Noise as a Source for Detecting Time-Lapse Changes

Roel Snieder

rsnieder@mines.edu

Noise as a Source for Detecting Time-Lapse Changes

Huub Douma, Alex Grêt, Chinaemerem Kanu, Ichiro Kuroda, Xun Li, Masatoshi Miyazawa, Nori Nakata, Ernst Niederleithinger, Carlos Pacheco, Thomas Planès, Kaoru Sawazaki, John Scales, Christoph Sens-Schönfelder, Kasper van Wijk, Roel Snieder

rsnieder@mines.edu

Geometry of L08-pad

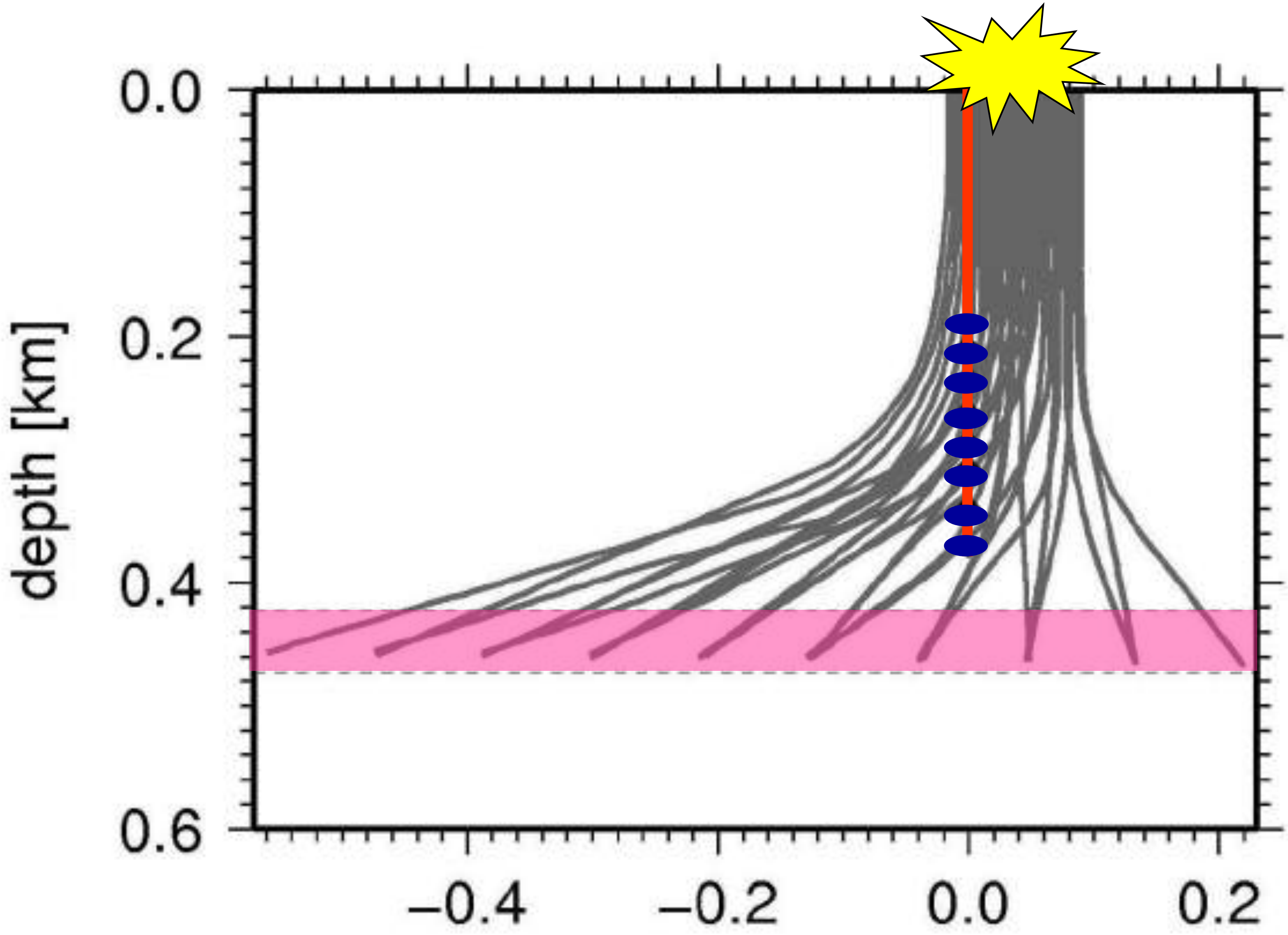

(Miyazawa, Snieder & Venkataraman, Geophysics, **73**, D35-D40, 2008)

from Noise to Signal

Top station

Bottom station

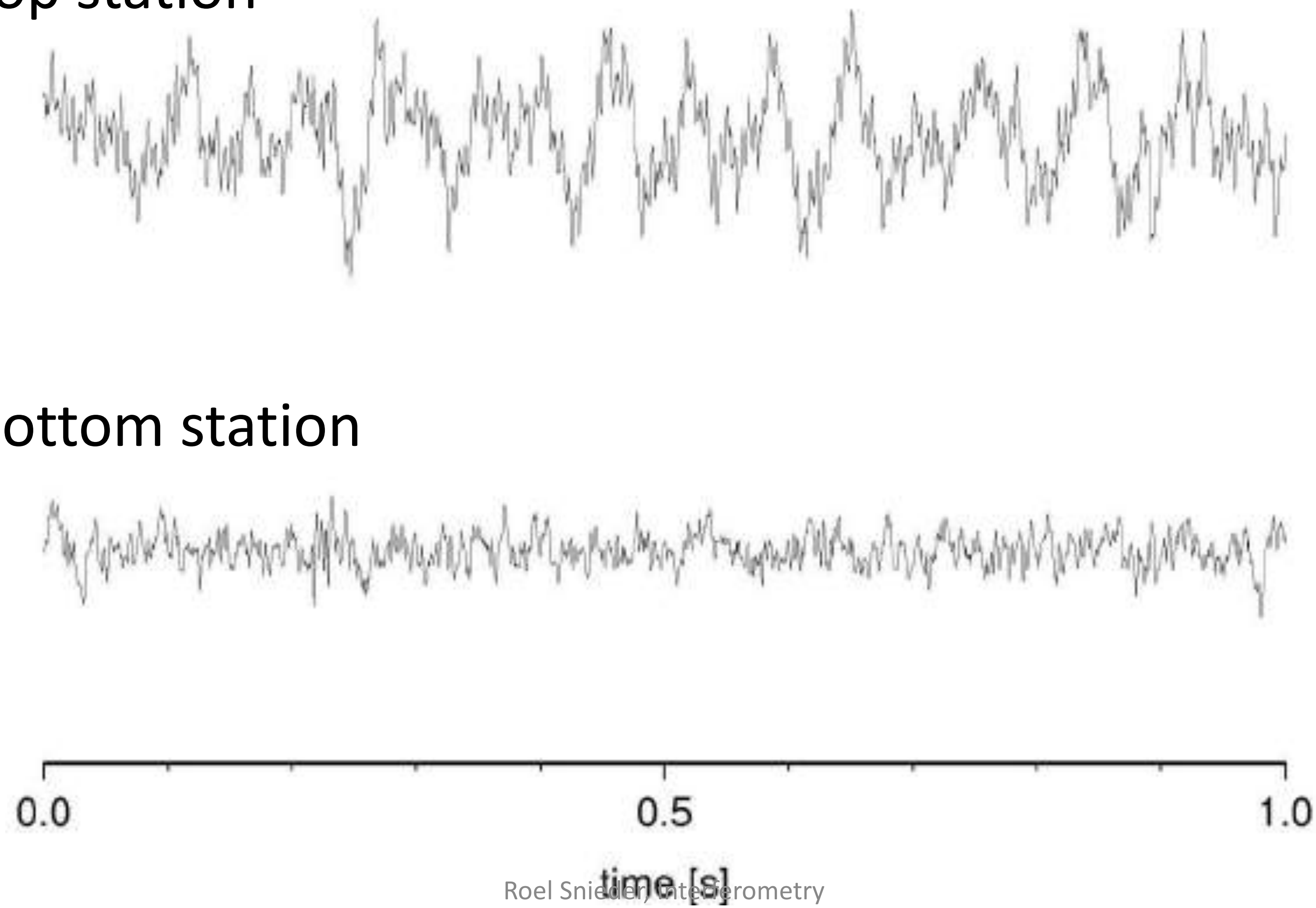

Cross-Correlation

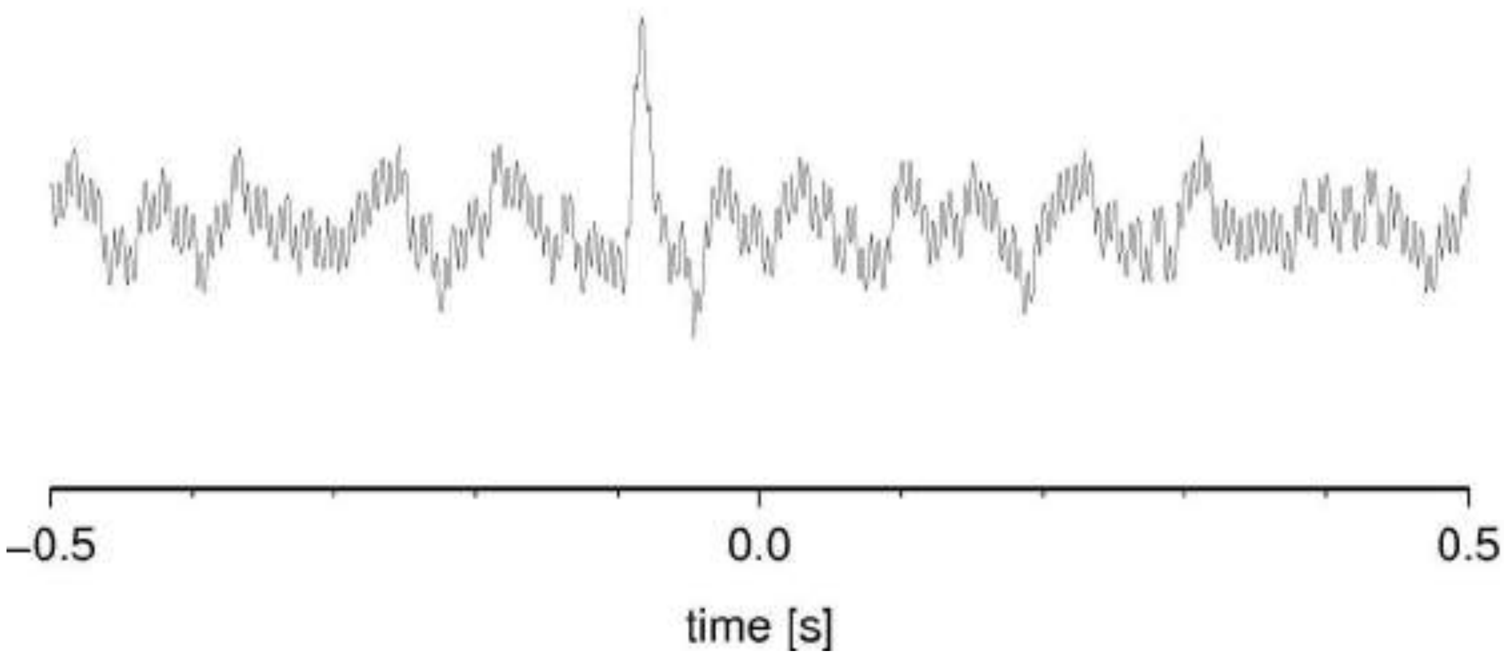

Cross-Correlation

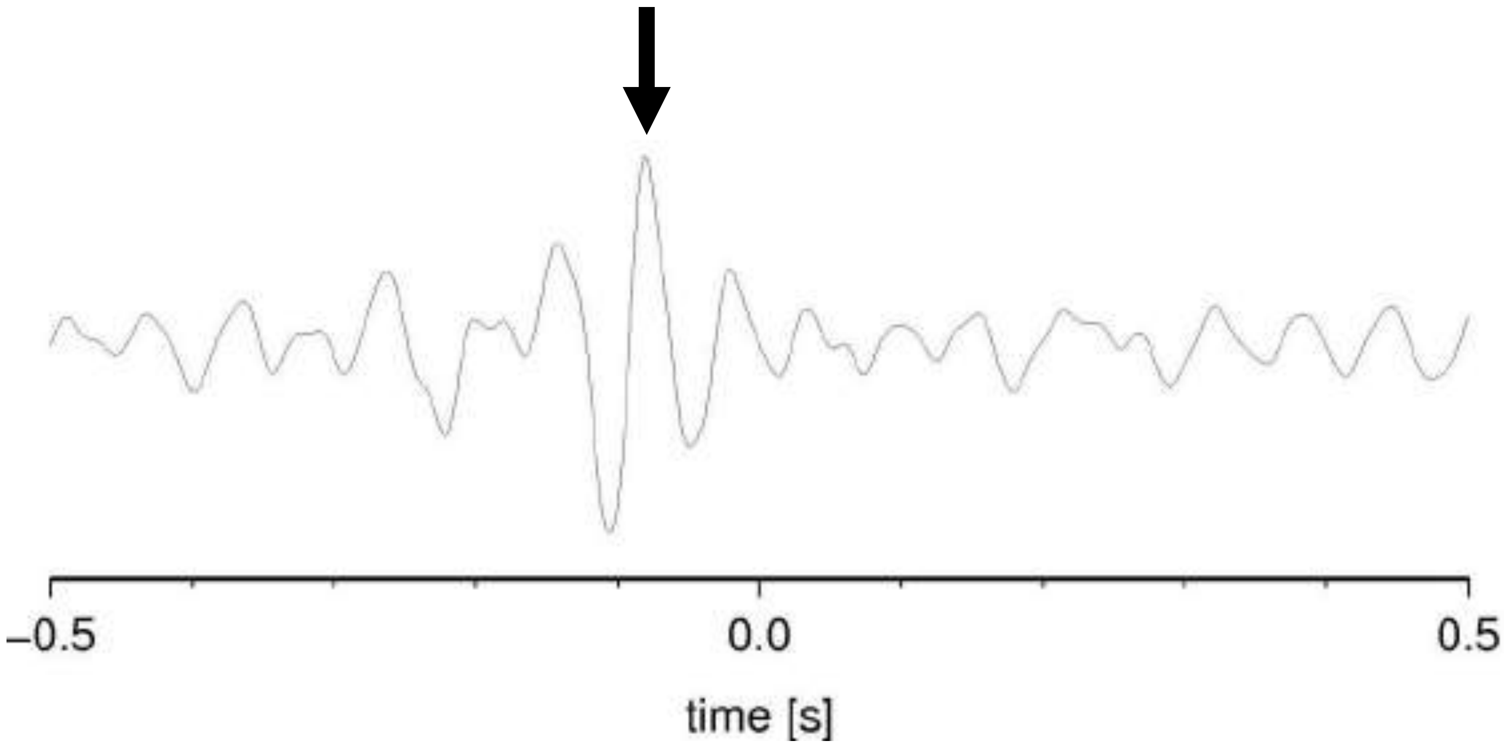

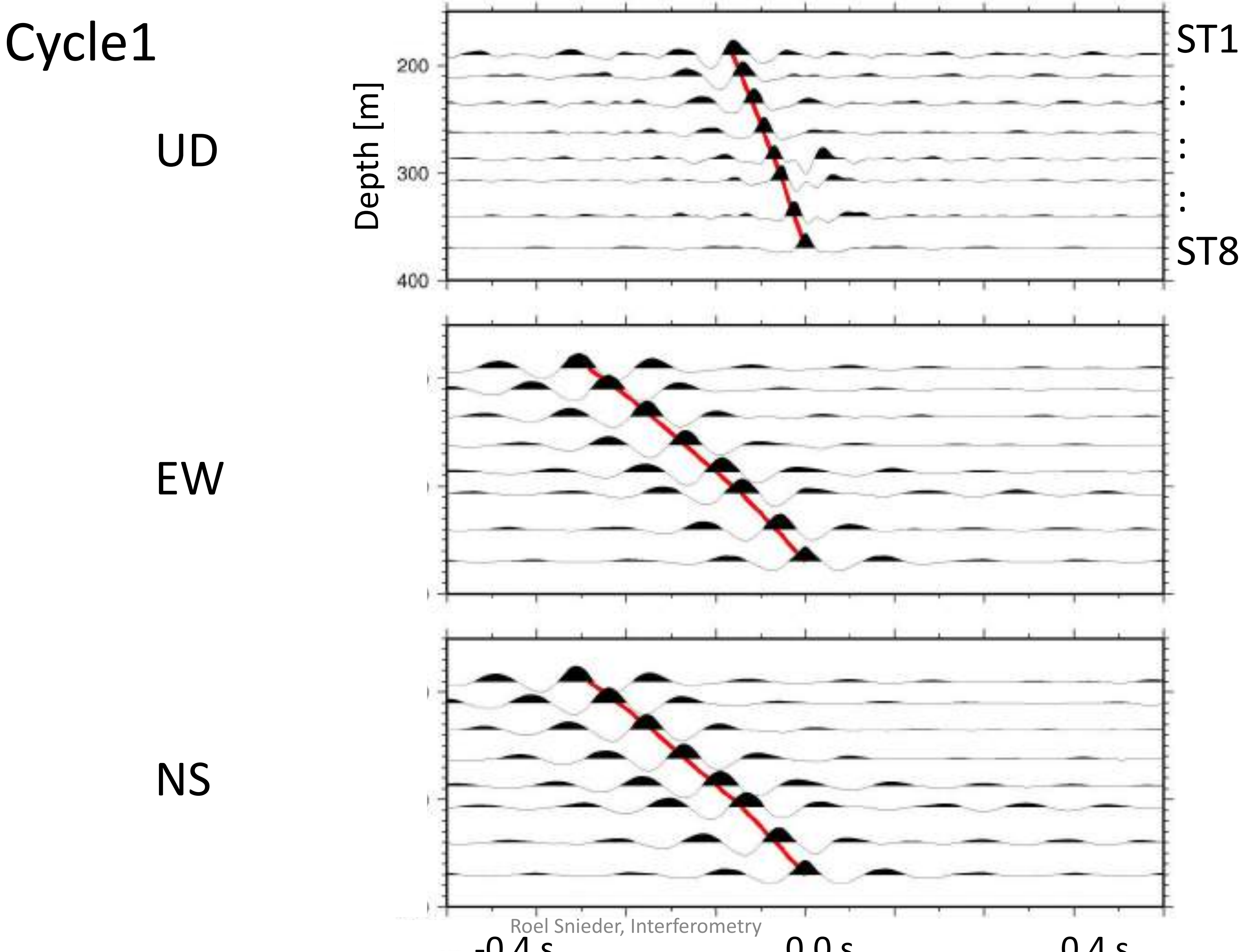

Roel Snieder, Interferometry

Surface waves

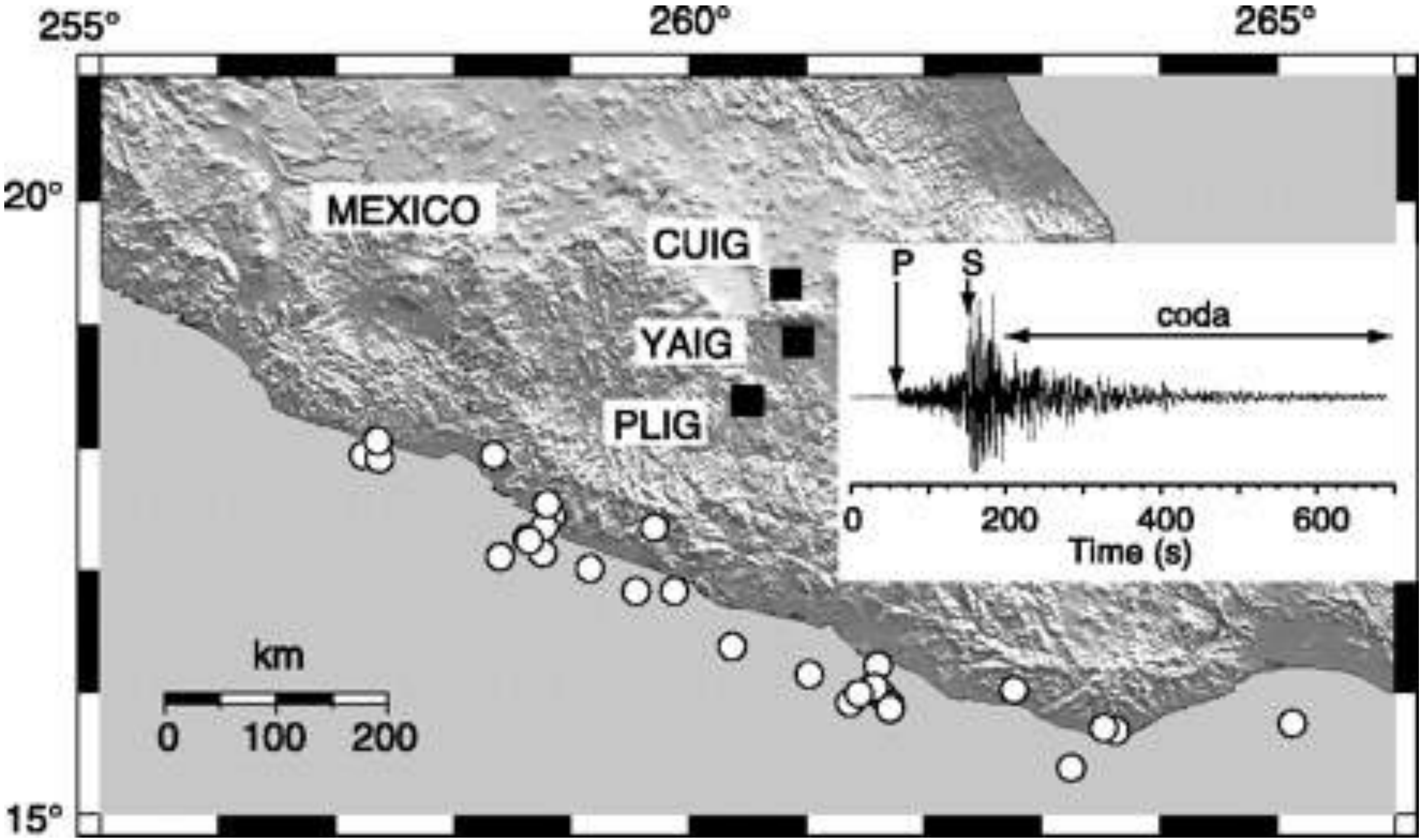

(Campillo and Paul, Science, **299**, 547-549, 2003)

correlation Green's tensor

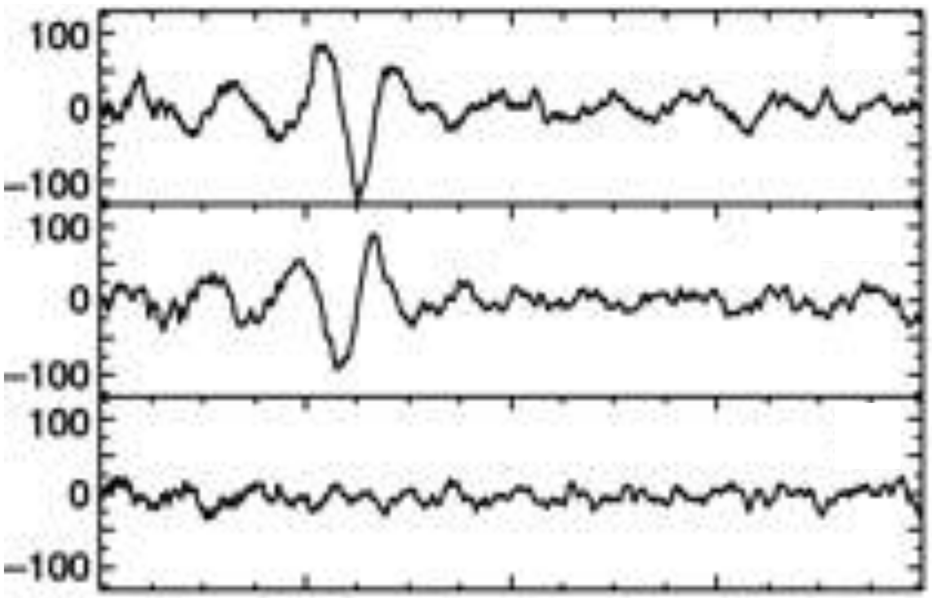

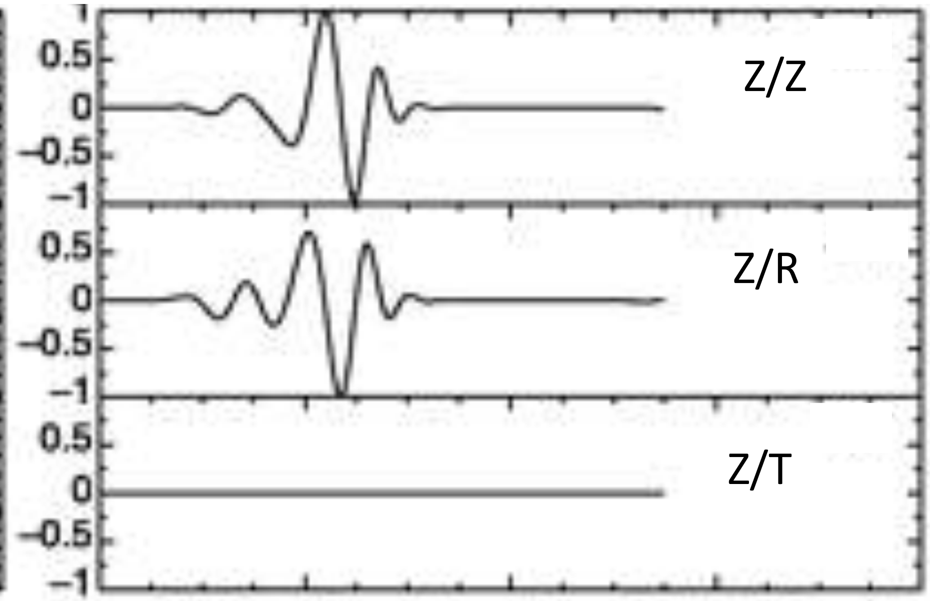

correlation   Green's tensor

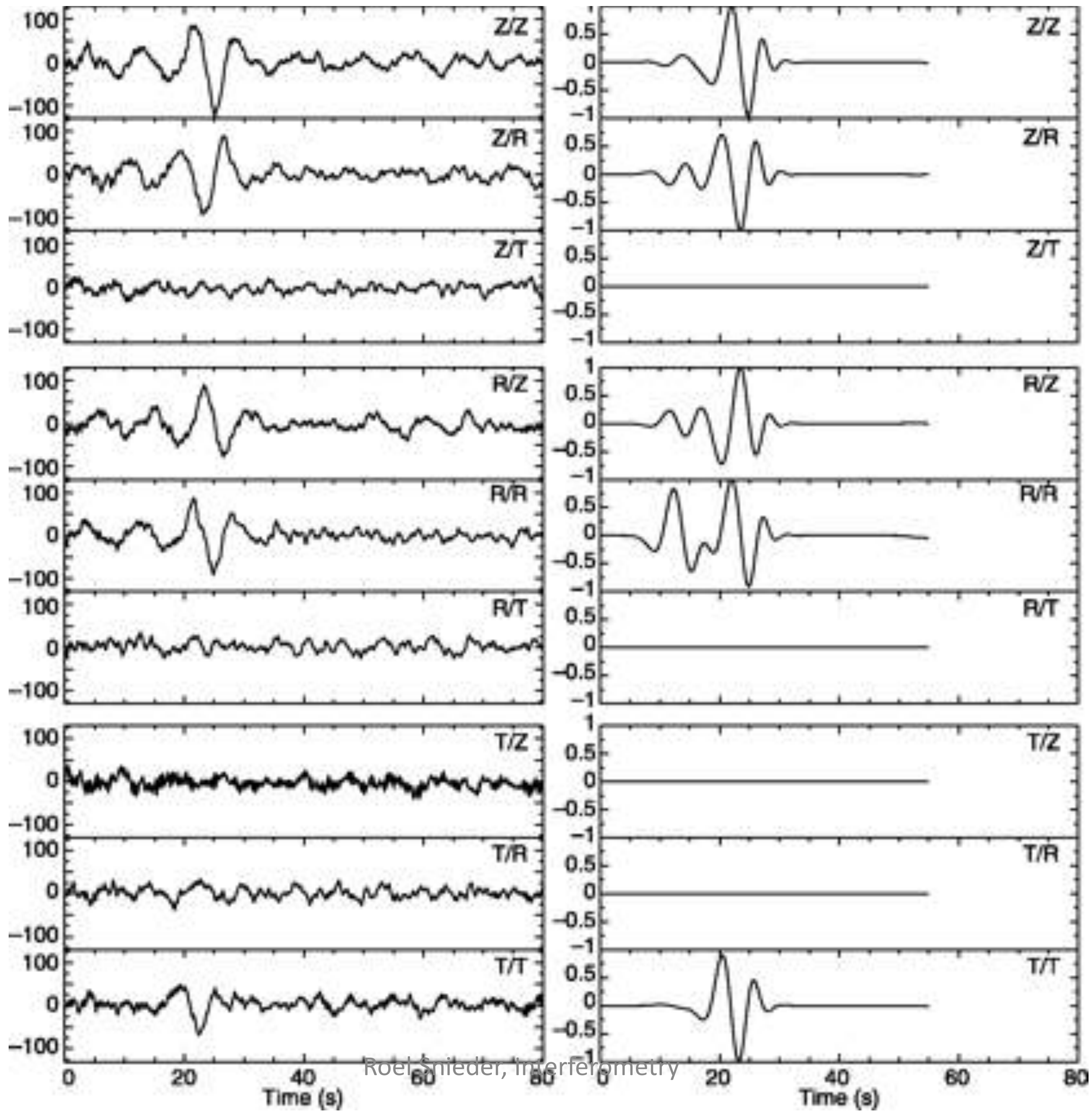

Z/Z

Z/R

Z/T

R/Z

R/R

R/T

T/Z

T/R

T/T

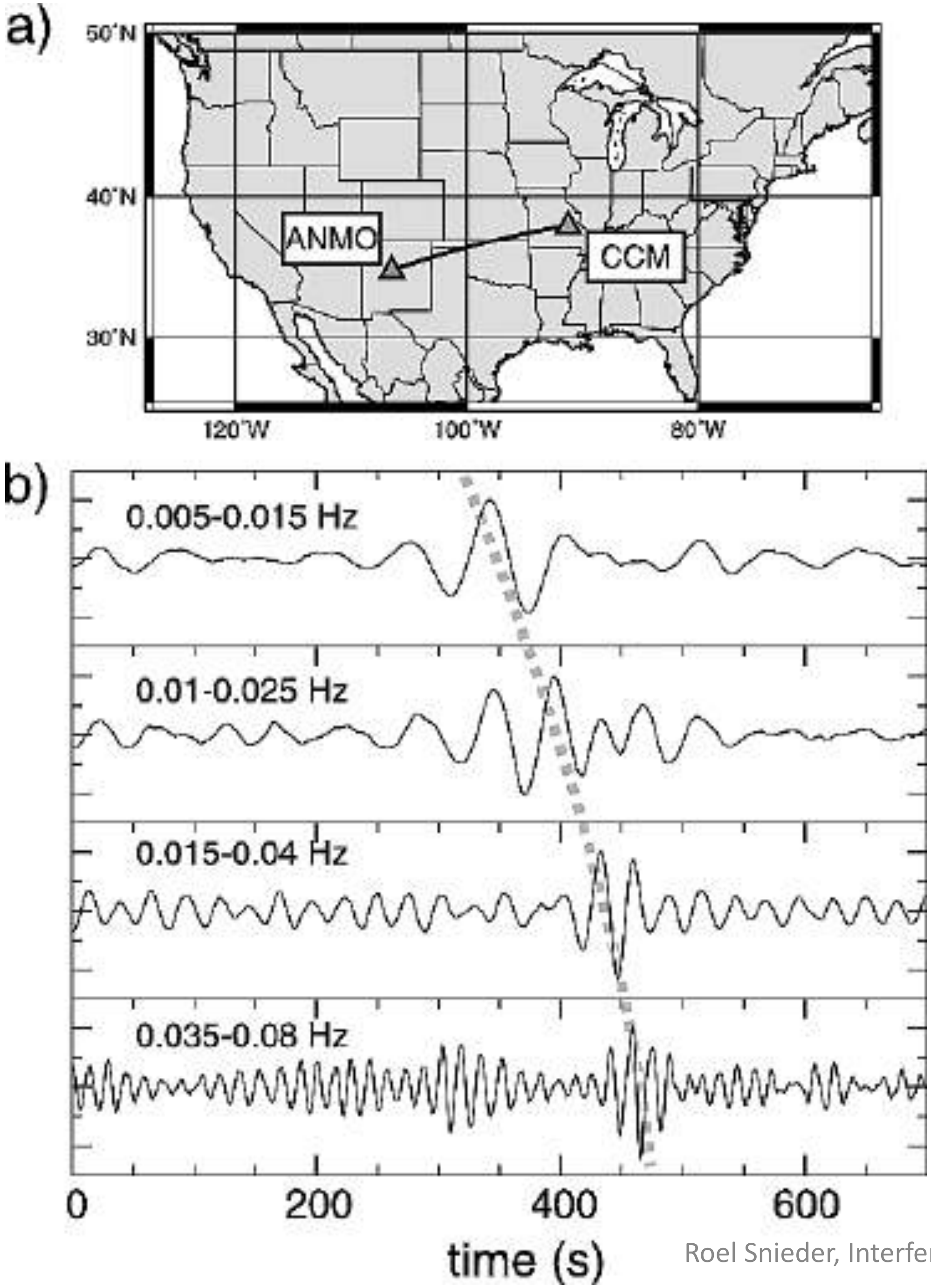

Surface wave dispersion from noise

(Shapiro and Campillo, Geophys. Res. Lett., **31**, L07614, 2004)

Raindrop model

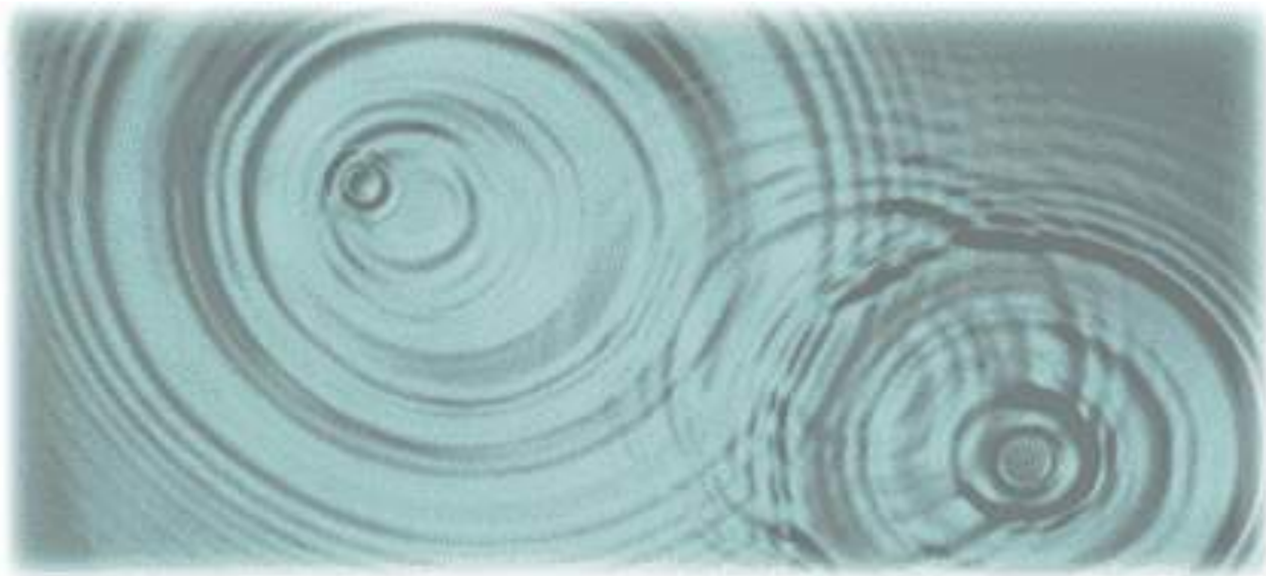

Correlation as volume integral

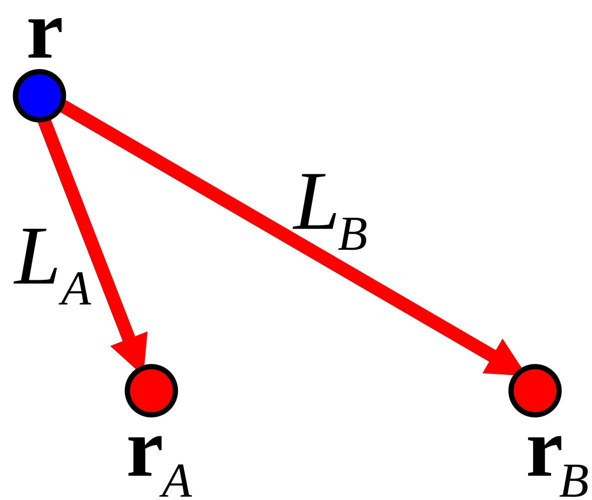

$$C_{AB}(\omega) = n\left|S(\omega)\right|^2 \int \frac{\exp\left(ik\left(L_A - L_B\right)\right)}{L_A L_B}\, dV$$

Stationary phase contribution

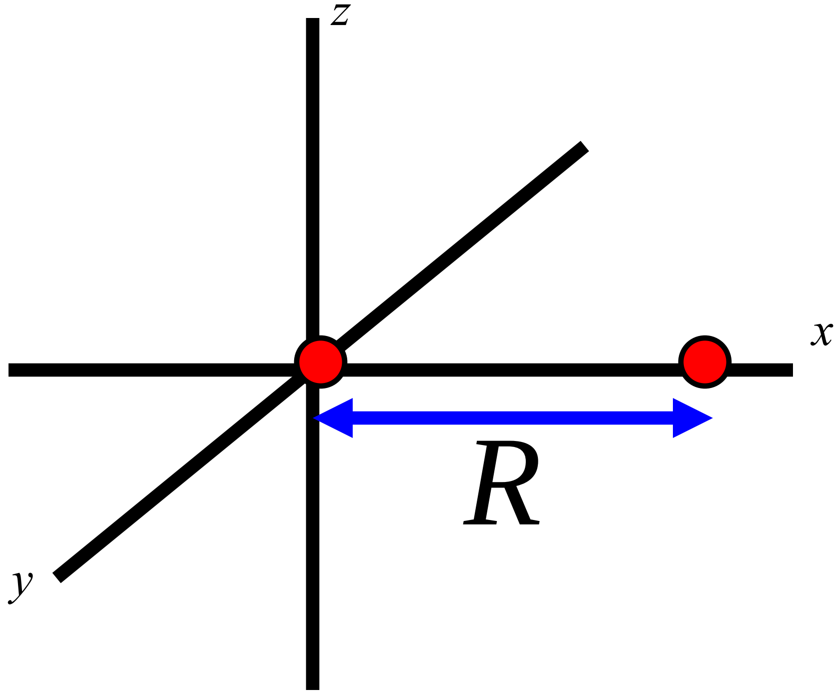

$$y = z = 0$$

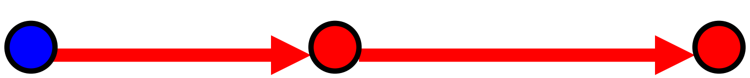

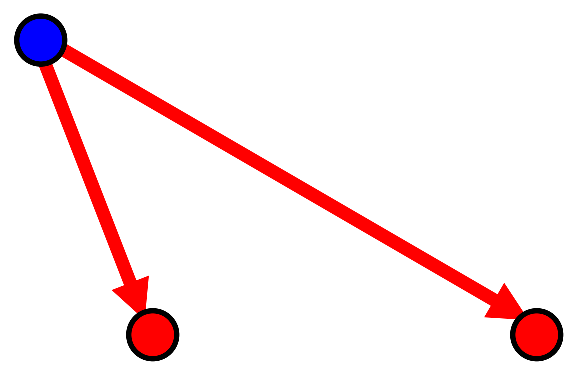

Stationary phase regions

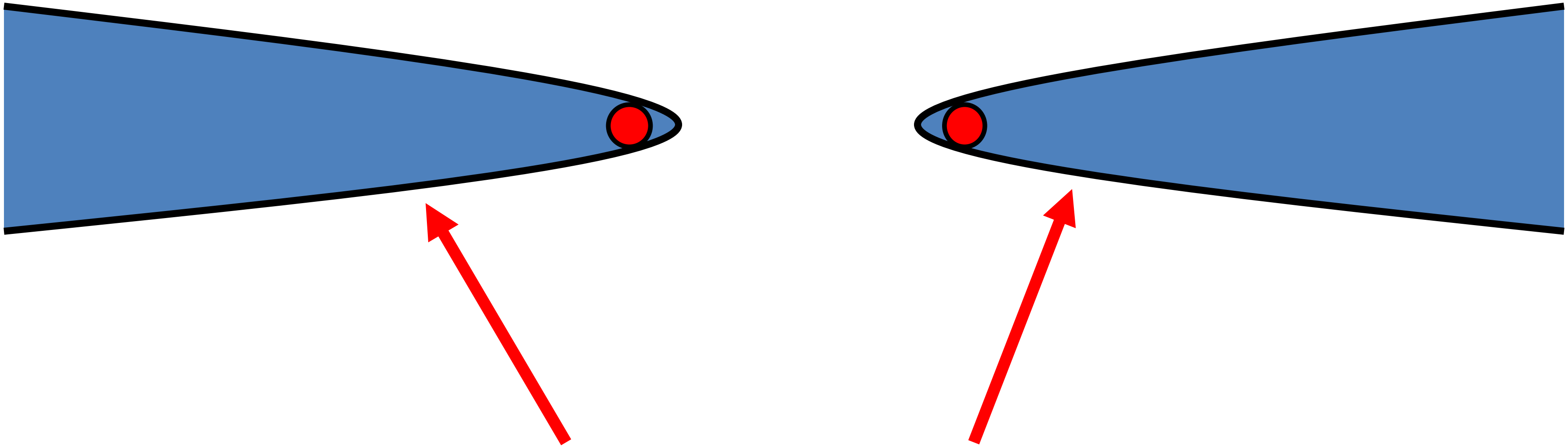

"anti-Fresnel zones"

(Snieder, Phys. Rev. E, **69**, 046610, 2004,
for reflected waves see:
Snieder, Wapenaar, and Larner, Geophysics, 71, SI111-SI124, 2006)

Four derivations

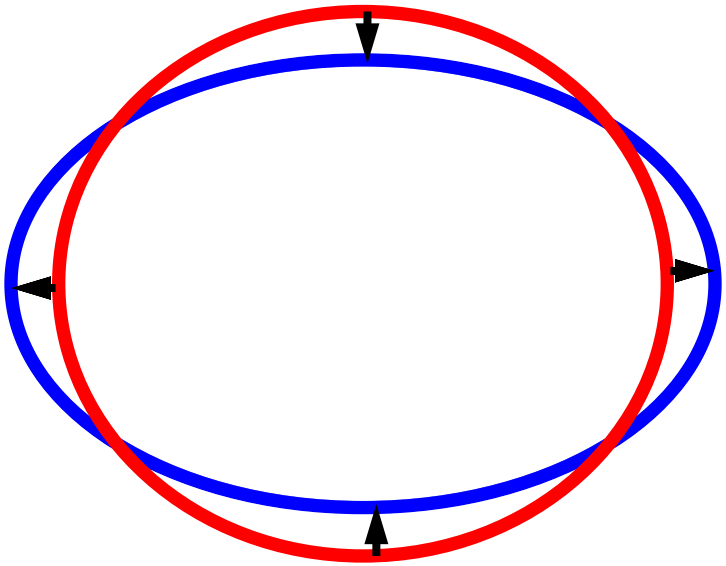

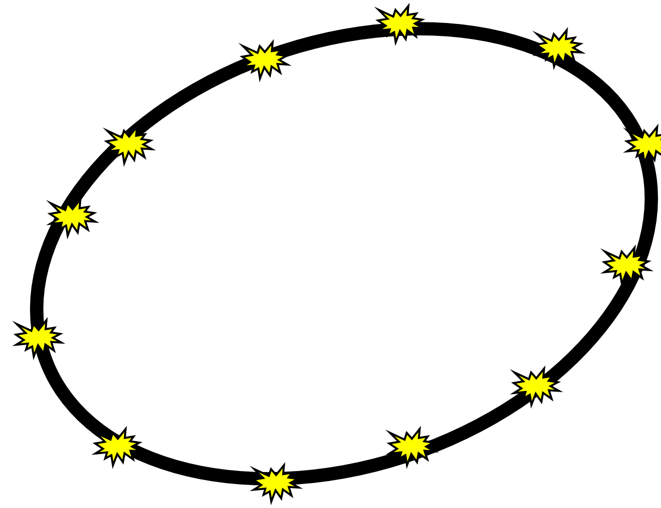

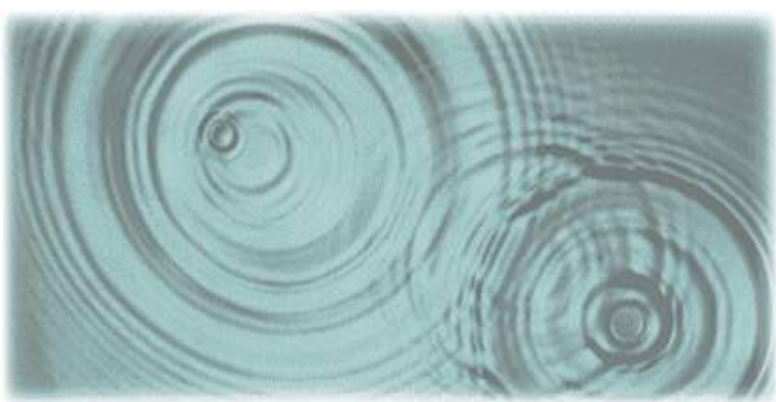

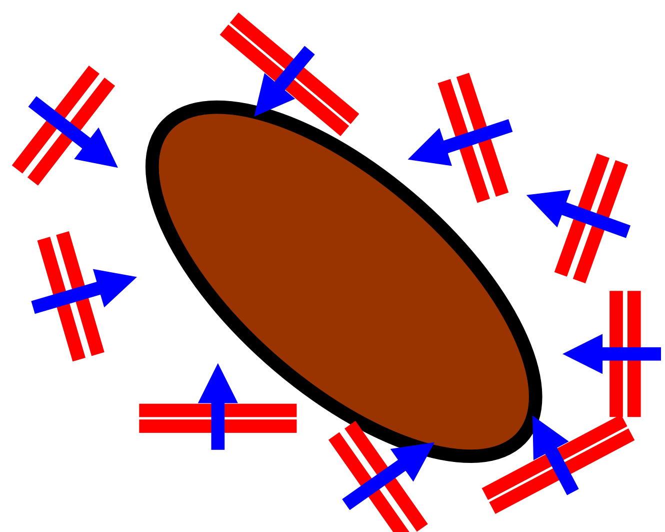

Derivation based on normal-modes

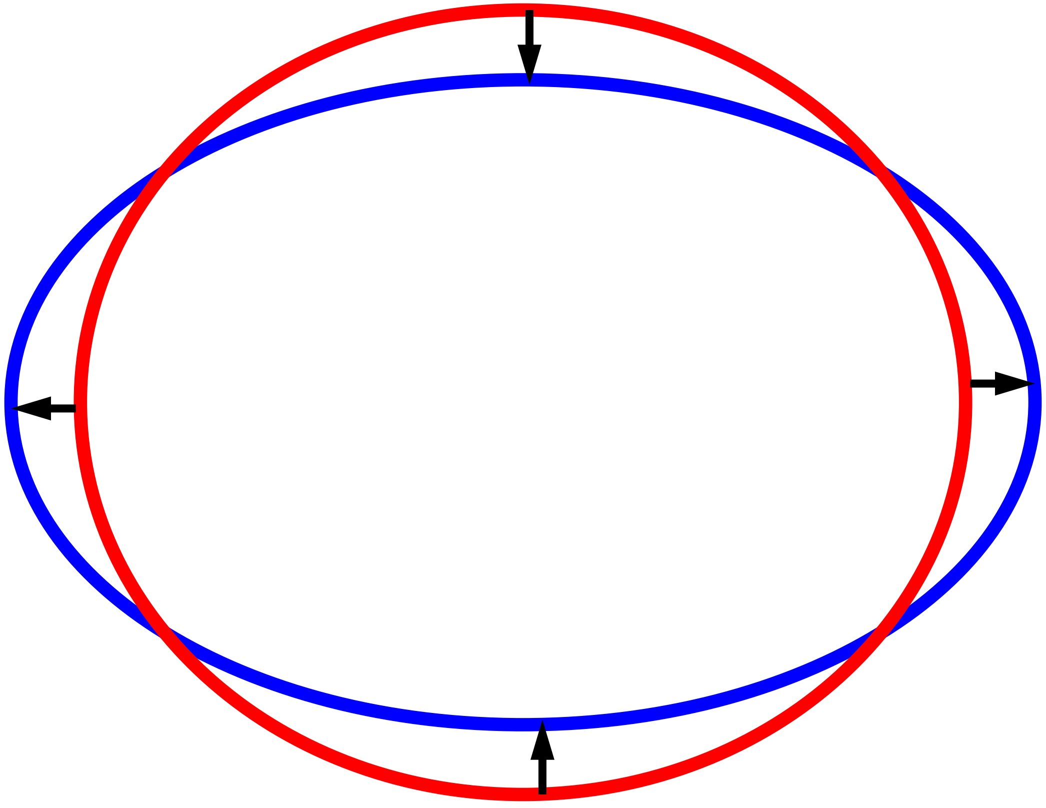

(Lobkis and Weaver, JASA, **110**, 3011-3017, 2001)

Displacement response

$$u(\mathbf{r},t)=\sum_m \frac{u_m(\mathbf{r})}{\omega_m}\left(a_m \sin\omega_m t + b_m \cos\omega_m t\right)$$

$$G(\mathbf{r},\mathbf{r}',t)=\sum_m \frac{u_m(\mathbf{r})u_m(\mathbf{r}')}{\omega_m}\sin\omega_m t \times H(t)$$

Heaviside function

Velocity response

$$v(\mathbf{r},t) = \sum_m u_m(\mathbf{r})\left(a_m \cos\omega_m t - b_m \sin\omega_m t\right)$$

$$G^{(v)}(\mathbf{r},\mathbf{r}',t) = \sum_m u_m(\mathbf{r})u_m(\mathbf{r}')\cos\omega_m t \times H(t)$$

Uncorrelated excitation

$$v(\mathbf{r},t) = \sum_m u_m(\mathbf{r})\left(a_m \cos\omega_m t - b_m \sin\omega_m t\right)$$

$$\langle a_n a_m \rangle = F^2 \delta_{nm}$$

$$\langle b_n b_m \rangle = F^2 \delta_{nm}$$

$$\langle a_n b_m \rangle = 0$$

Correlation

$$C_{AB}^{(v)}(\tau) = \left\langle v(\mathbf{r}_A, t)\, v(\mathbf{r}_B, t+\tau) \right\rangle$$

$$v(\mathbf{r}_{A,B}, t) = \sum_m u_m(\mathbf{r}_{A,B})\left(a_m \cos\omega_m t - b_m \sin\omega_m t\right)$$

Correlation as a sum of modes

$$
\begin{aligned}
C_{AB}^{(v)}(\tau) \quad = \sum_{n,m} & u_n(\mathbf{r}_A) u_m(\mathbf{r}_B) \\
& \times \Big\{ \langle a_n a_m \rangle \cos\omega_n t \cos\omega_m (t+\tau) \\
& \quad - \langle a_n b_m \rangle \cos\omega_n t \sin\omega_m (t+\tau) \\
& \quad - \langle b_n a_m \rangle \sin\omega_n t \cos\omega_m (t+\tau) \\
& \quad + \langle b_n b_m \rangle \sin\omega_n t \sin\omega_m (t+\tau) \Big\}
\end{aligned}
$$

For uncorrelated modes

$$C_{AB}^{(v)}(\tau) = \sum_{n,m} u_n(\mathbf{r}_A) u_m(\mathbf{r}_B)$$

$$\times \left\{ \langle a_n a_m \rangle \cos\omega_n t \cos\omega_m (t+\tau) \right.$$

$$- \cancel{\langle a_n b_m \rangle} \cos\omega_n t \sin\omega_m (t+\tau)$$

$$- \cancel{\langle b_n a_m \rangle} \sin\omega_n t \cos\omega_m (t+\tau)$$

$$\left. + \langle b_n b_m \rangle \sin\omega_n t \sin\omega_m (t+\tau) \right\}$$

$$F^2 \delta_{nm}$$

For uncorrelated modes

$$
\begin{aligned}
C^{(v)}_{AB}(\tau) &= \sum_{n,m} u_n(\mathbf{r}_A)\, u_m(\mathbf{r}_B) \\
&\quad \times \Big\{ \langle a_n a_m \rangle \cos\omega_n t \cos\omega_m (t+\tau) \\
&\quad - \cancel{\langle a_n b_m \rangle} \cos\omega_n t \sin\omega_m (t+\tau) \\
&\quad - \cancel{\langle b_n a_m \rangle} \sin\omega_n t \cos\omega_m (t+\tau) \\
&\quad + \langle b_n b_m \rangle \sin\omega_n t \sin\omega_m (t+\tau) \Big\}
\end{aligned}
$$

$$F^2 \delta_{nm}$$

$$= \cos\omega_m \tau$$

Correlation

$$C_{AB}^{(v)}(\tau) = F^2 \sum_m u_m(\mathbf{r}_A) u_m(\mathbf{r}_B) \cos\omega_m \tau$$

Green's function

$$G^{(v)}(\mathbf{r}_A, \mathbf{r}_B, \tau) = \sum_m u_m(\mathbf{r}_A) u_m(\mathbf{r}_B) \cos\omega_m \tau \times H(\tau)$$

Correlation

$$C_{AB}^{(v)}(\tau) = F^2 \sum_m u_m(\mathbf{r}_A) u_m(\mathbf{r}_B) \cos \omega_m \tau$$

Green's function

$$G^{(v)}(\mathbf{r}_A, \mathbf{r}_B, \tau) = \sum_m u_m(\mathbf{r}_A) u_m(\mathbf{r}_B) \cos \omega_m \tau \times H(\tau)$$

$$\tau > 0 \longrightarrow C_{AB}^{(v)}(\tau) = F^2 G^{(v)}(\mathbf{r}_A, \mathbf{r}_B, \tau)$$

Correlation

$$C_{AB}^{(v)}(\tau) = F^2 \sum_m u_m(\mathbf{r}_A) u_m(\mathbf{r}_B) \cos \omega_m \tau$$

Green's function

$$G^{(v)}(\mathbf{r}_A, \mathbf{r}_B, \tau) = \sum_m u_m(\mathbf{r}_A) u_m(\mathbf{r}_B) \cos \omega_m \tau \times H(\tau)$$

$$\tau < 0 \longrightarrow C_{AB}^{(v)}(\tau) = F^2 G^{(v)}(\mathbf{r}_A, \mathbf{r}_B, -\tau)$$

Correlation and Green's function

$$\boxed{C_{AB}^{(v)}(t) = F^2\left\{G^{(v)}(\mathbf{r}_A,\mathbf{r}_B,t) + G^{(v)}(\mathbf{r}_A,\mathbf{r}_B,-t)\ \right\}}$$

- sum of causal and acausal Green's function

- holds for arbitrary heterogeneity

Displacement instead of velocity

$$C_{AB}^{(v)} = \frac{d^2 C_{AB}^{(disp)}}{dt^2}$$

$$G^{(v)}(\mathbf{r}_A, \mathbf{r}_B, t) = \frac{\partial G^{(disp)}(\mathbf{r}_A, \mathbf{r}_B, t)}{\partial t}$$

$$\frac{dC_{AB}^{(disp)}}{dt}(t) = F^2 \left\{ G^{(disp)}(\mathbf{r}_A, \mathbf{r}_B, t) - G^{(disp)}(\mathbf{r}_A, \mathbf{r}_B, -t) \right\}$$

Conclusion: time derivative may appear

Wave field reconstruction

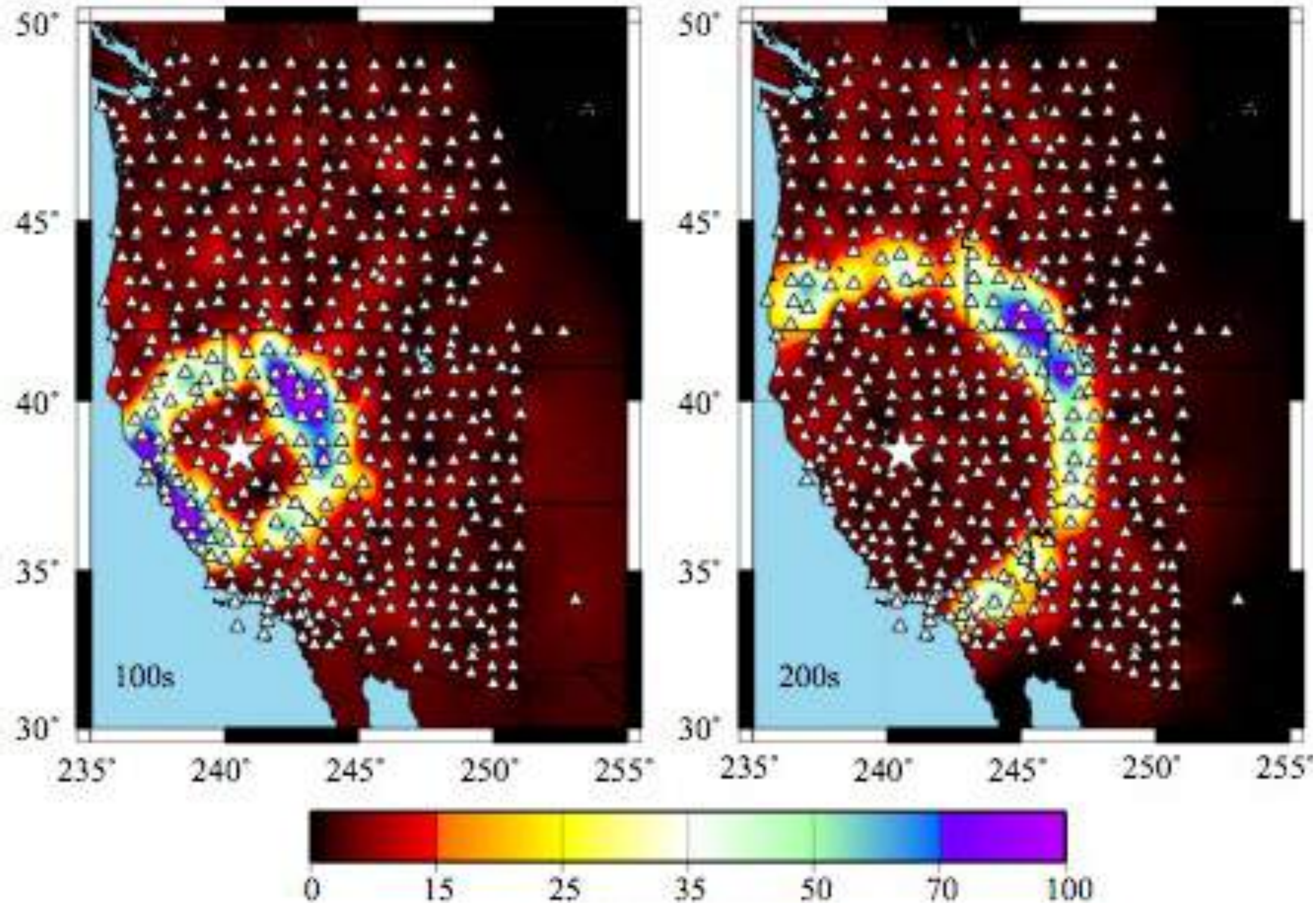

(Lin, Ritzwoller and Snieder, Geophys. J. Int., 177, 1091–1110, 2009)

Seismic interferometry

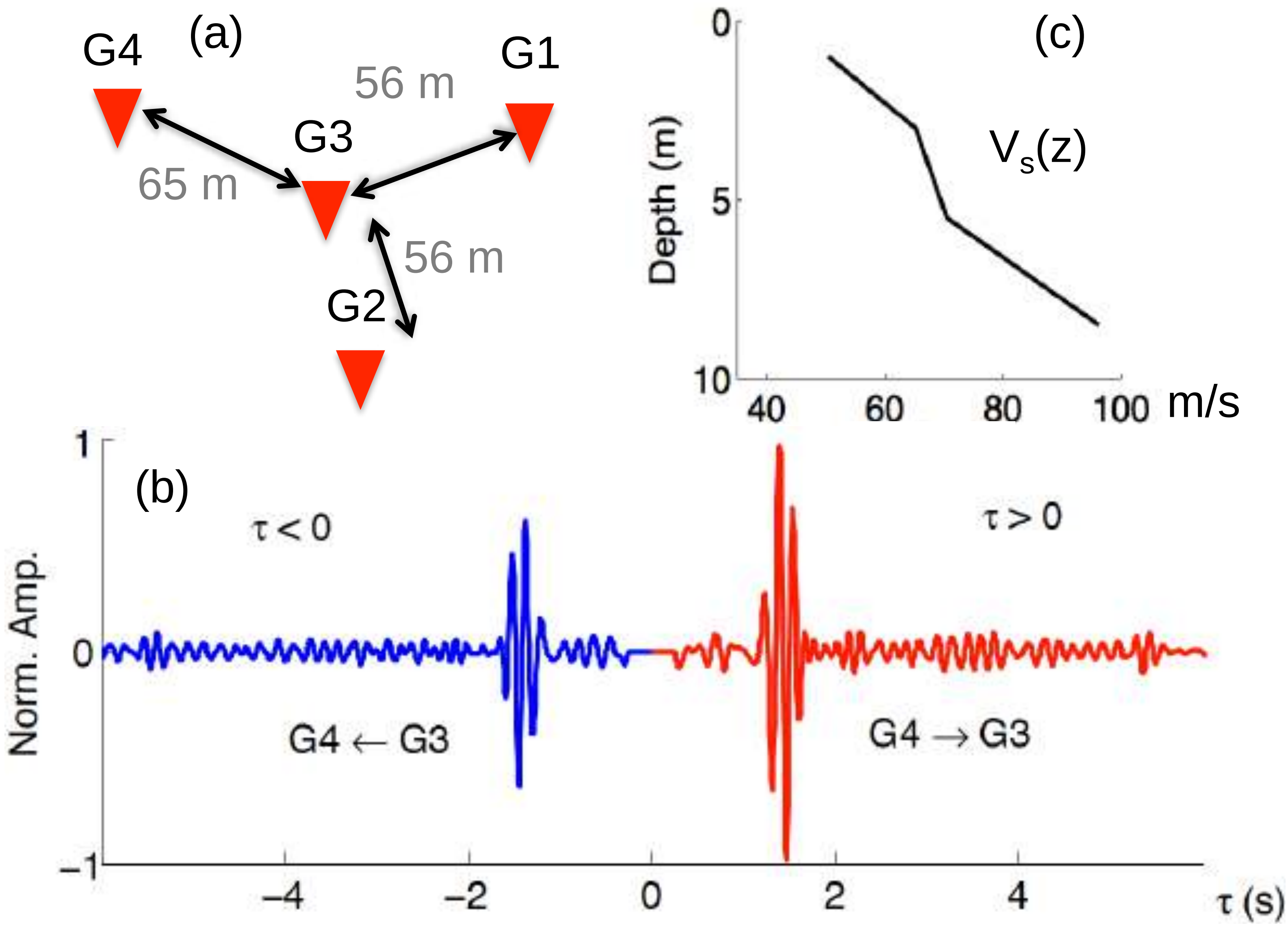

(Larose et al., Geophys. Res. Lett., 32, L16201, 2005)

Seismic interferometry on the moon!

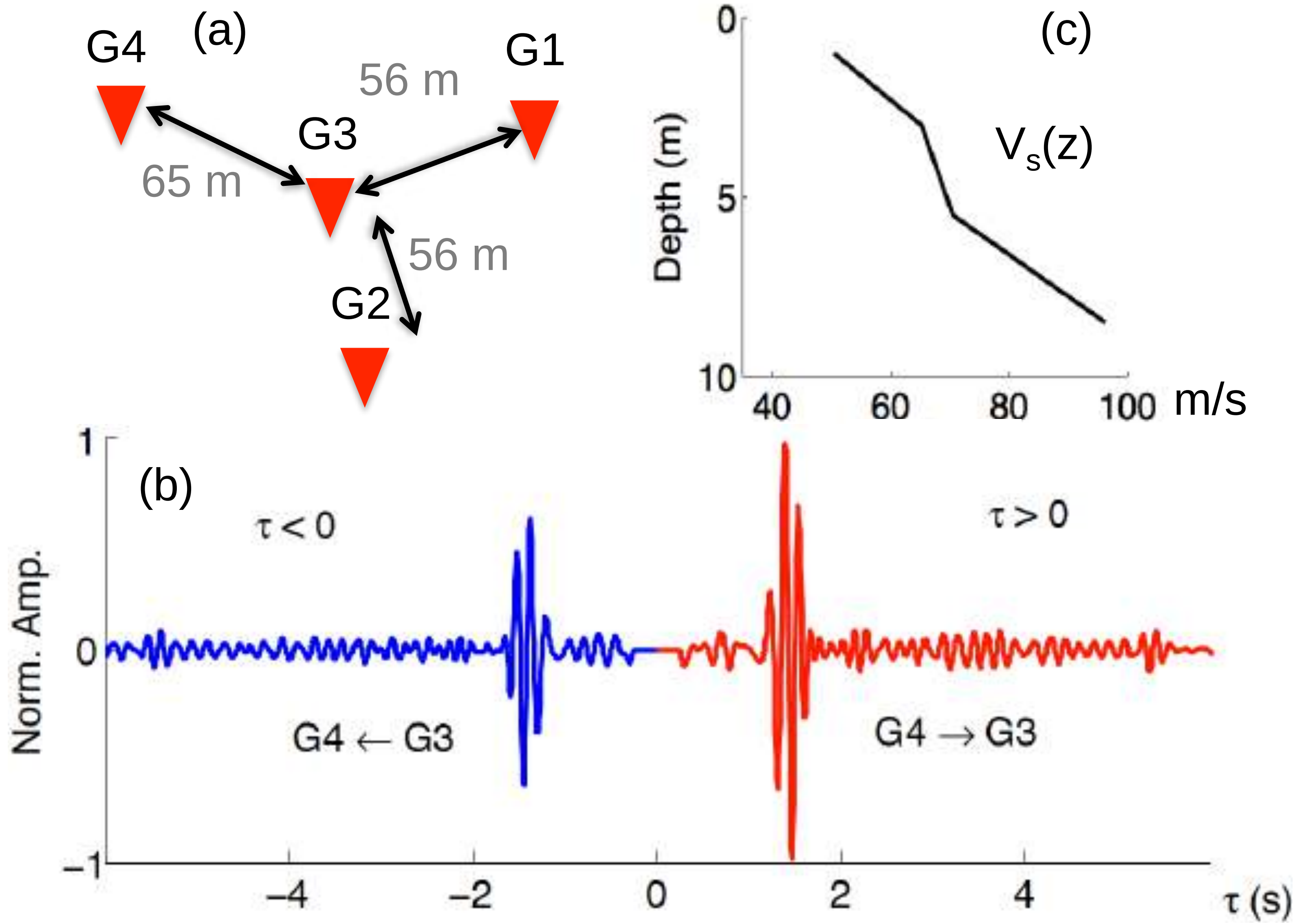

(Larose et al., Geophys. Res. Lett., 32, L16201, 2005)

Seismic interferometry on the moon

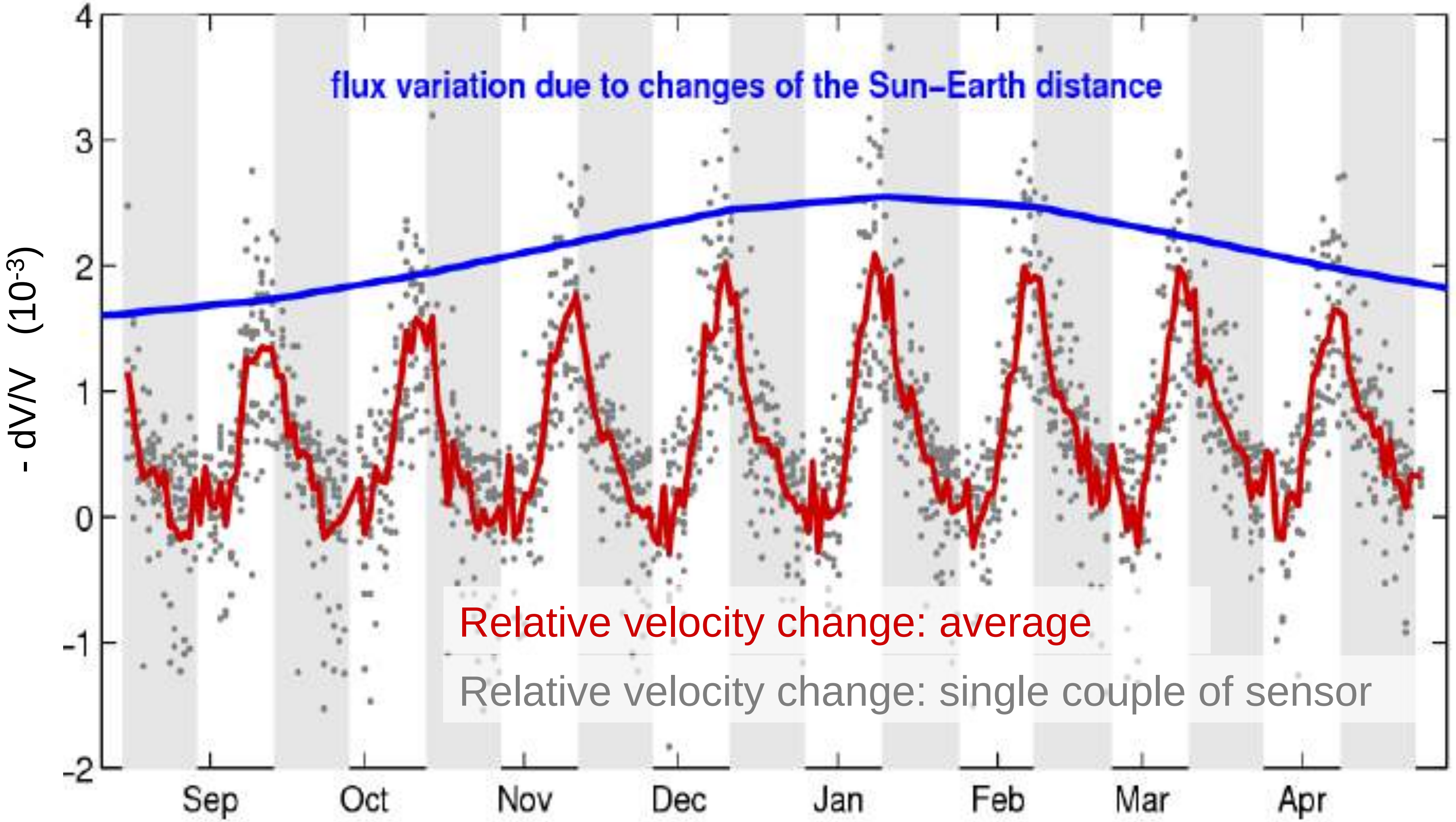

(Sens-Schönfelder & Larose, Phys. Rev. E, 78, 045601, 2008)

INSIGHTS

PERSPECTIVES

ENVIRONMENT

Why coal ash and tailings dam disasters occur

Knowledge gaps and management shortcomings contribute to catastrophic dam failures

By **J. Carlos Santamarina[1], Luis A. Torres-Cruz[2], Robert C. Bachus[3]**

On 25 January 2019, the structure damming a pond filled with iron ore mining wastes (tailings) burst at Brumadinho, Brazil (*1*), causing a massive mudslide that killed at least 232 people. This tailings dam failure was only the most recent in a long list of catastrophic tailings dam accidents (see the first figure) (*2*, *3*). Similar accidents also occur at electric power stations, where ponds are used to store coal combustion residuals such as fly and bottom ash. There are about 1000 operating ash ponds in the United States (*4*), and coal consumption patterns suggest that there may be more than 9000 worldwide. The catastrophic accident at the Kingston fossil power plant in Tennessee in 2008 (*5*) highlights the destructive potential of ash pond failures. Detailed analysis of tailings dam and ash pond failures shows that little-understood processes such as time-delayed triggering mechanisms are more likely to manifest when best engineering practices are disregarded.

Failure of the containment structure around mine tailings and coal ash is often followed by a fast-moving mudflow, which can run downstream for several miles, with catastrophic consequences. This liquefaction of the impounded materials may sug-

PHOTO: DOUGLAS MAGNO/AFP/GETTY IMAGES

Roel Snieder, Interferometry

Mechanisms and processes of tailings dam and ash pond failures

Many different aspects of impounded ash and mine tailings and the associated dams can contribute to dam failures and the resulting fast-moving mudflows. The figure shows upstream construction as an example; most processes and mechanisms shown also apply to centerline and downstream construction methods.

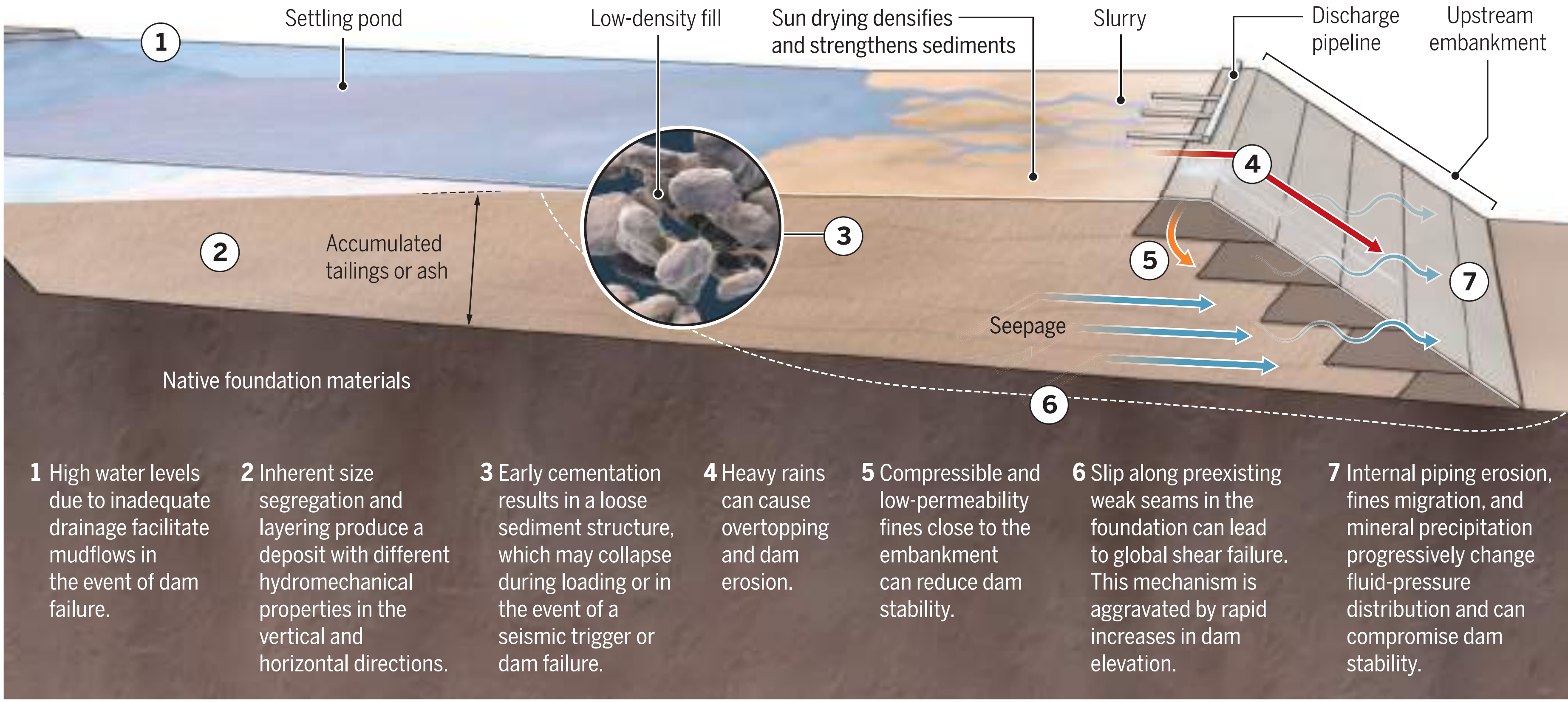

(Santamarina et al., Science, 364, 526-528, 2019)

Monitoring a dam

breach created by pulling a metal rod out of the dam

(Planès et al., Geotechnique, 66, 301-312, 2016)

Change in shear velocity in a dam

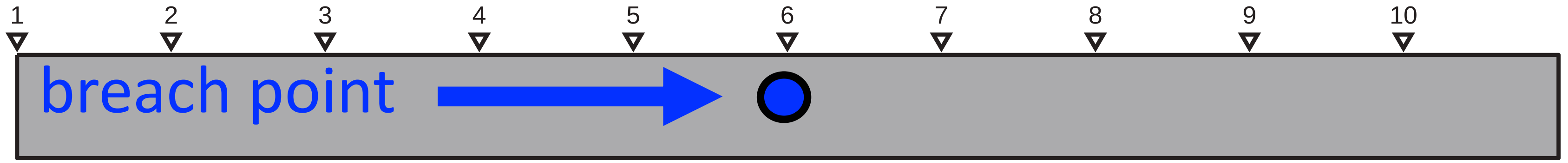

(Planes et al., Geotechnique, 66, 301-312, 2016)

Sensor 1 as virtual source

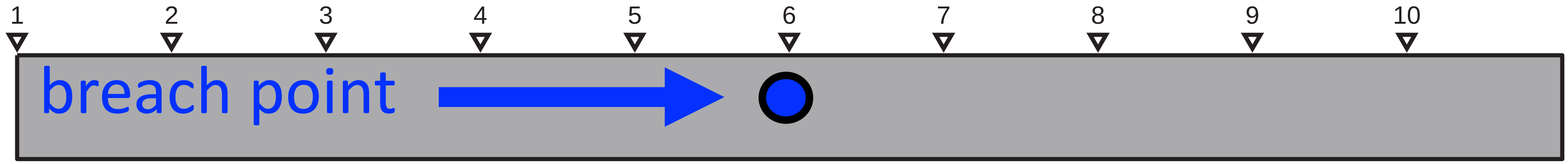

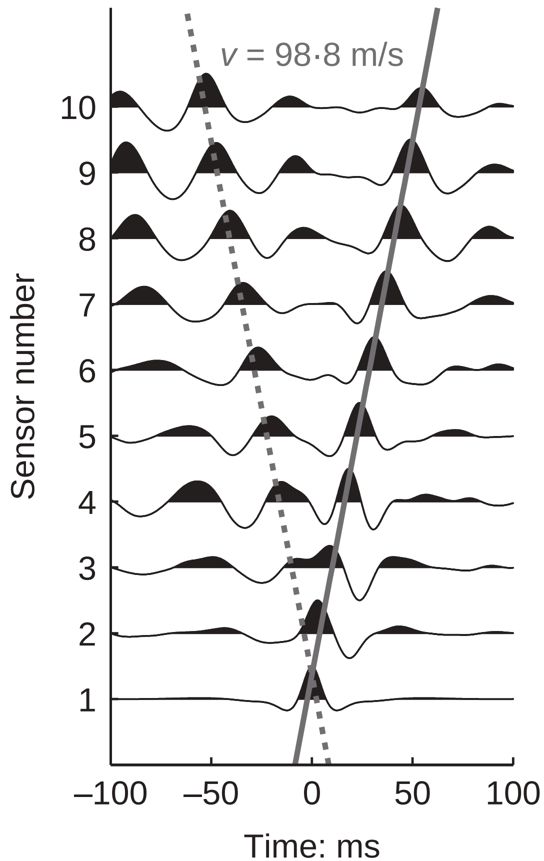

(Planes et al., Geotechnique, 66, 301-312, 2016)

Change in shear velocity in a dam

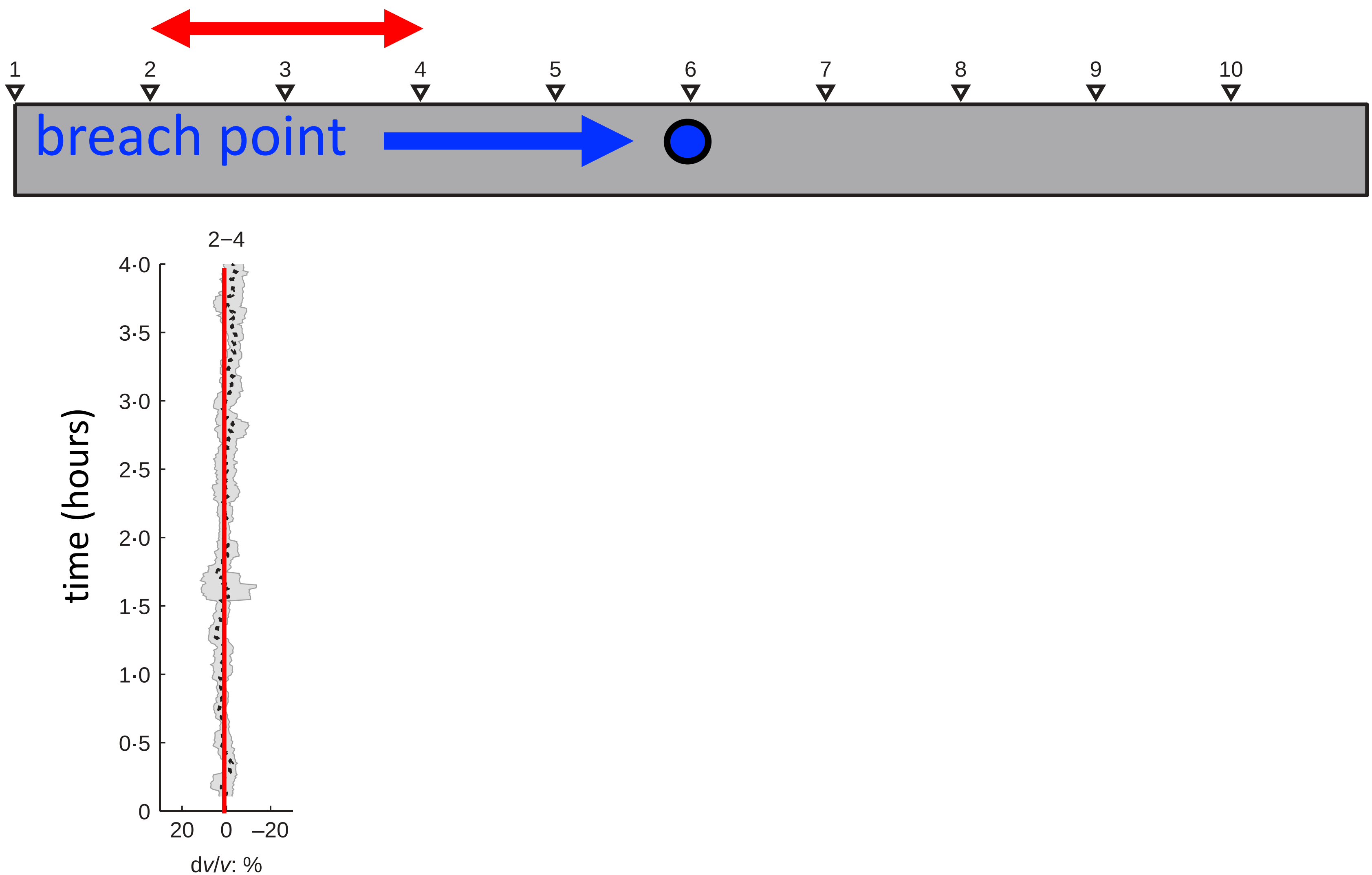

(Planes et al., Geotechnique, 66, 301-312, 2016)

Change in shear velocity in a dam

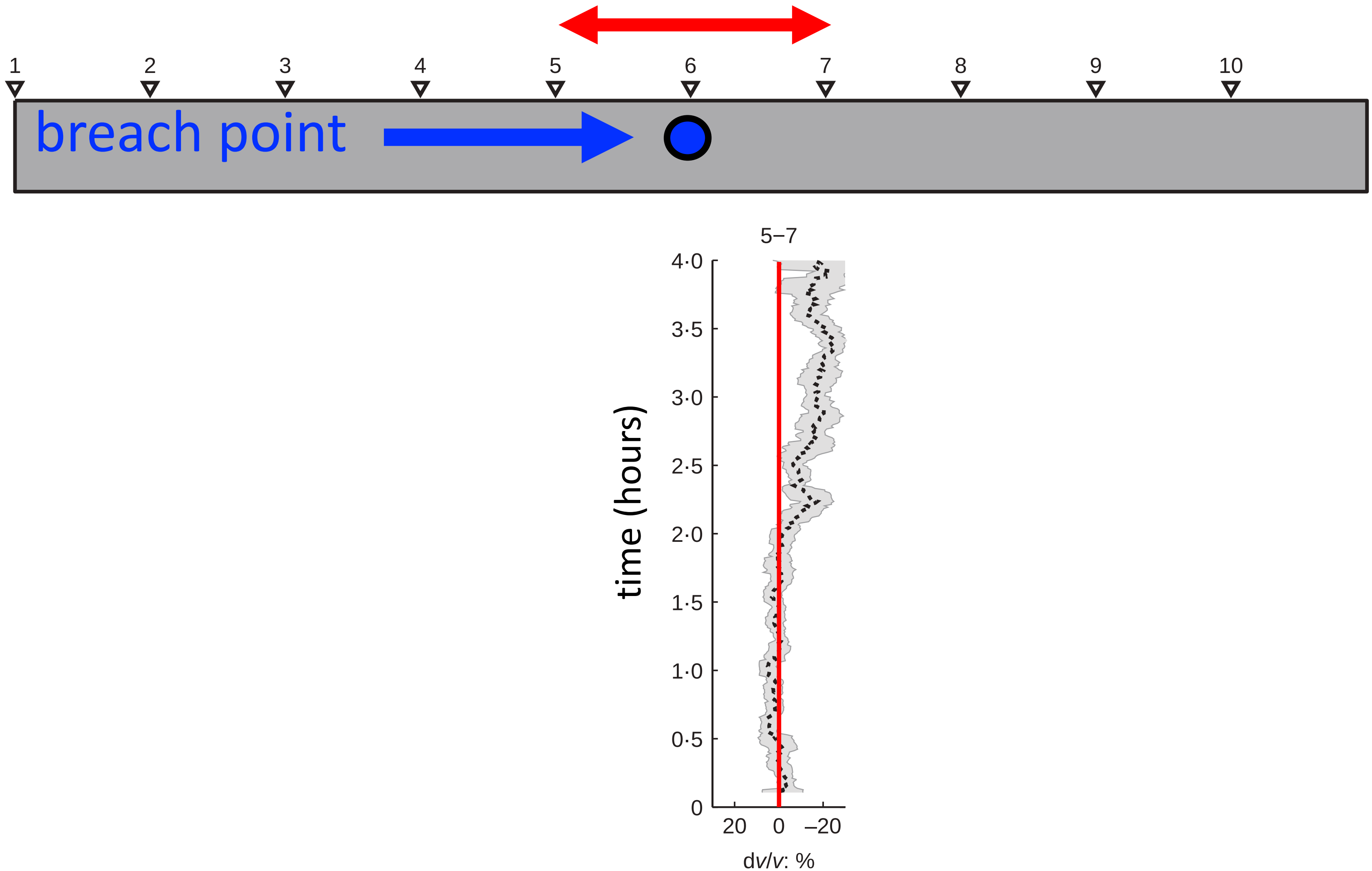

(Planes et al., Geotechnique, 66, 301-312, 2016)

Near-surface structure from Kik-Net

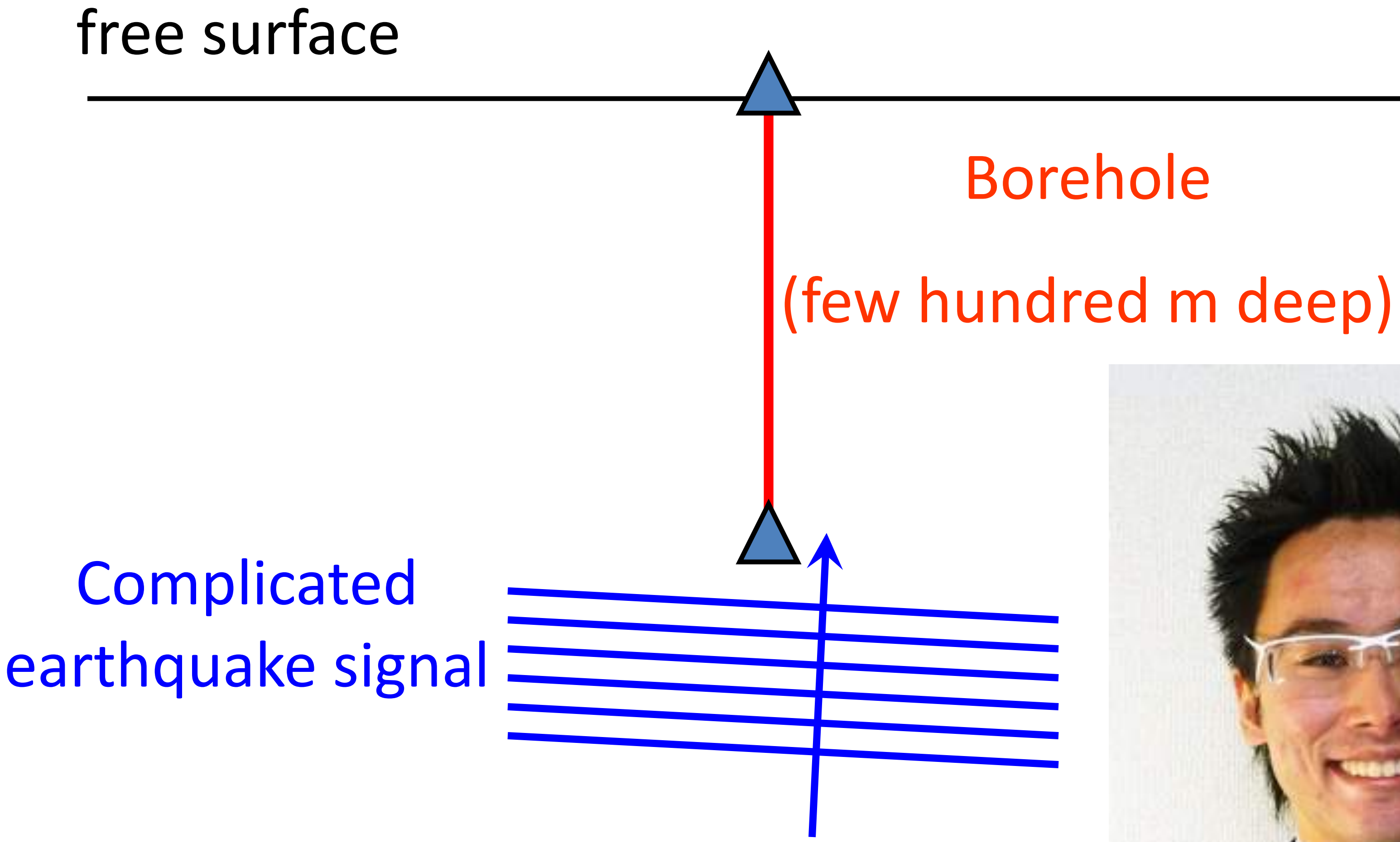

Data at station NIGH13

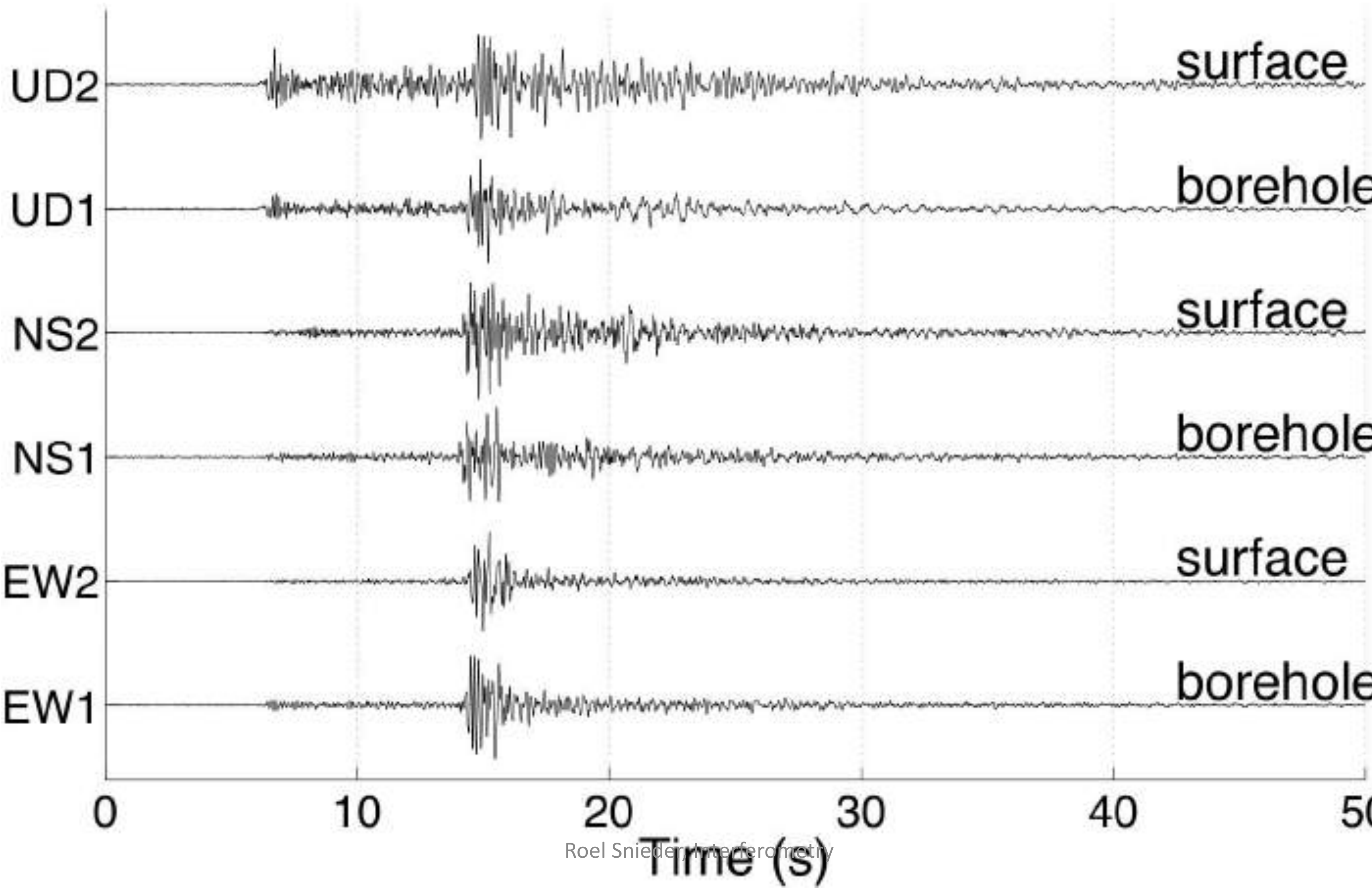

Annual stacks at station NIGH13

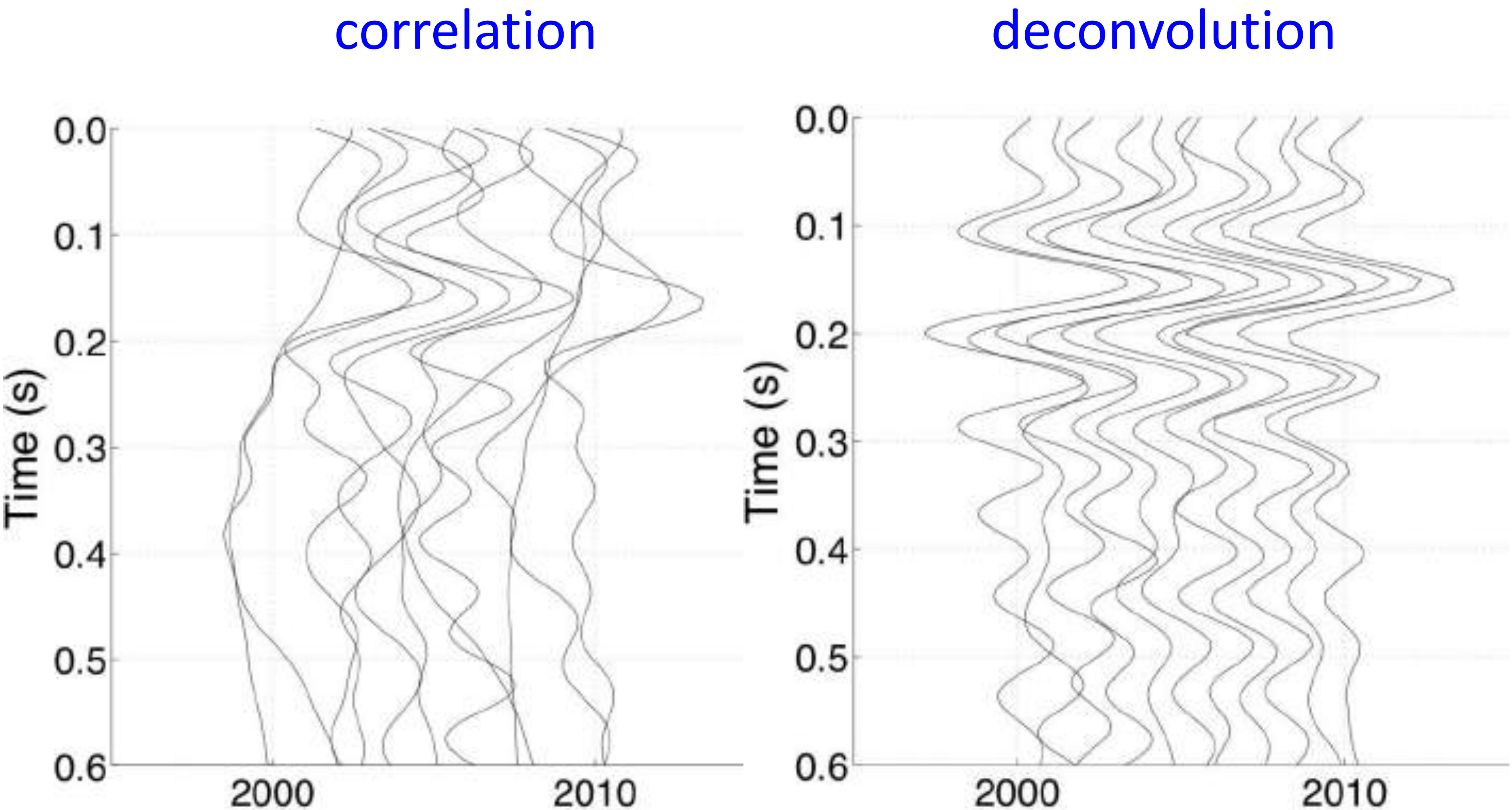

Correlation vs. deconvolution

$$u(z,\omega) = S(\omega)e^{-ikz}$$

$$correlation = u(z=0,\omega)u^{*}(z=D,\omega) = \left|S(\omega)\right|^{2} e^{ikz}$$

$$deconvolution = \frac{u(z=0,\omega)}{u(z=D,\omega)} = e^{ikz}$$

When there is one source

$$u_A = G_{AS} S$$

$$u_B = G_{BS} S$$

$$D = \frac{u_A}{u_B} = \frac{G_{AS} S}{G_{BS} S} = \frac{G_{SA}}{G_{SB}}$$

Independent of source signal

When there are two sources

$$u_A = G_{AS_1} S_1 + G_{AS_2} S_2$$

$$u_B = G_{BS_1} S_1 + G_{BS_2} S_2$$

$$D = \frac{u_A}{u_B} = \frac{G_{AS_1} S_1 + G_{AS_2} S_2}{G_{BS_1} S_1 + G_{BS_2} S_2}$$

Source signal does not divide out

Arrival time of shear wave

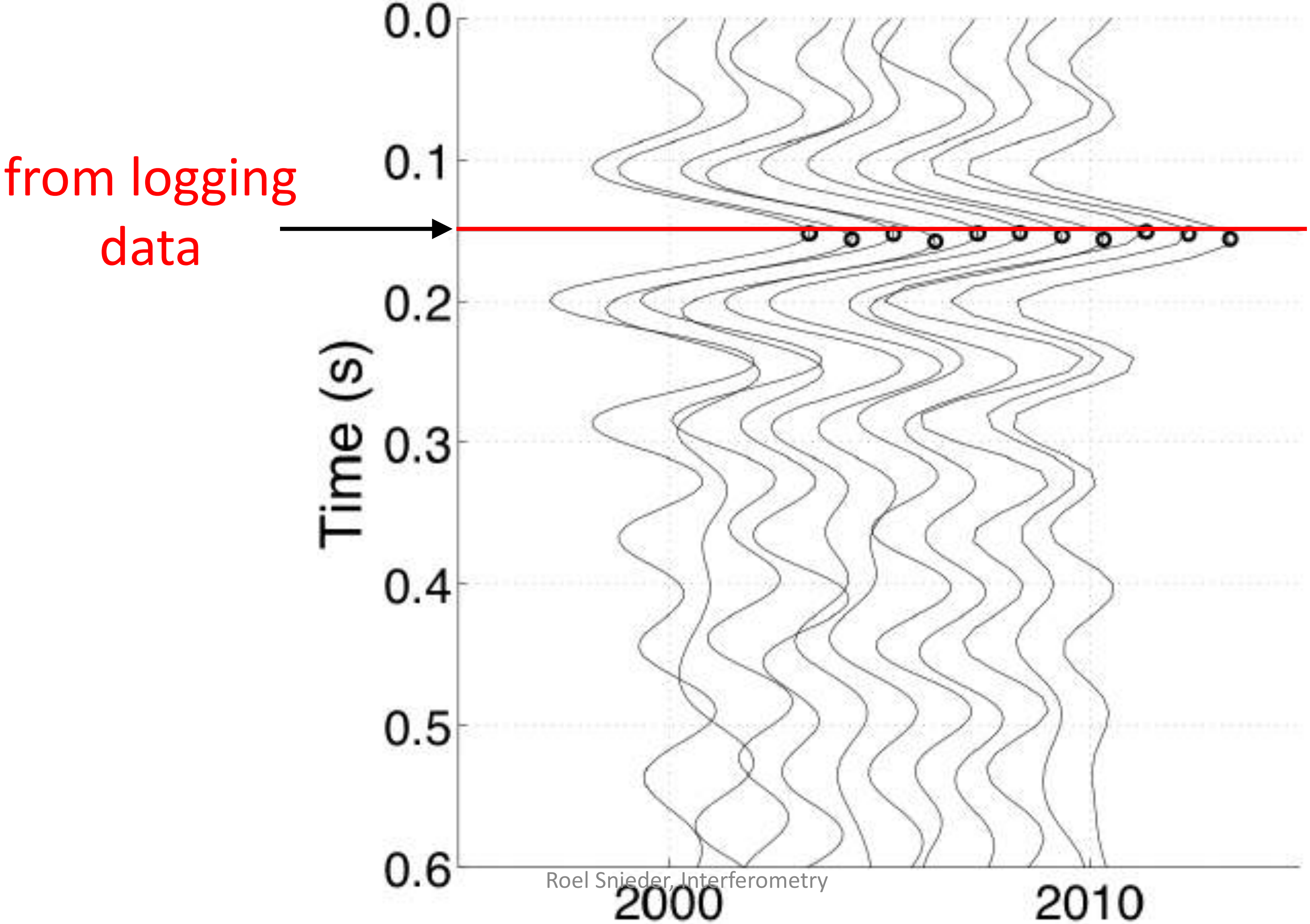

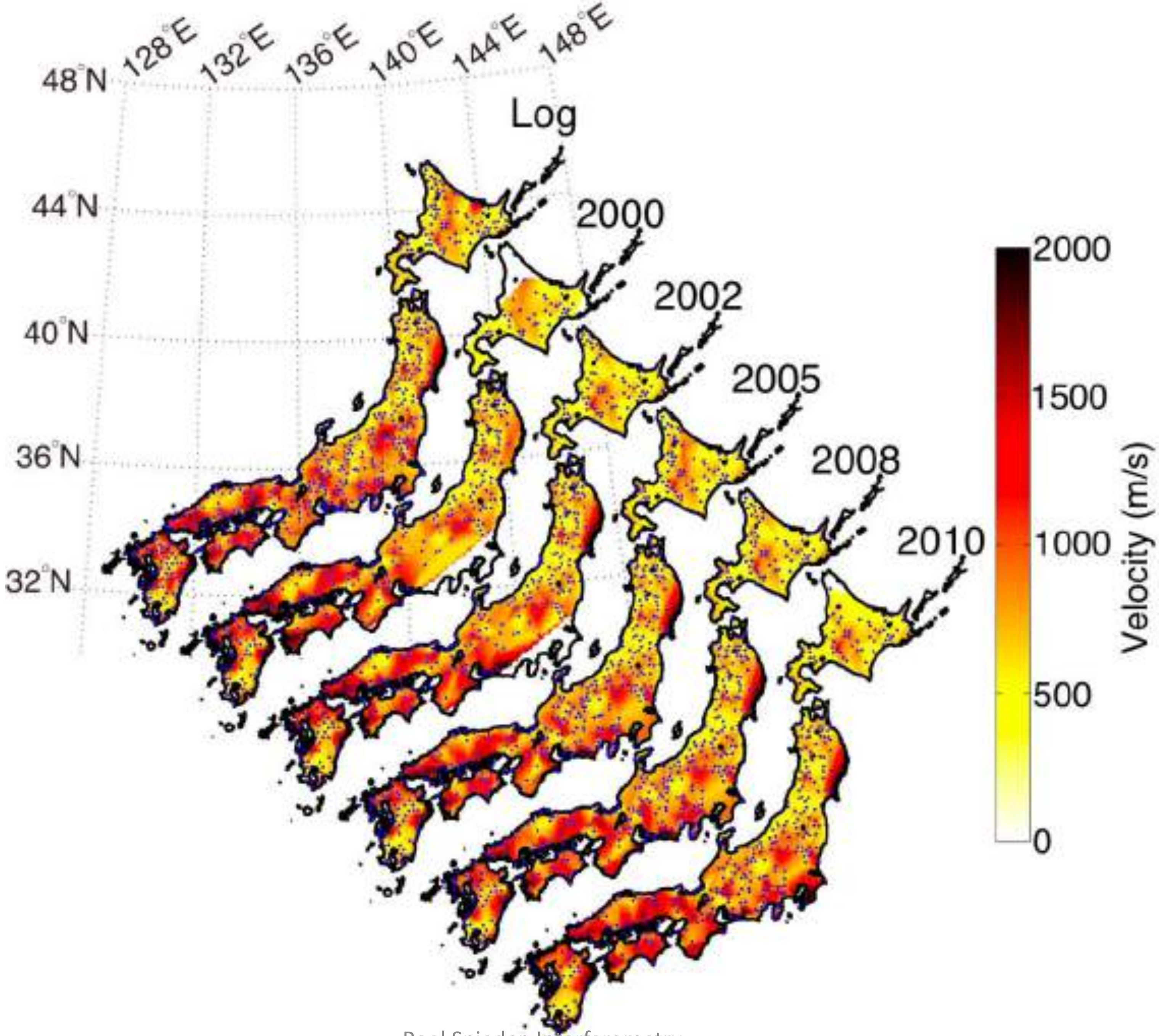

(Nakata and Snieder, JGR, 117, B01308, 2012)

S-waves in Niigata and earthquakes

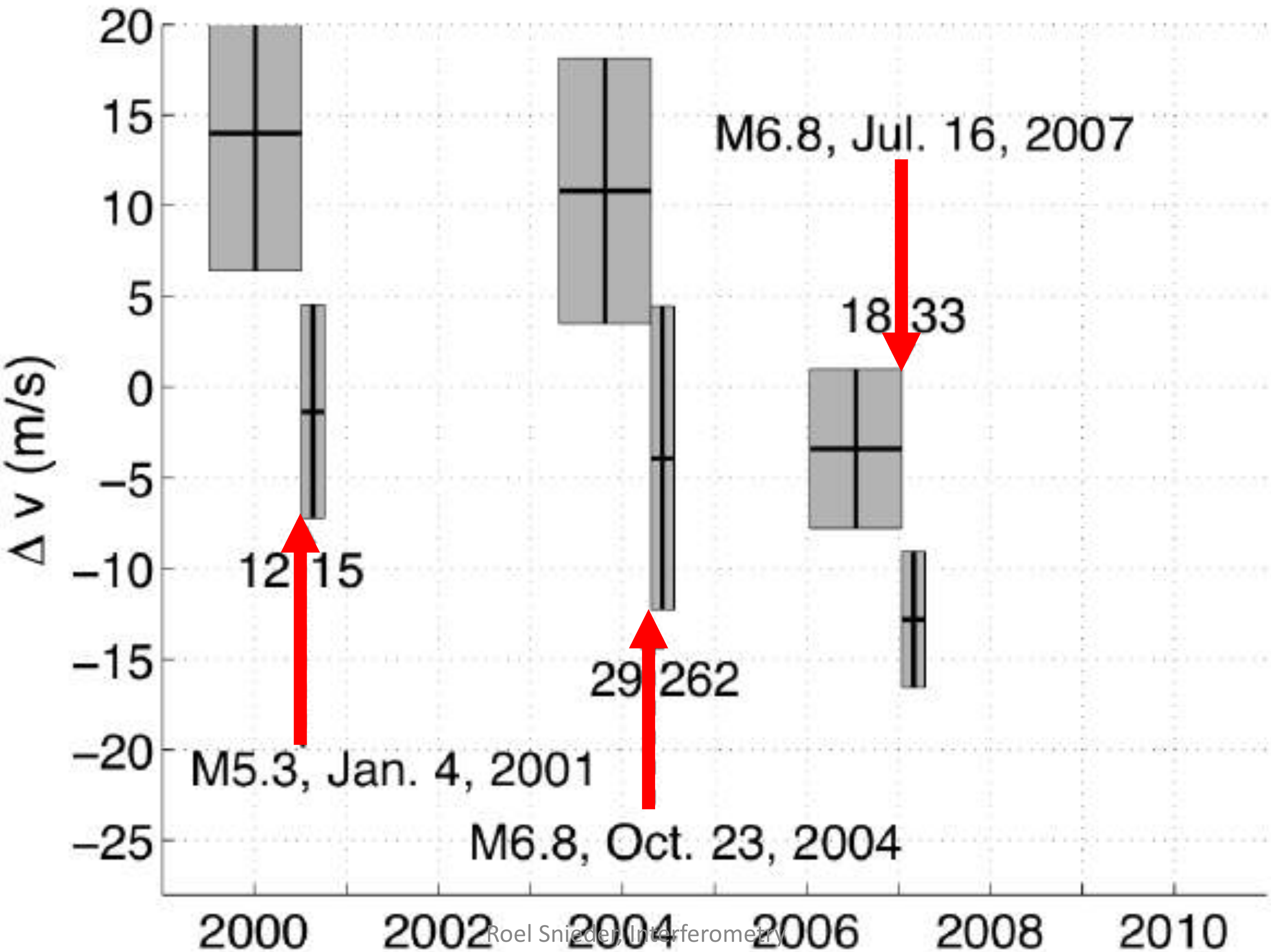

Time-lapse change

Tohoku-Oki earthquake

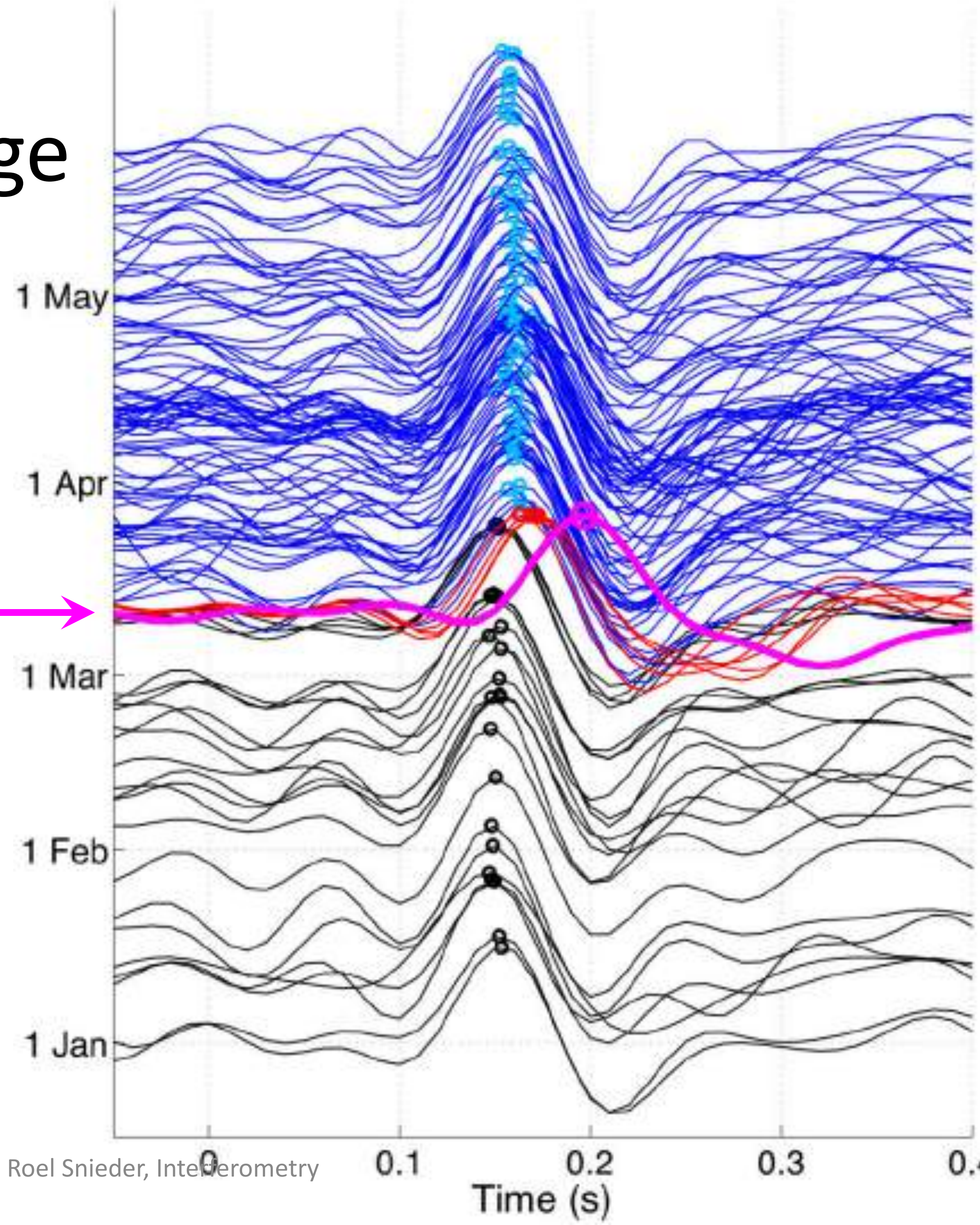

(Nakata and Snieder, Geophys. Res. Lett.,18, L17302, 2011)

Time-lapse change

Tohoku-Oki earthquake

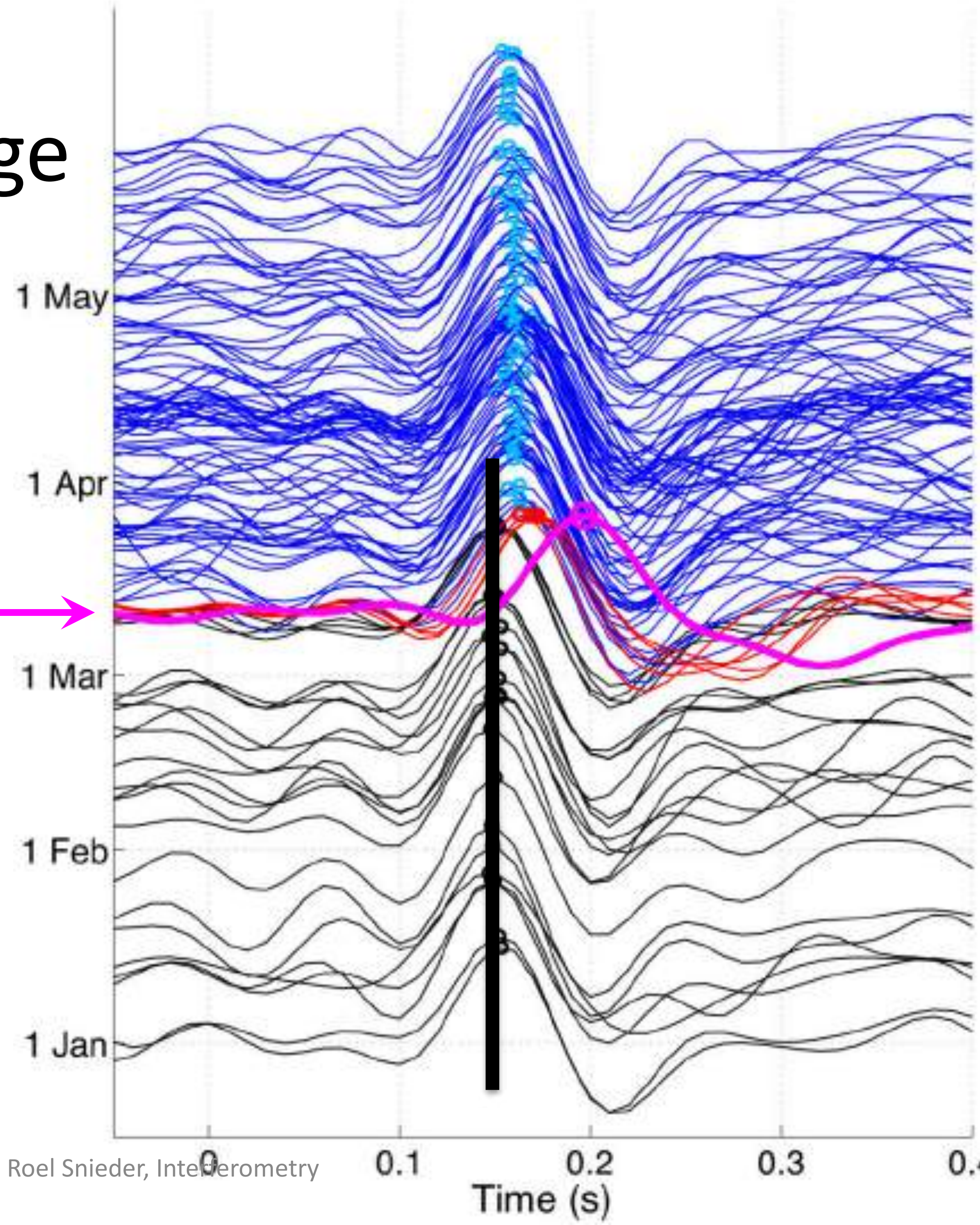

(Nakata and Snieder, Geophys. Res. Lett.,18, L17302, 2011)

Time-lapse change

Tohoku-Oki earthquake

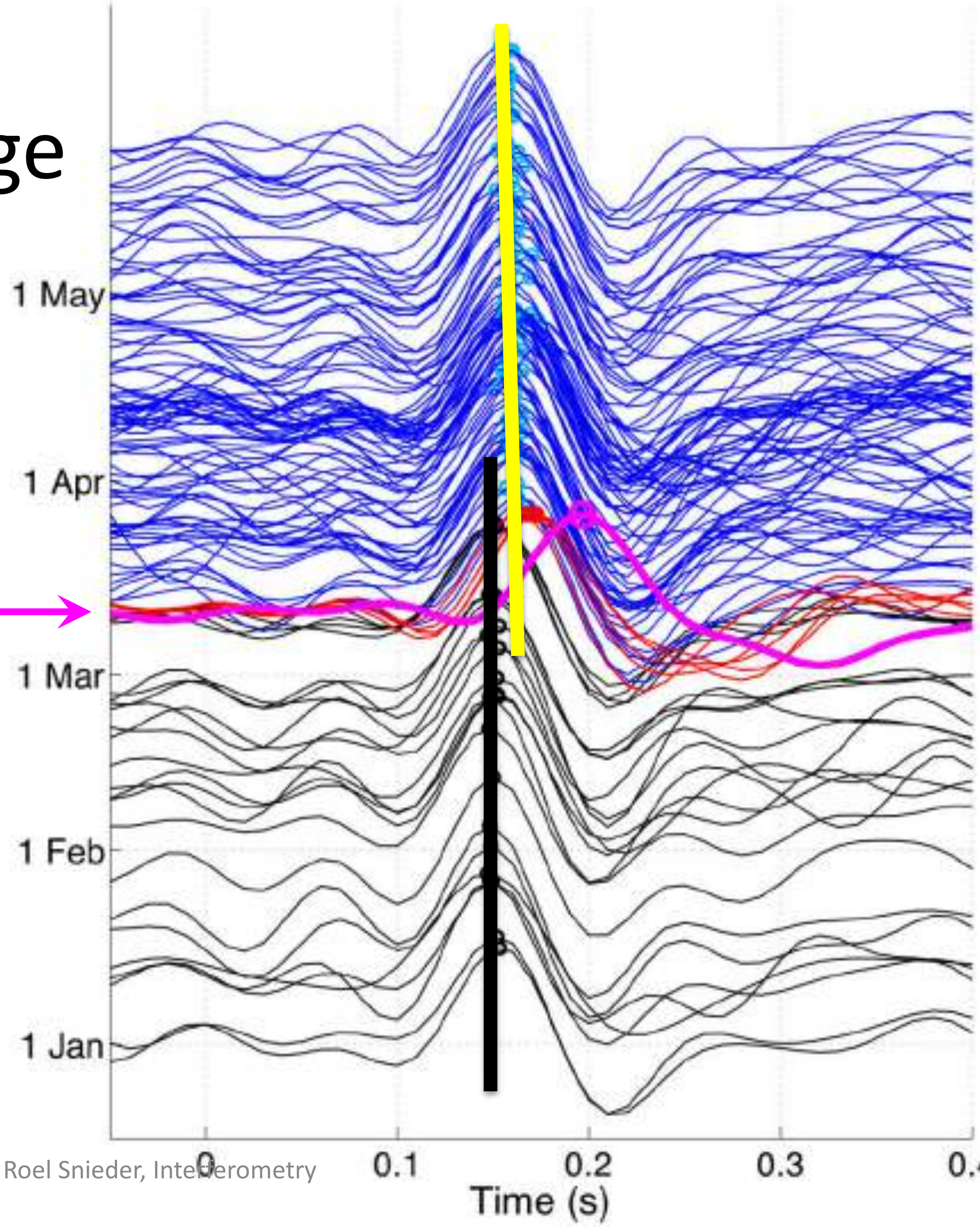

(Nakata and Snieder, Geophys. Res. Lett.,18, L17302, 2011)

Velocity change

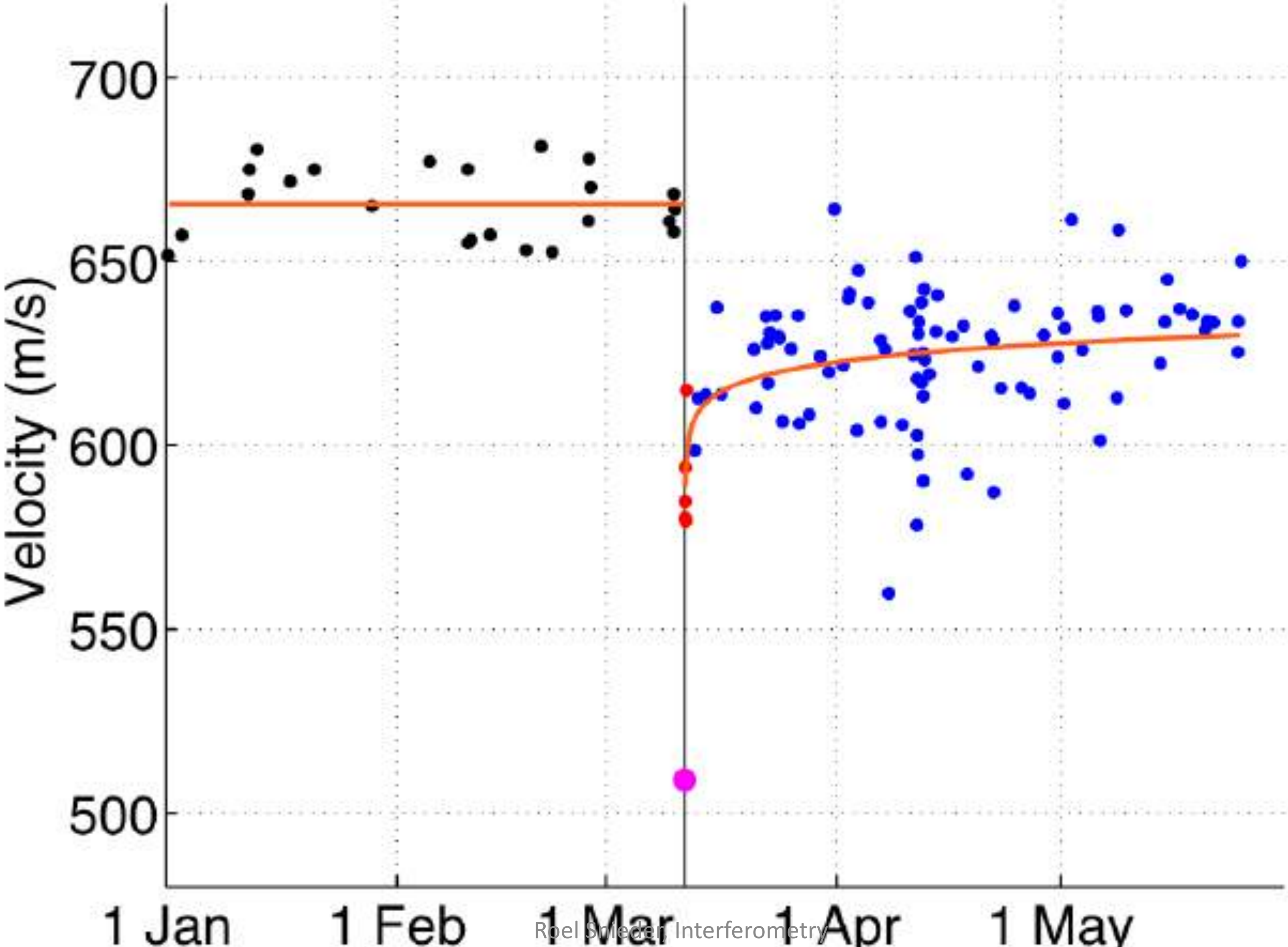

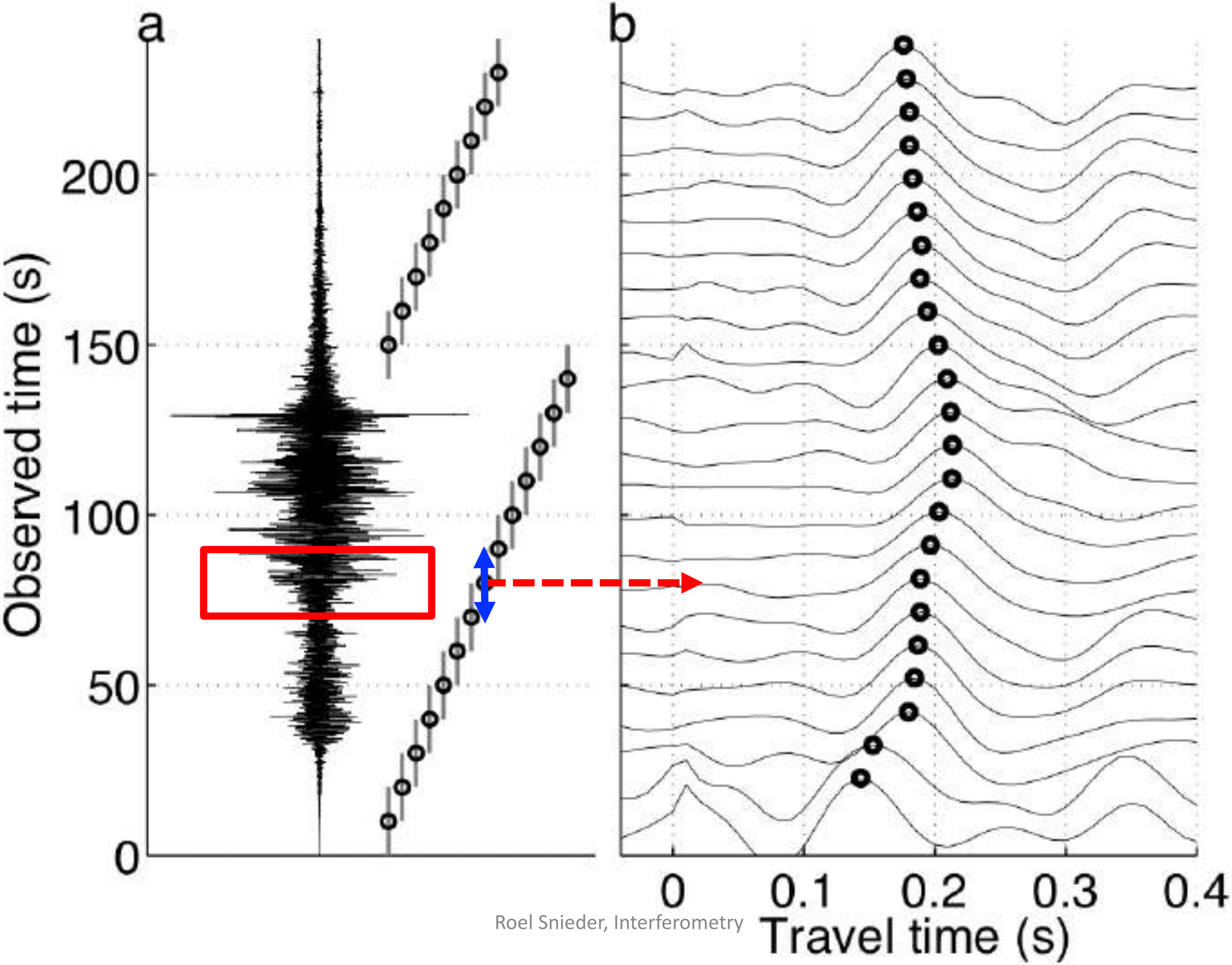
a
b
Observed time (s)
200
150
100
50
0
0
0.1
0.2
0.3
0.4
Travel time (s)

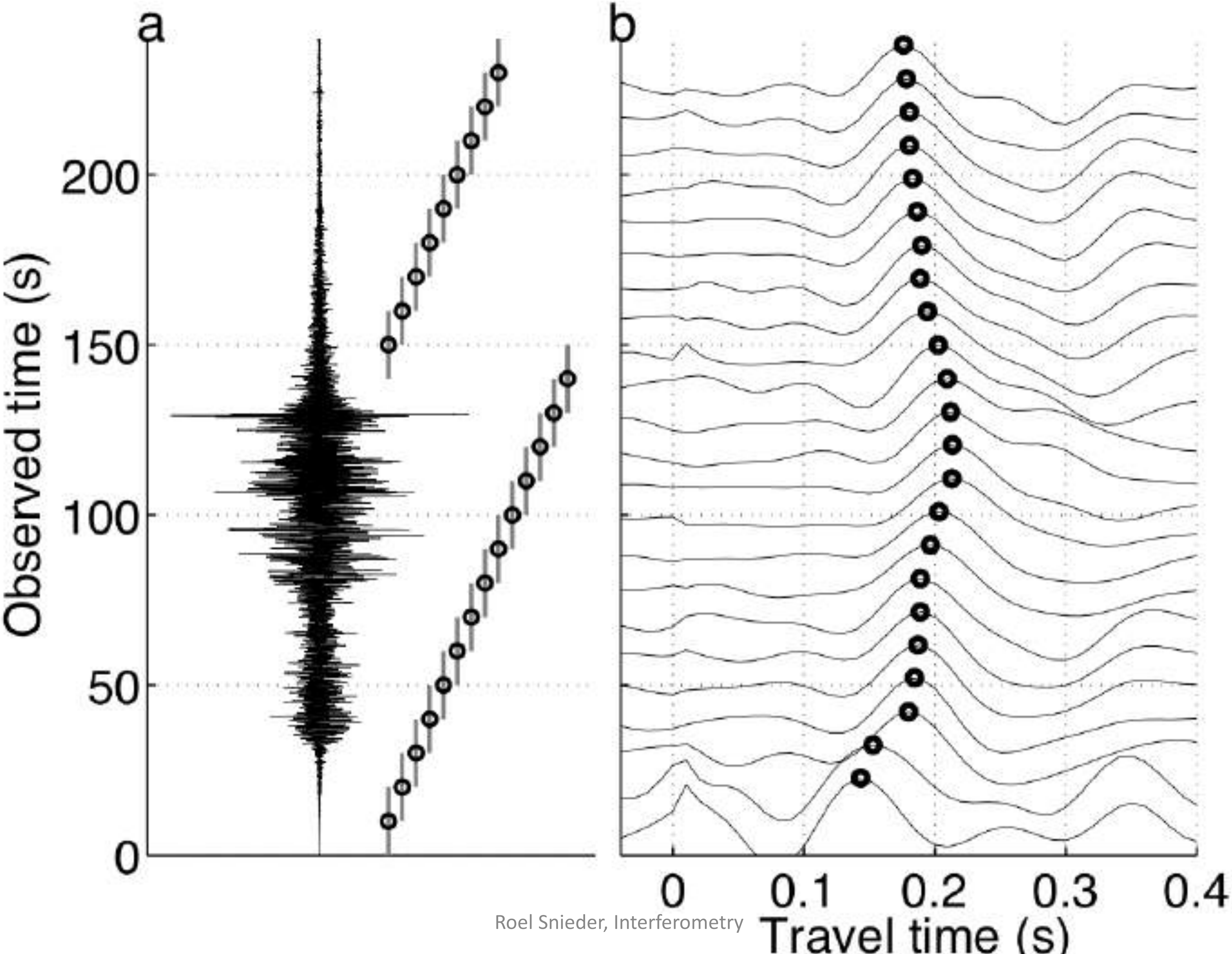
a
b
Observed time (s)
0
50
100
150
200
0
0.1
0.2
0.3
0.4
Travel time (s)

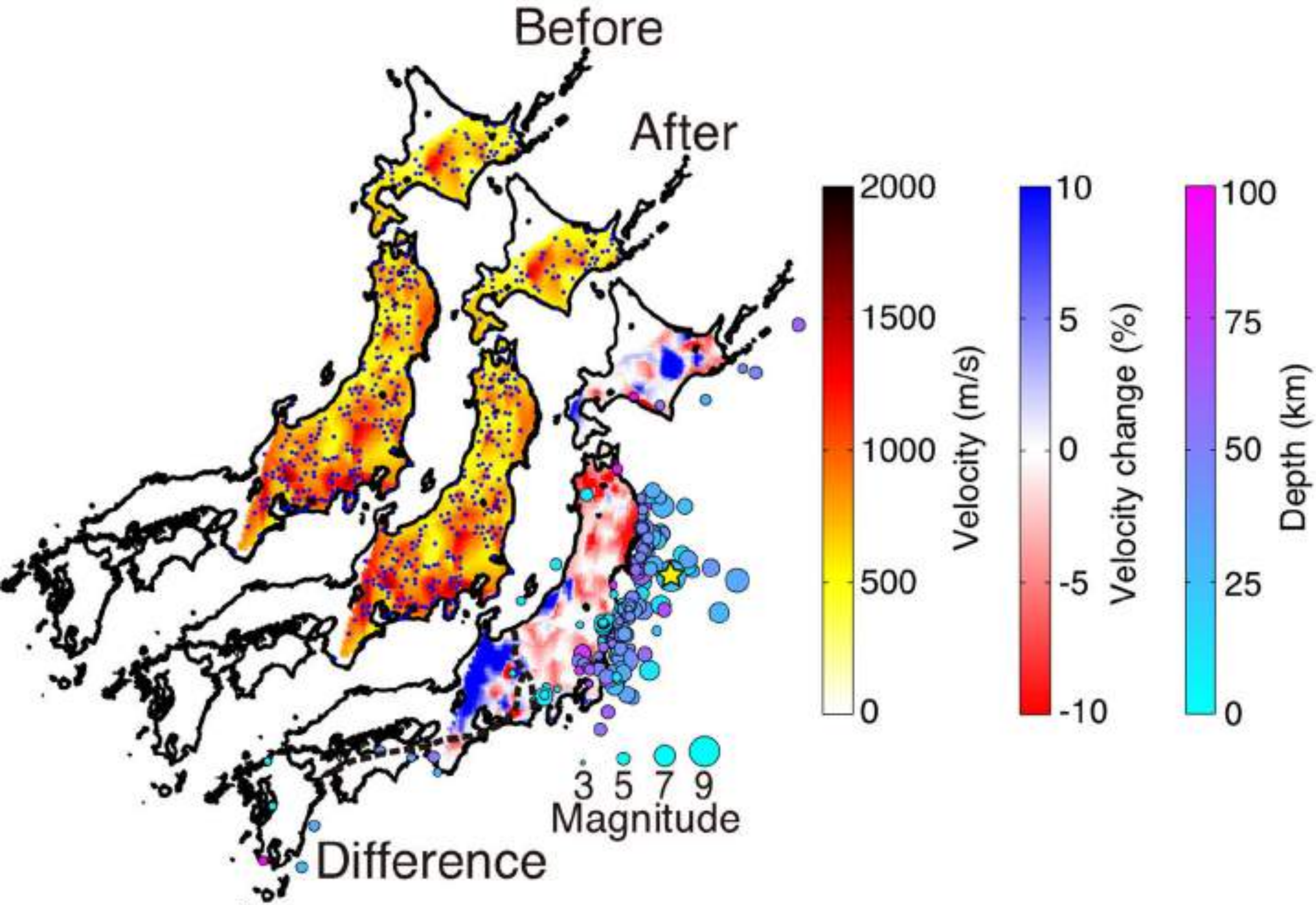

(Nakata and Snieder, Geophys. Res. Lett.,18, L17302, 2011)

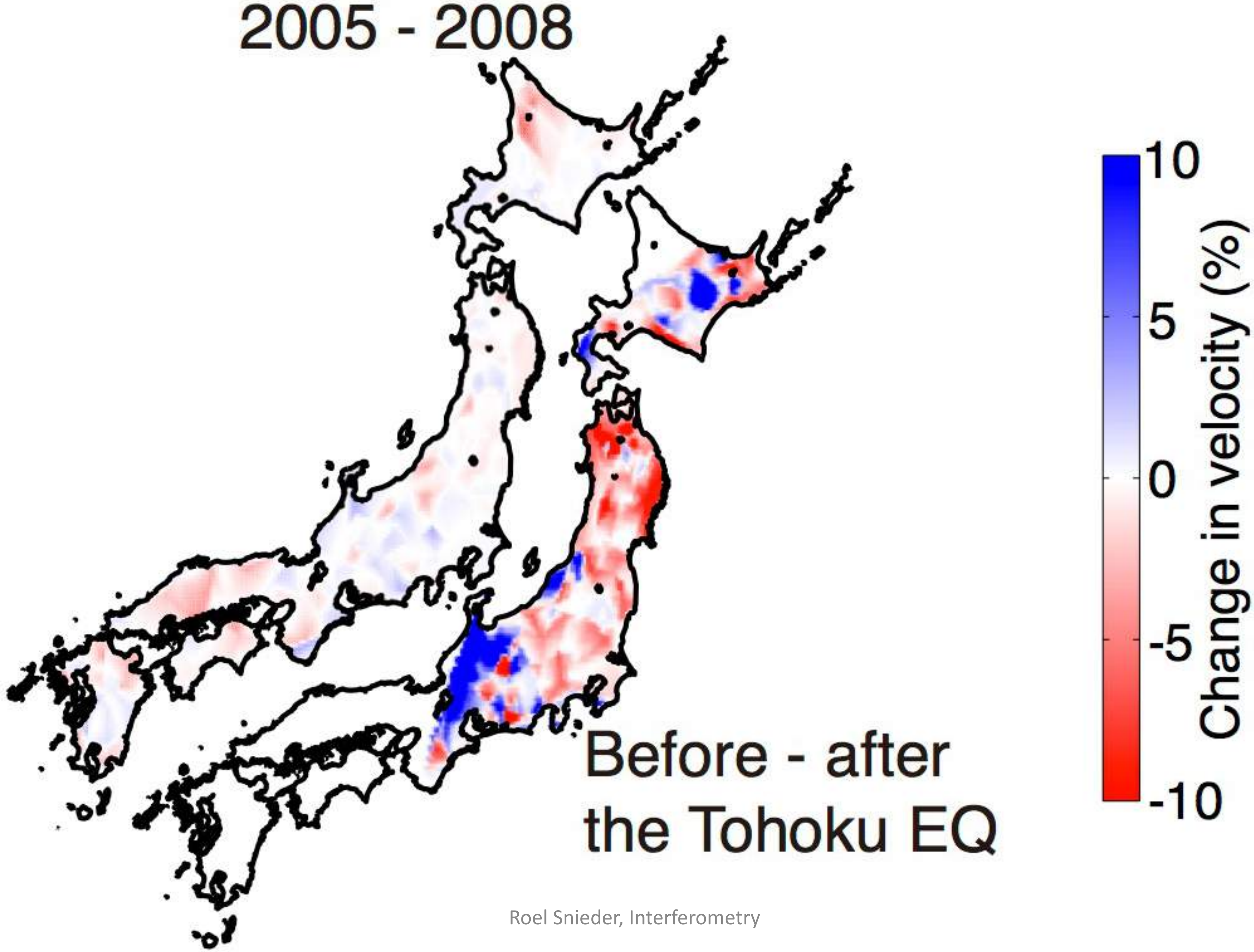
2005 - 2008
Before - after
the Tohoku EQ
Change in velocity (%)
10
5
0
-5
-10

S-velocity changes with seasons

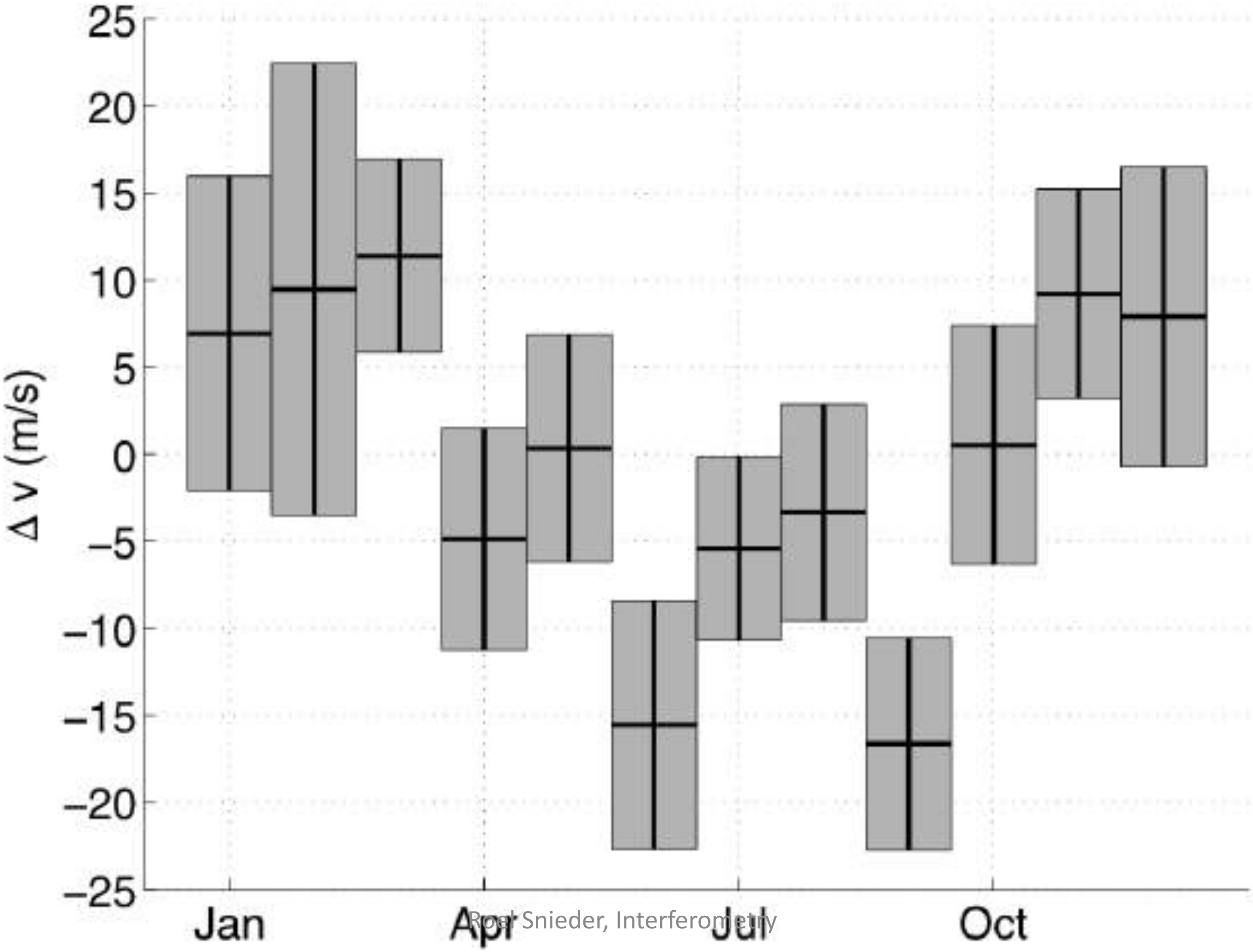

Rainfall/v_s for soft-rock sites

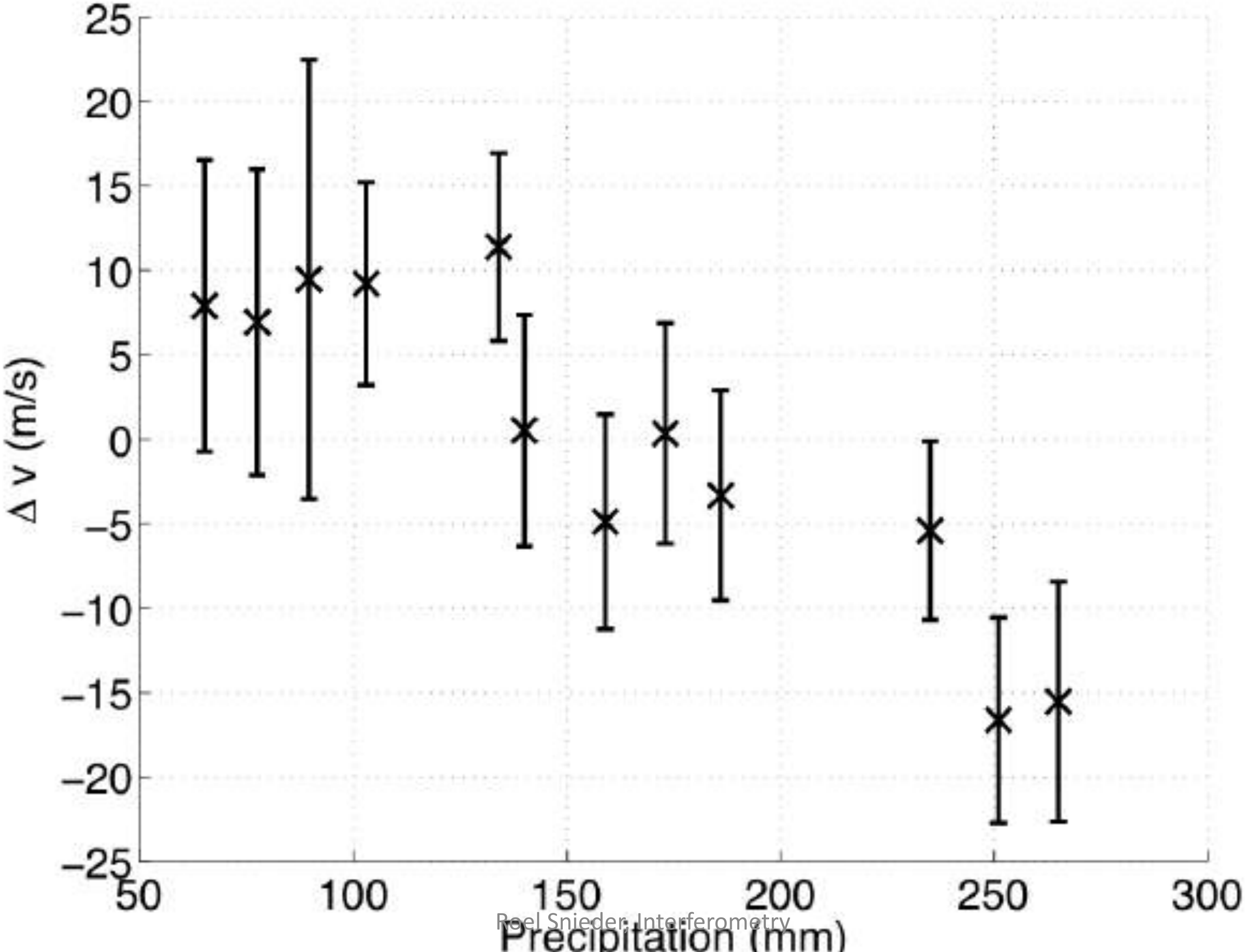

Rainfall/v_s for hard-rock sites

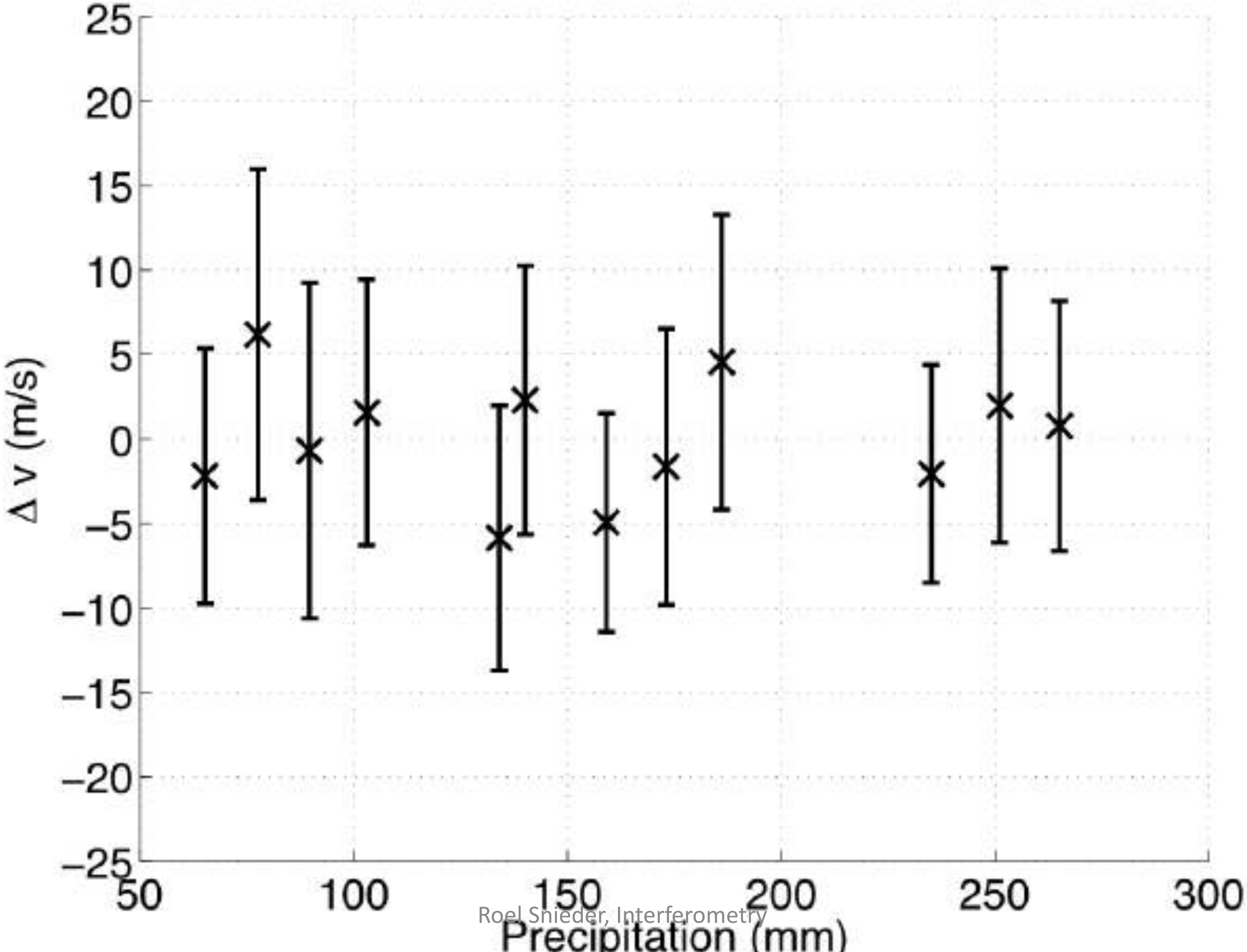

Seismic interferometry in Millikan Library

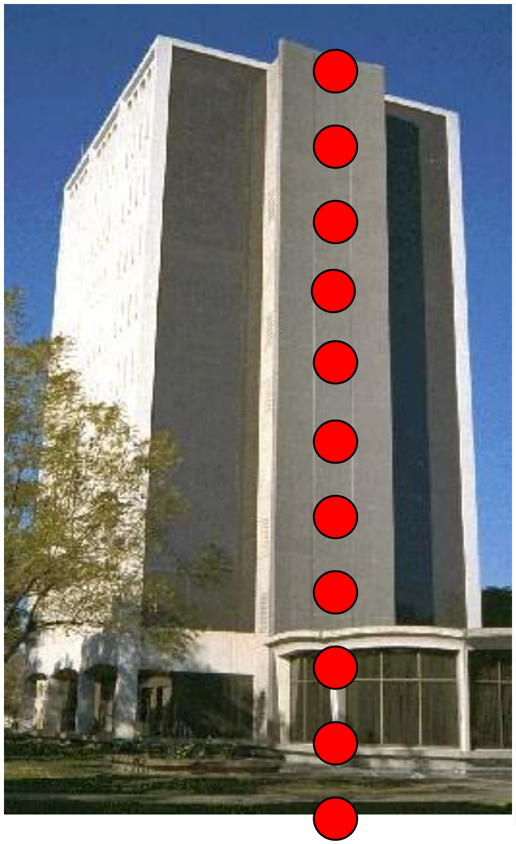

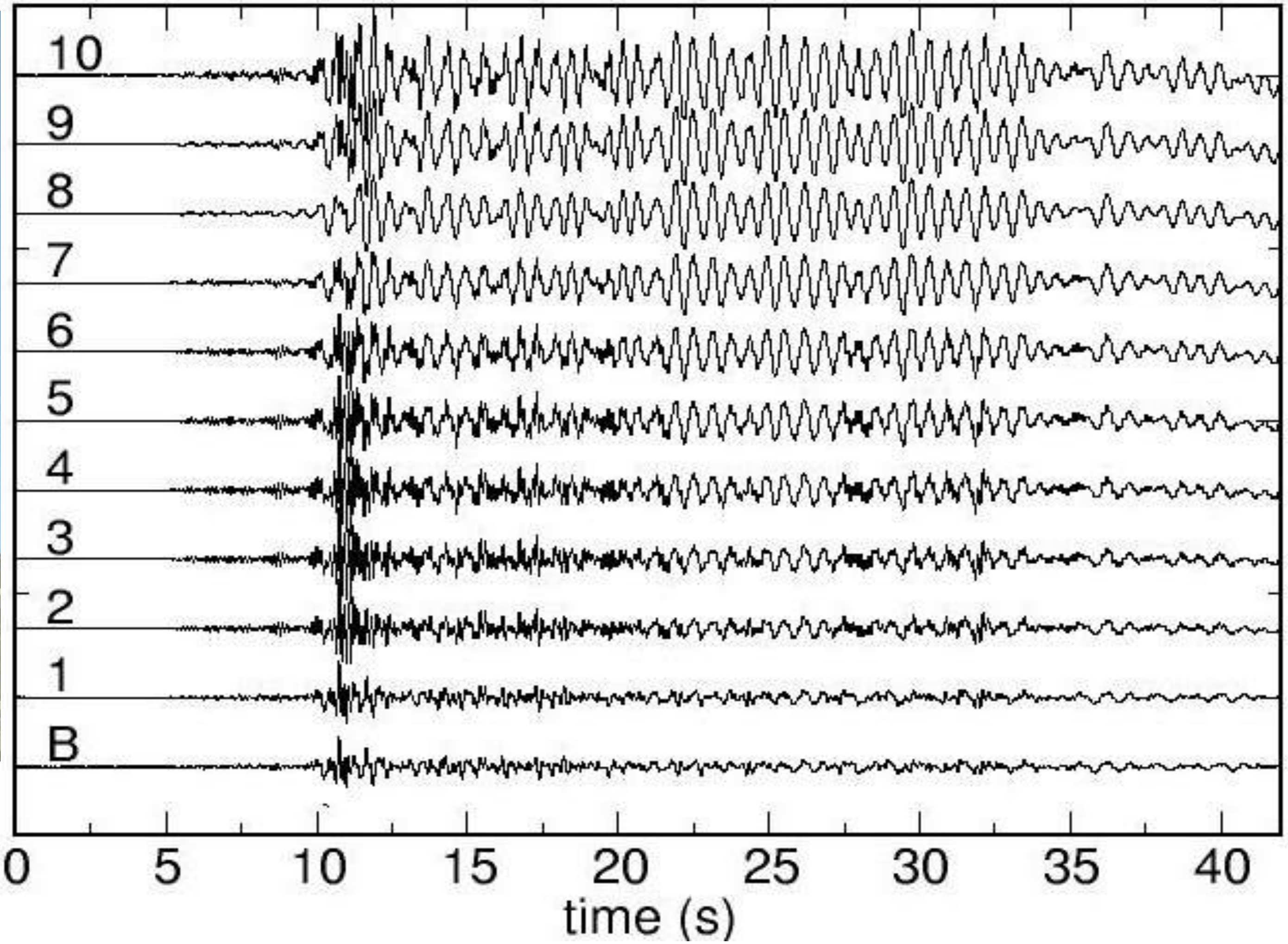

(Snieder and Safak, Bull. Seismol. Soc. Am., **96**, 586-598, 2006)

Deconvolution with top floor

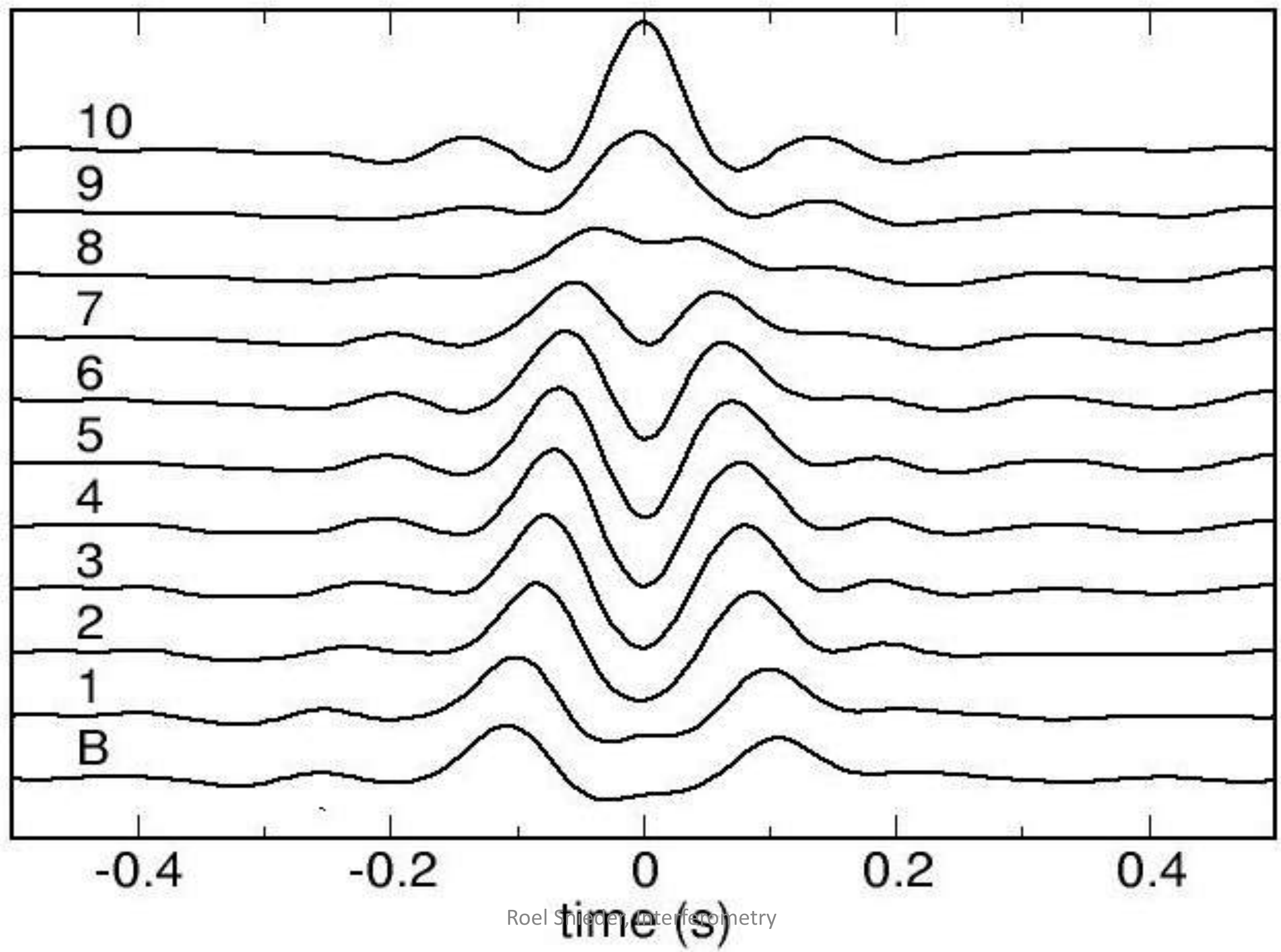

Deconvolution with bottom floor

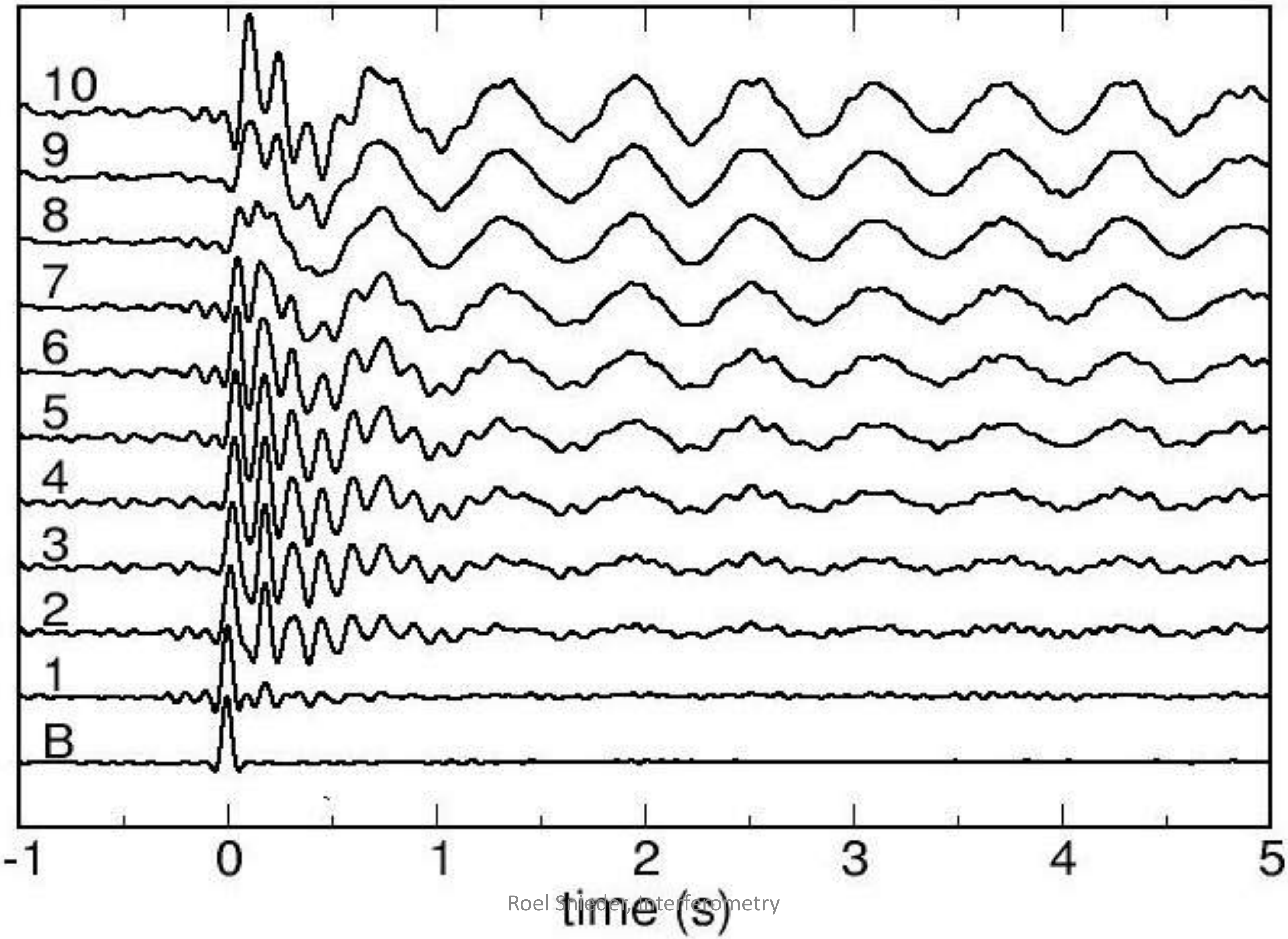

Deconvolution with bottom floor

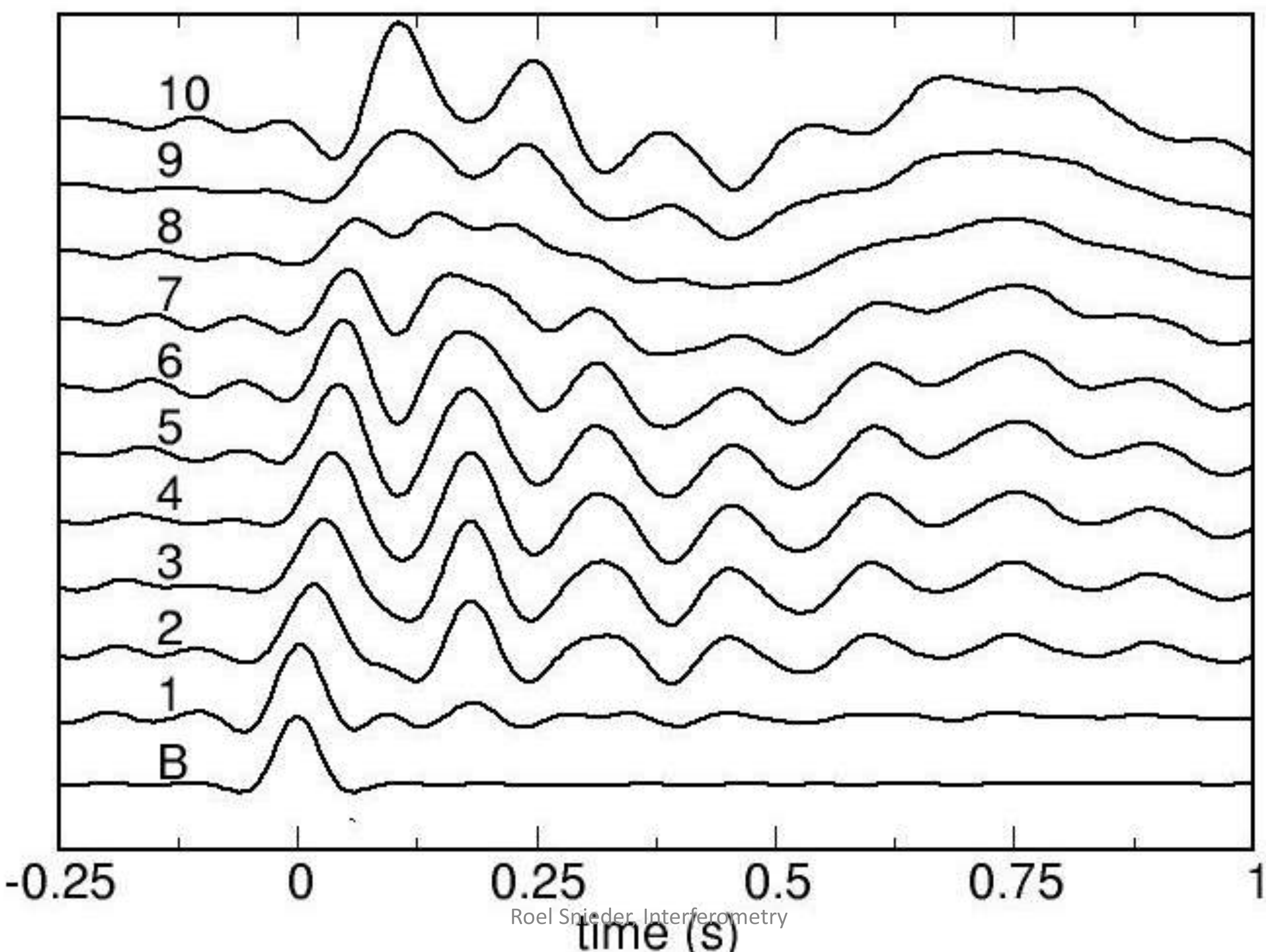

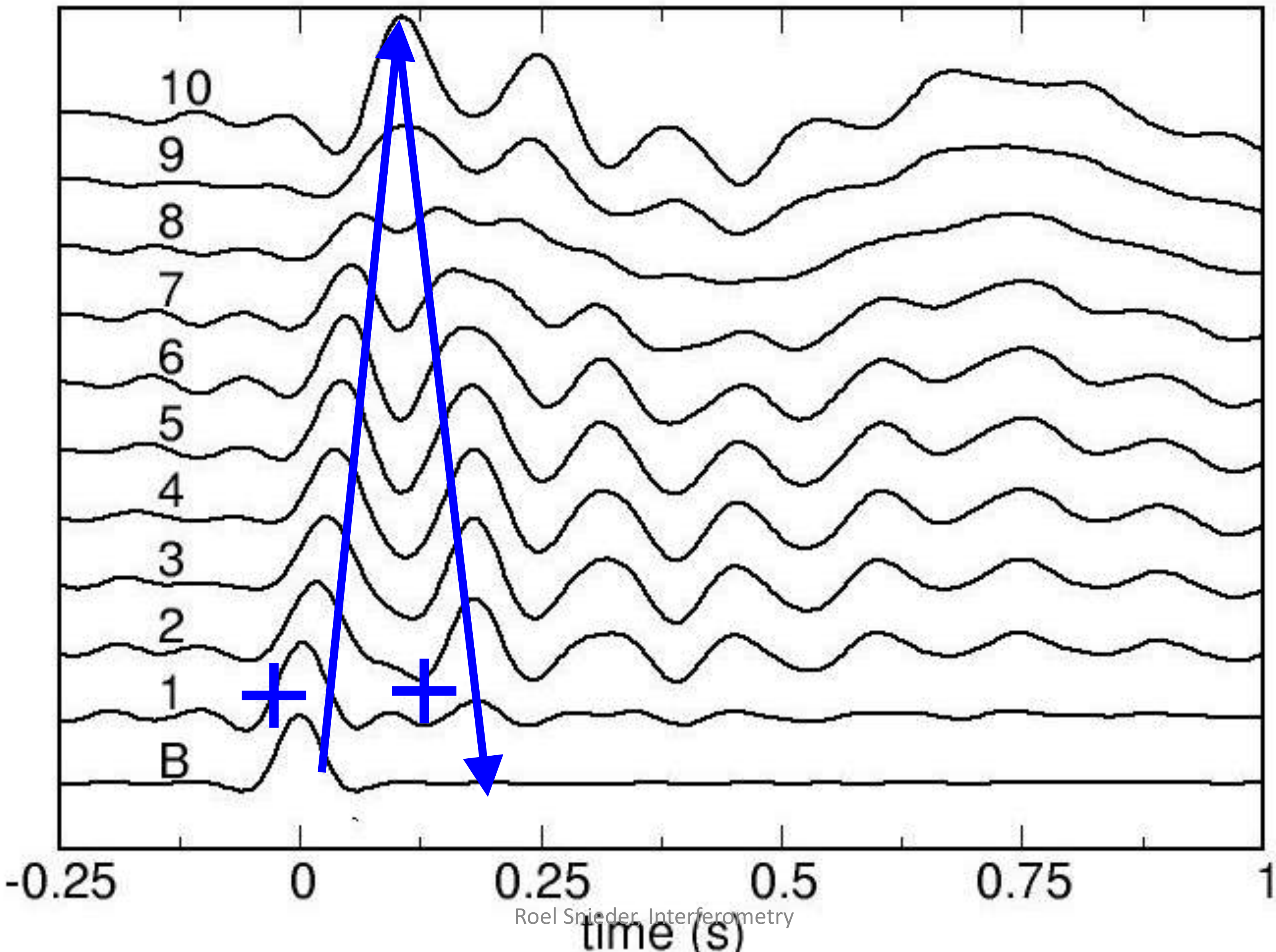
10
9
8
7
6
5
4
3
2
1
B
-0.25
0
0.25
0.5
0.75
1
time (s)

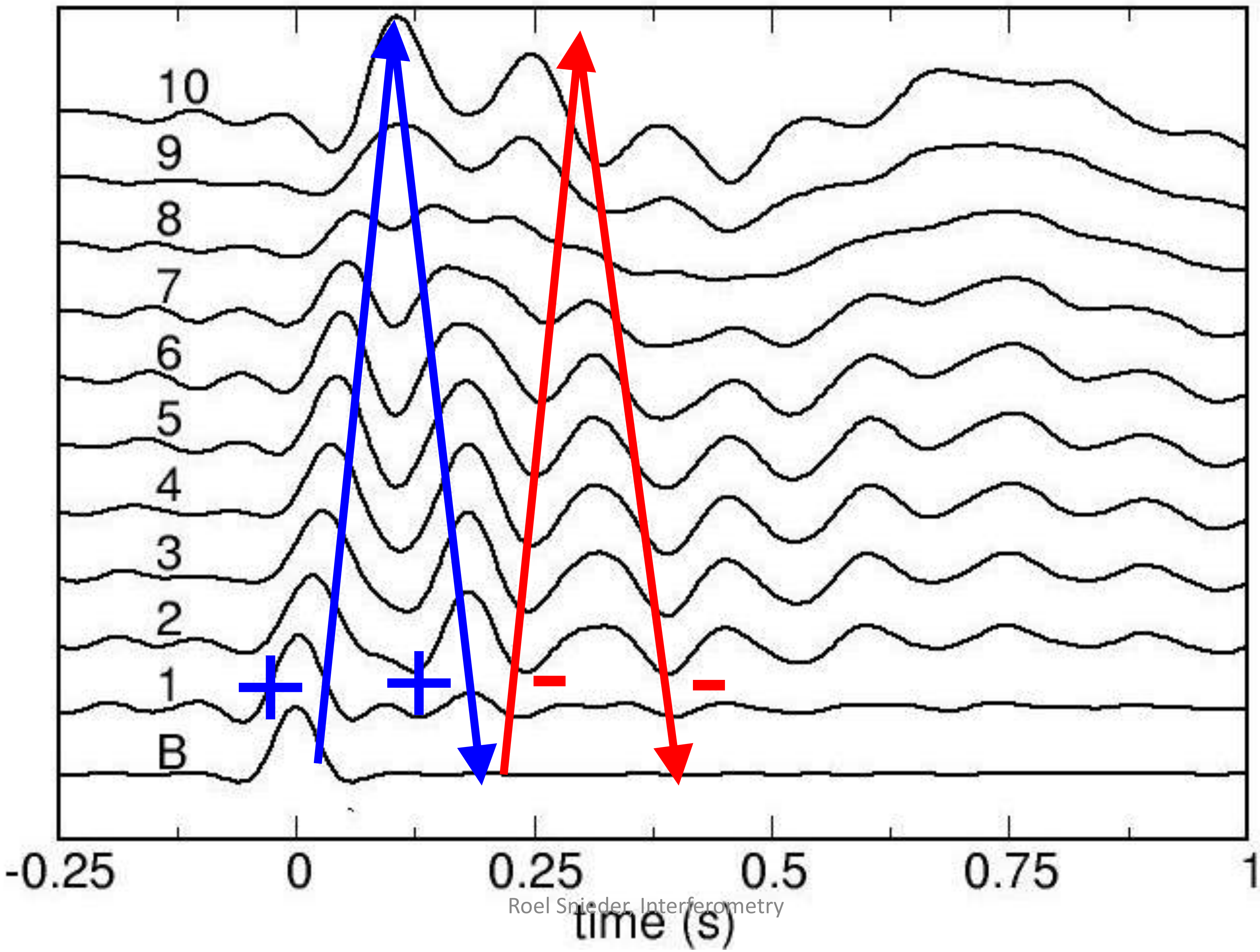

10
9
8
7
6
5
4
3
2
1
B
+
+
-
-
-0.25
0
0.25
0.5
0.75
1
time (s)

Fundamental mode: $T = 4H/c$

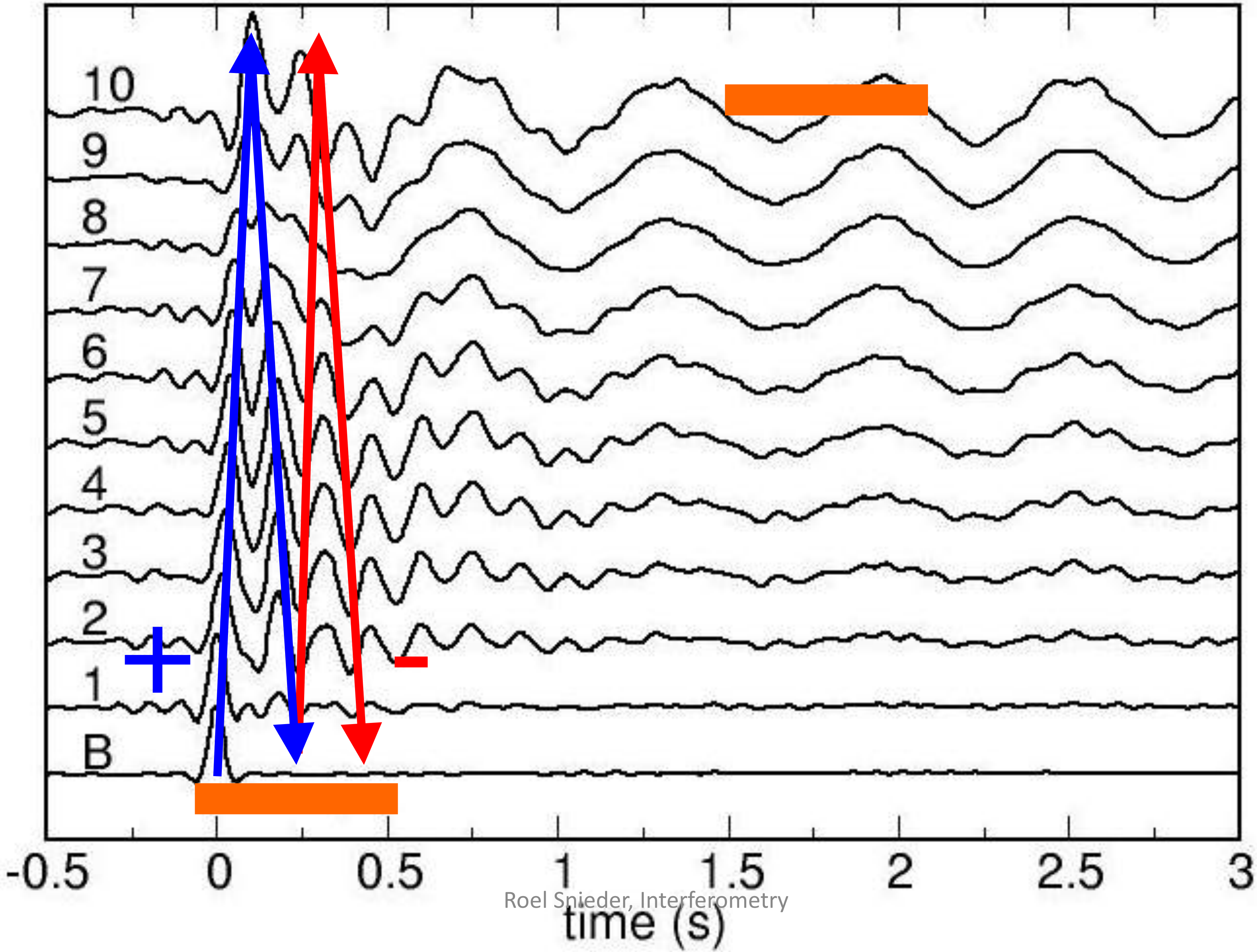

traveling waves

normal modes

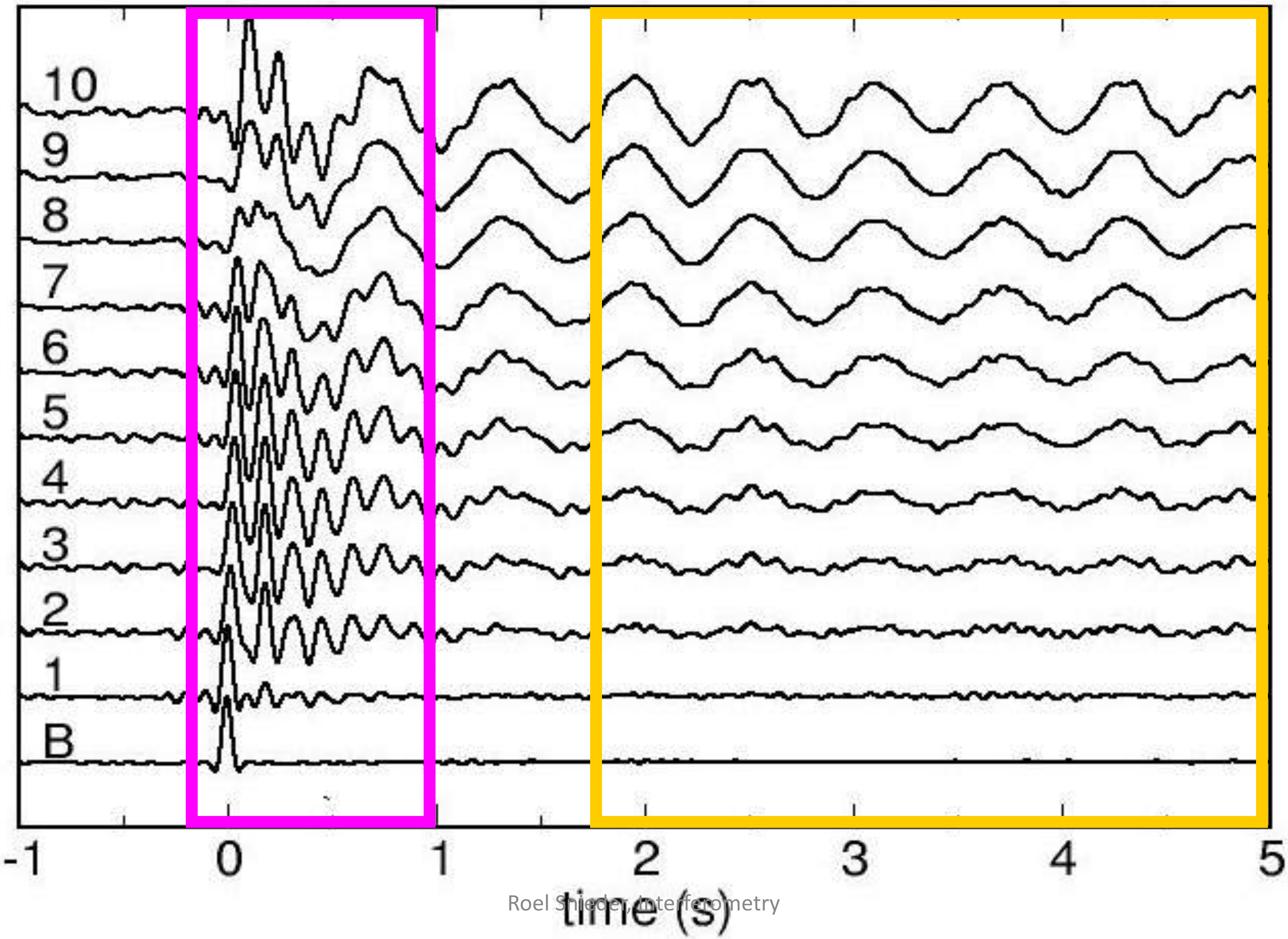

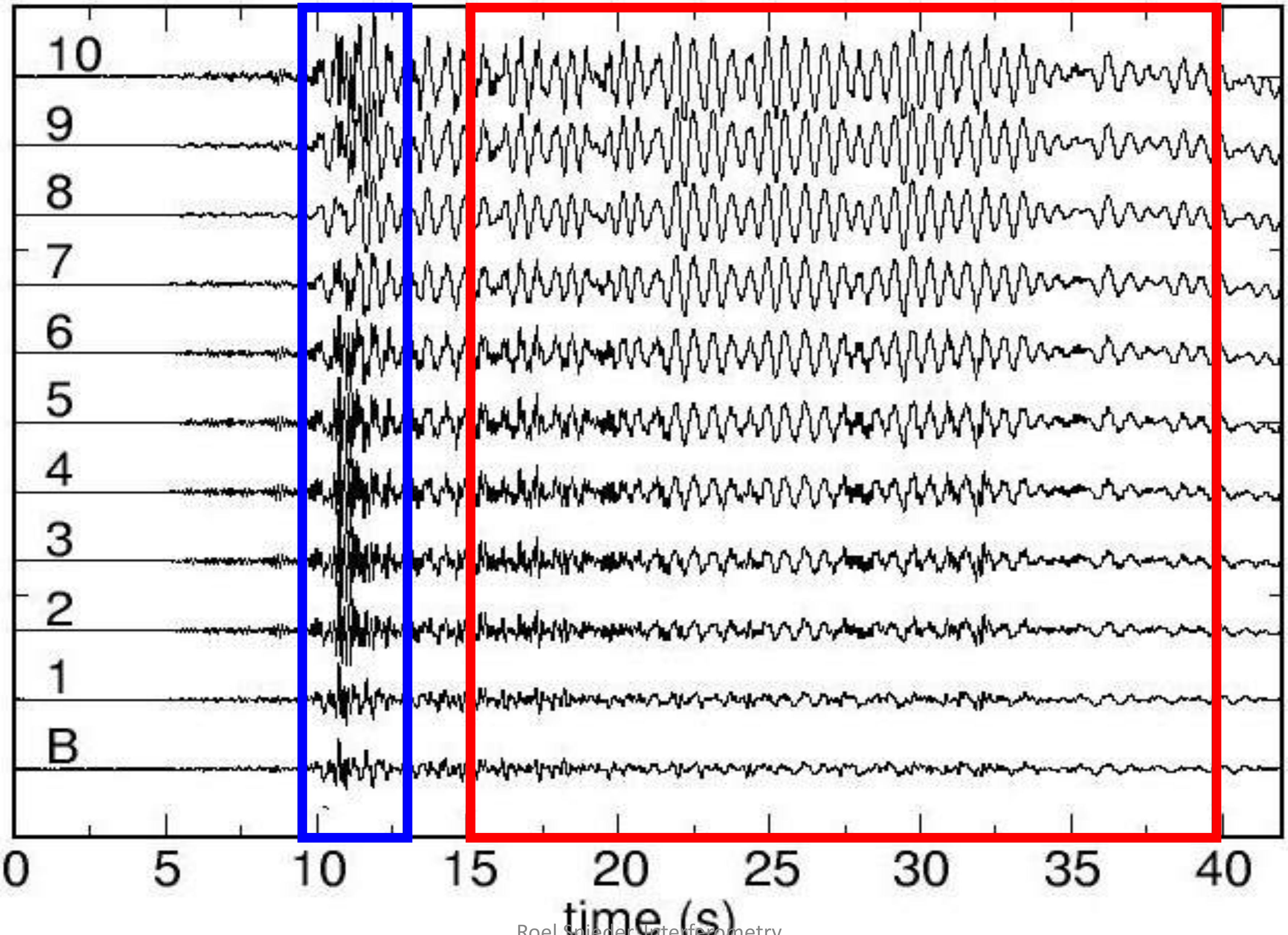
10
9
8
7
6
5
4
3
2
1
B
0
5
10
15
20
25
30
35
40
time (s)

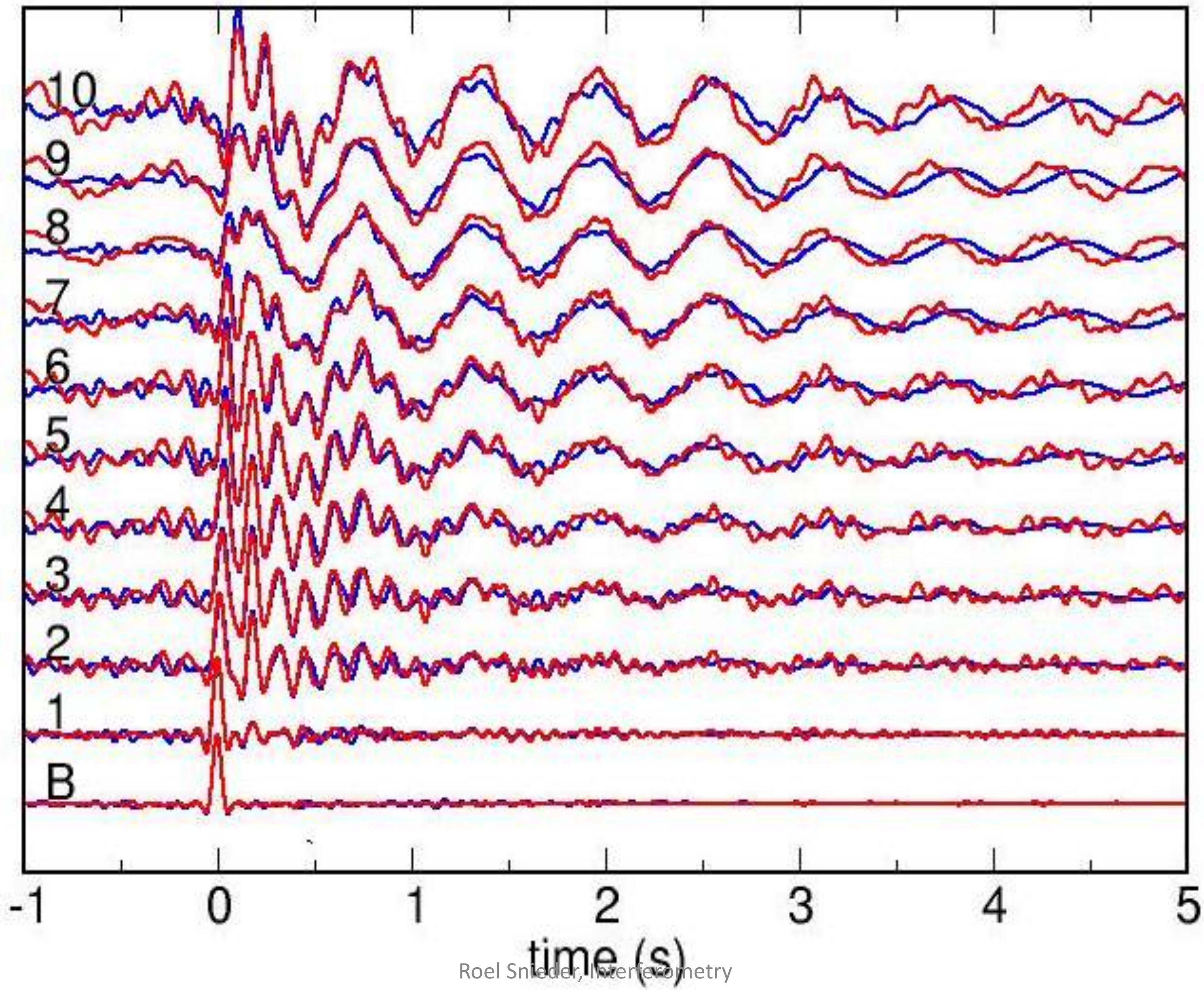
10
9
8
7
6
5
4
3
2
1
B
-1
0
1
2
3
4
5
time (s)

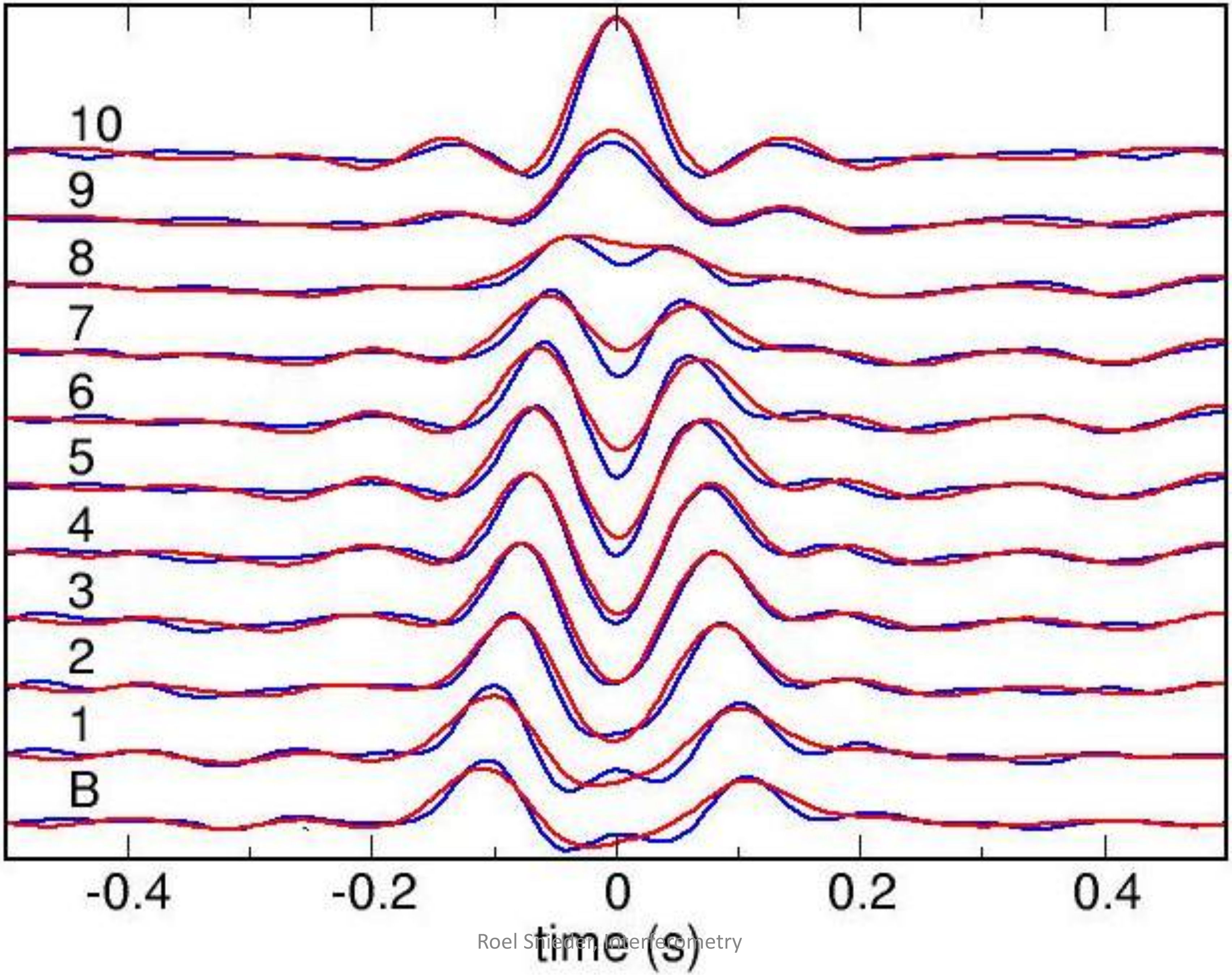
10
9
8
7
6
5
4
3
2
1
B
-0.4
-0.2
0
0.2
0.4
time (s)

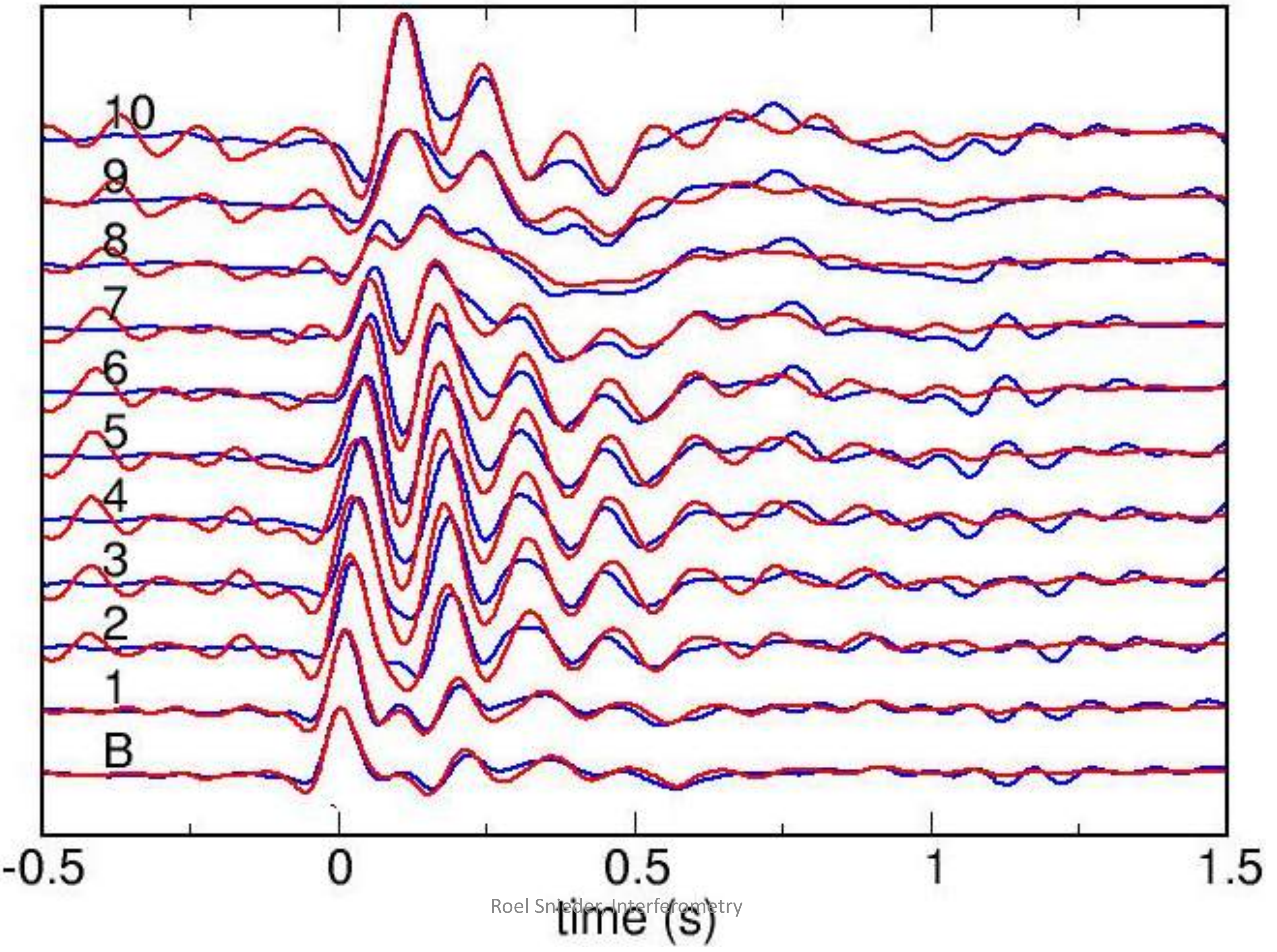
10
9
8
7
6
5
4
3
2
1
B
-0.5
0
0.5
1
1.5
time (s)

Location of building and earthquakes

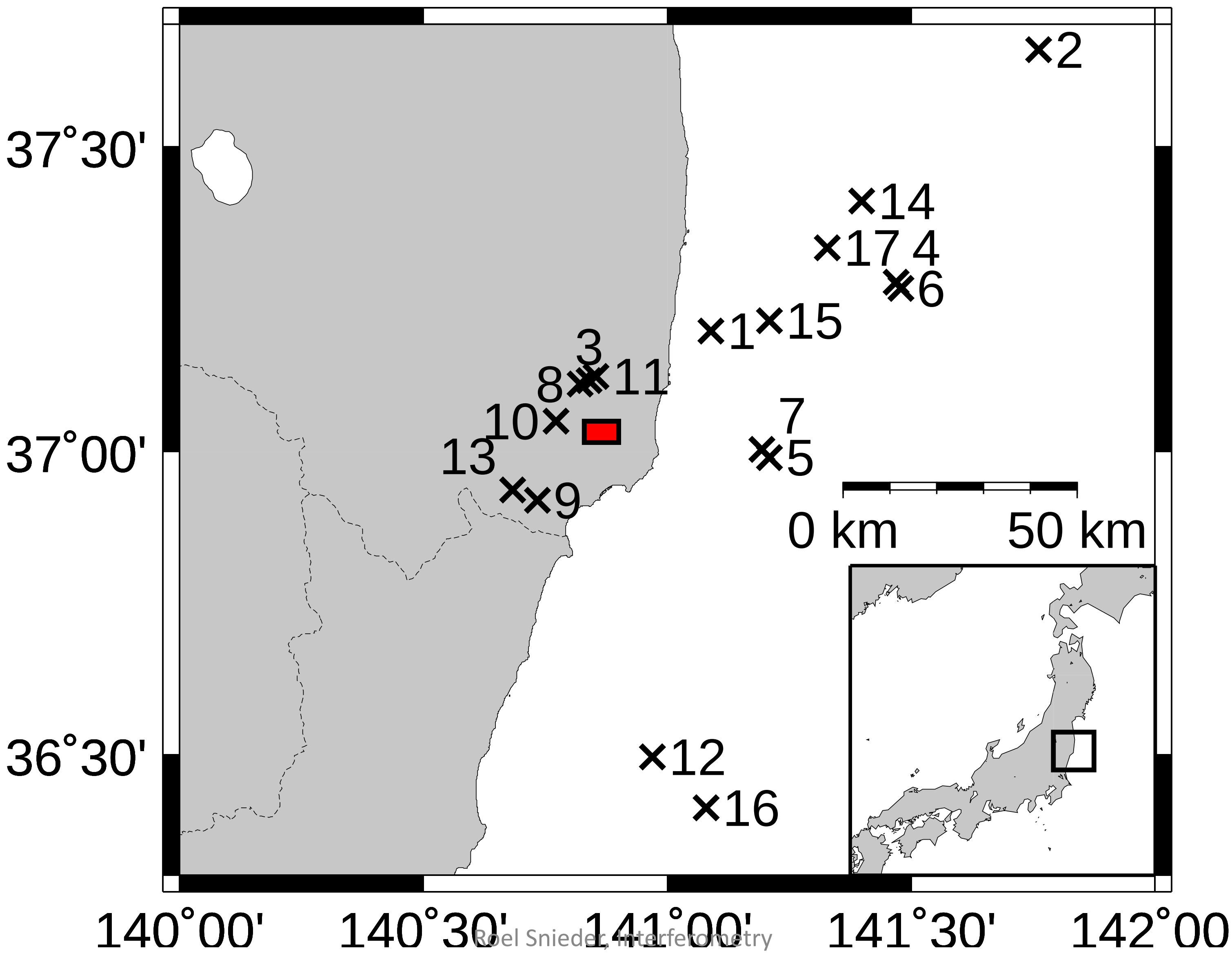

Building and accelerometers

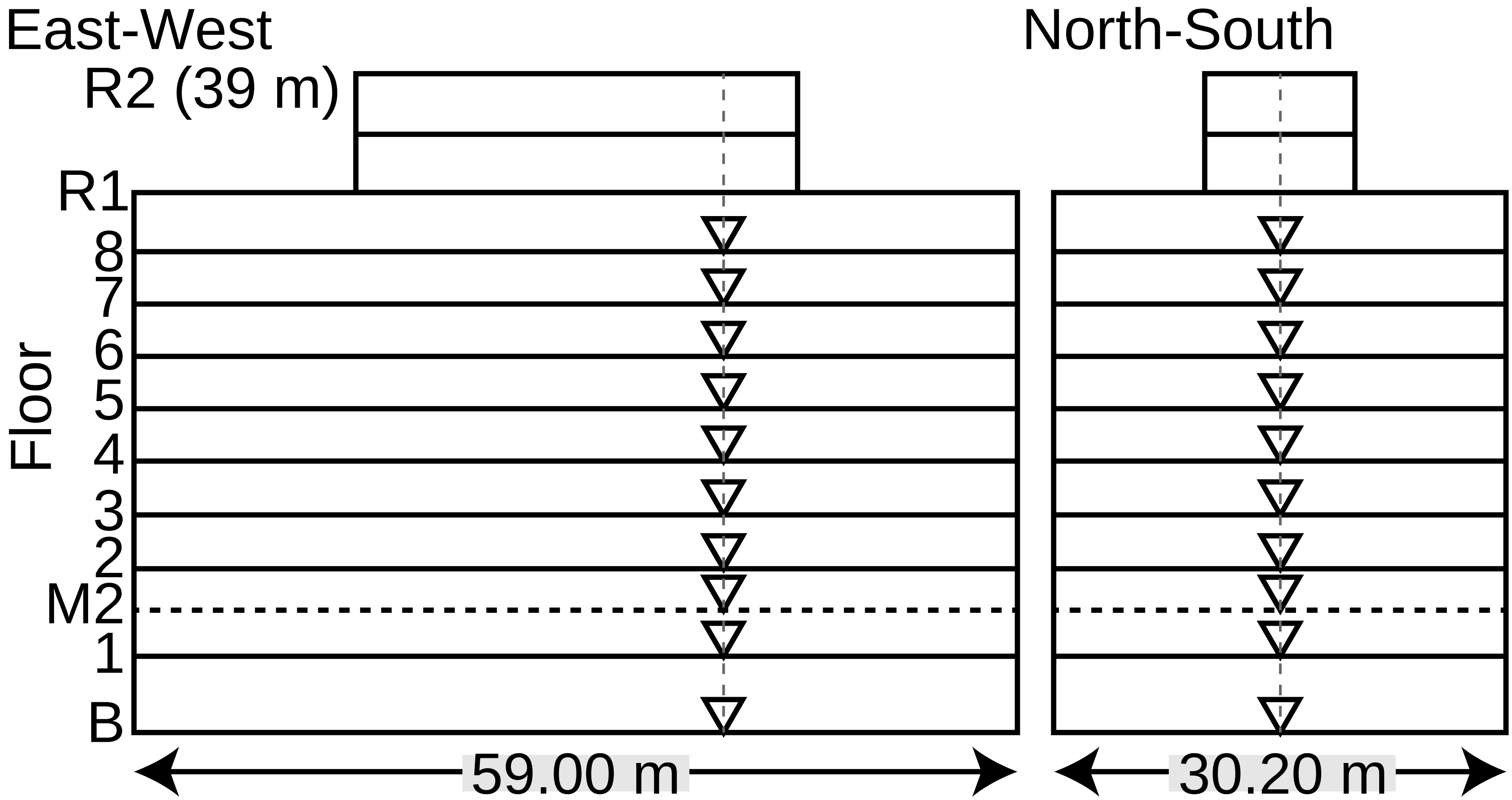

Recorded motion

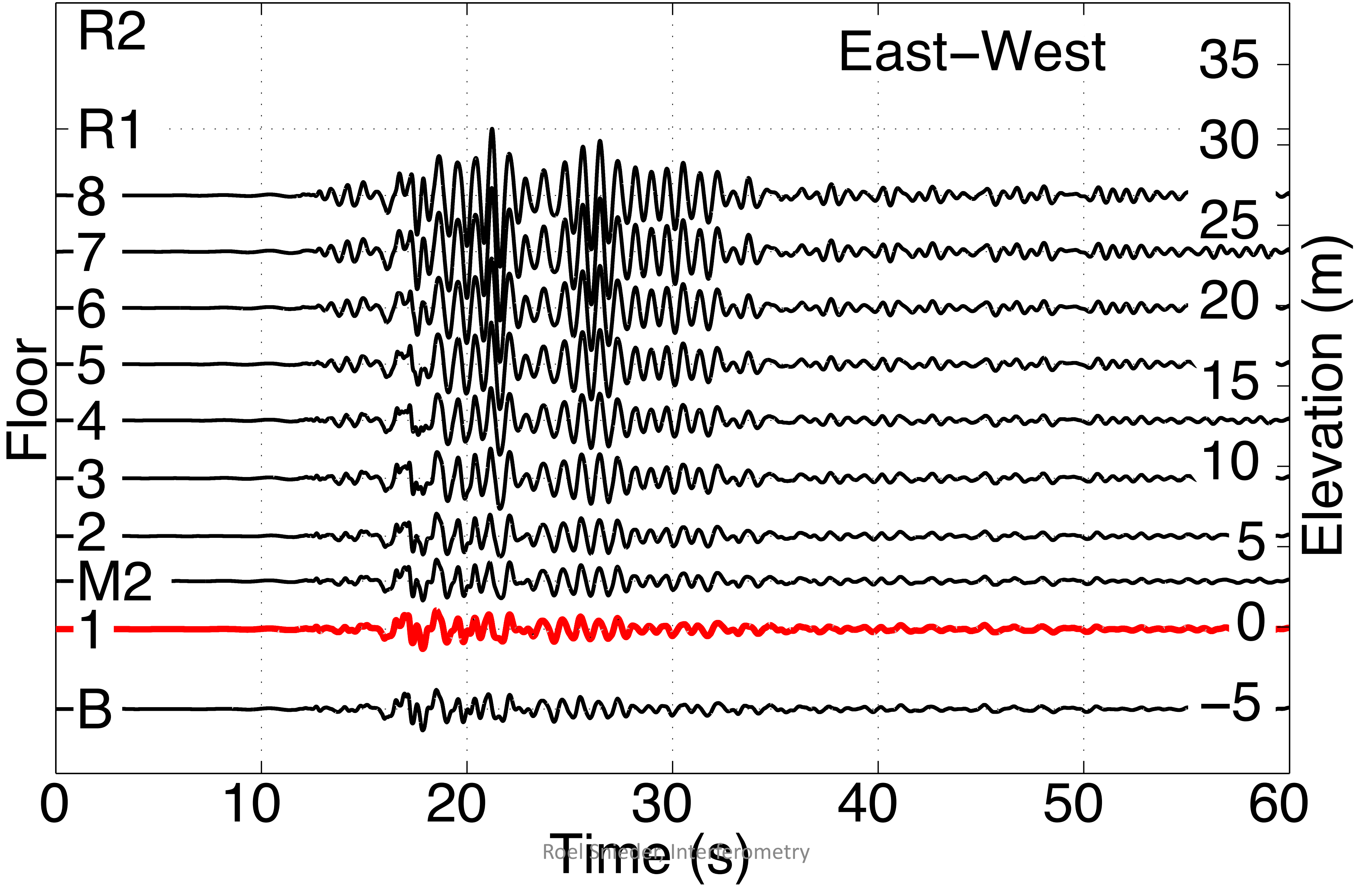

Earthquake after deconvolution

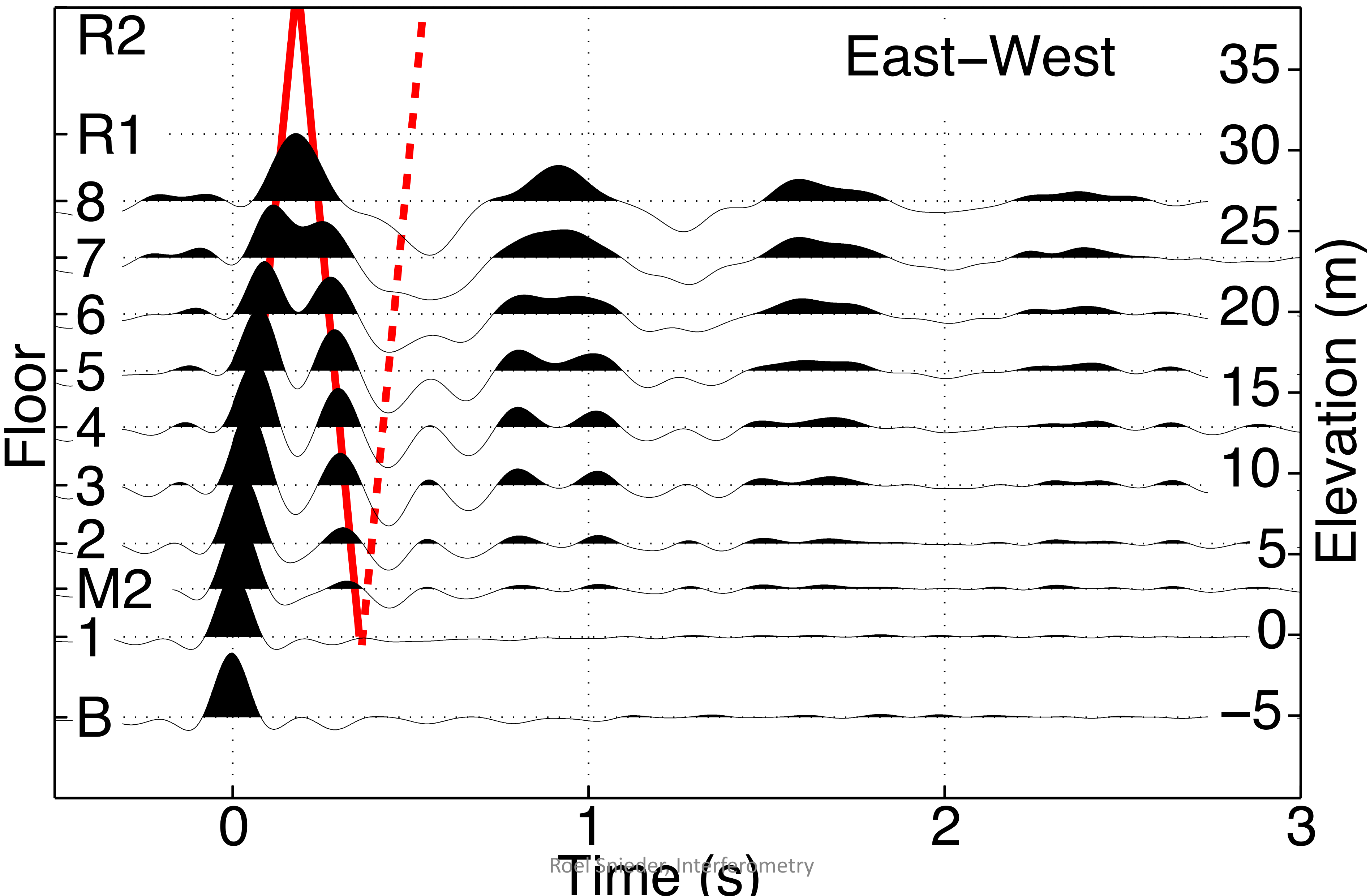

Earthquake after deconvolution

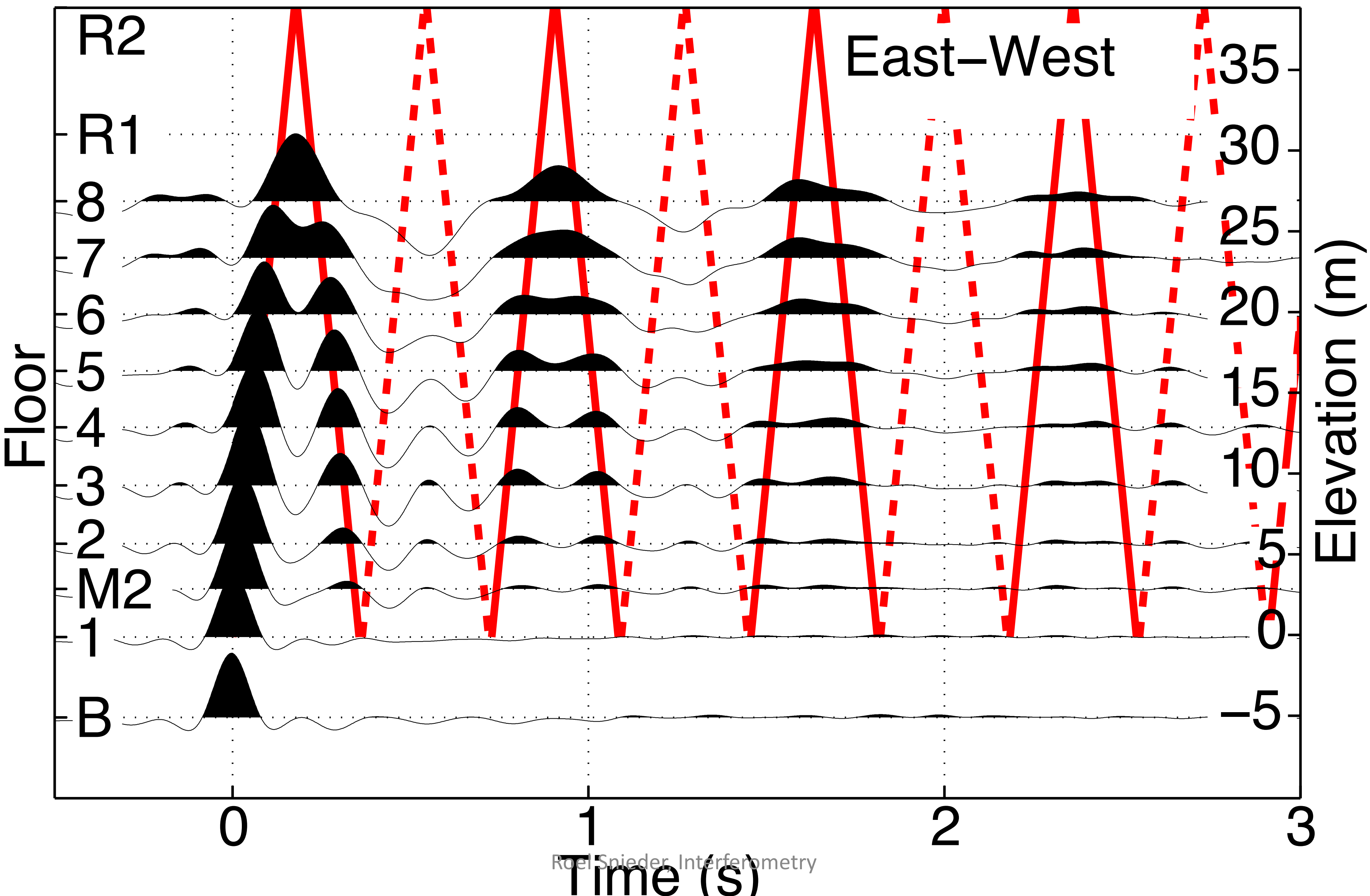

Shear velocity from different quakes

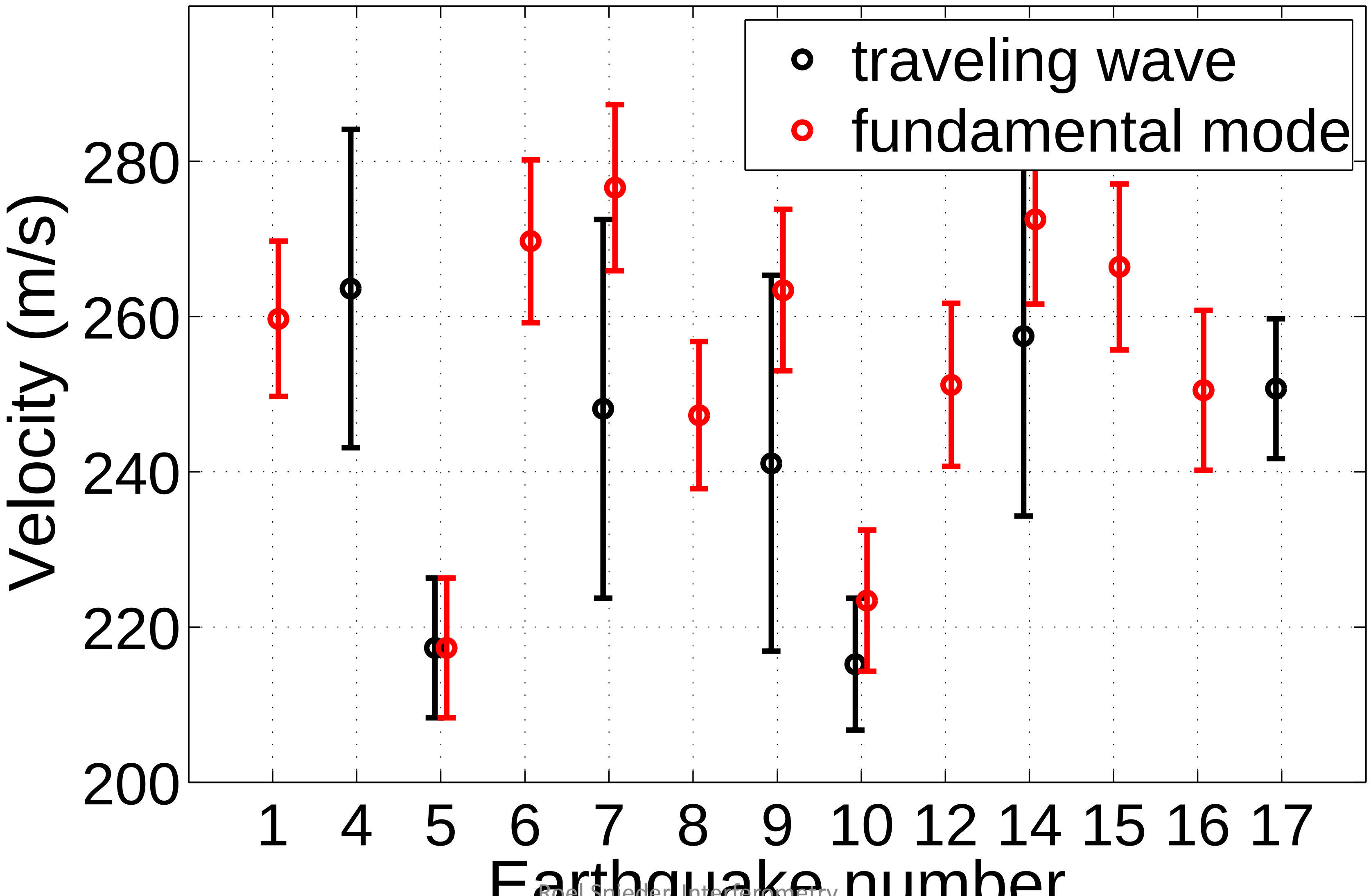

Shear velocity vs. shaking

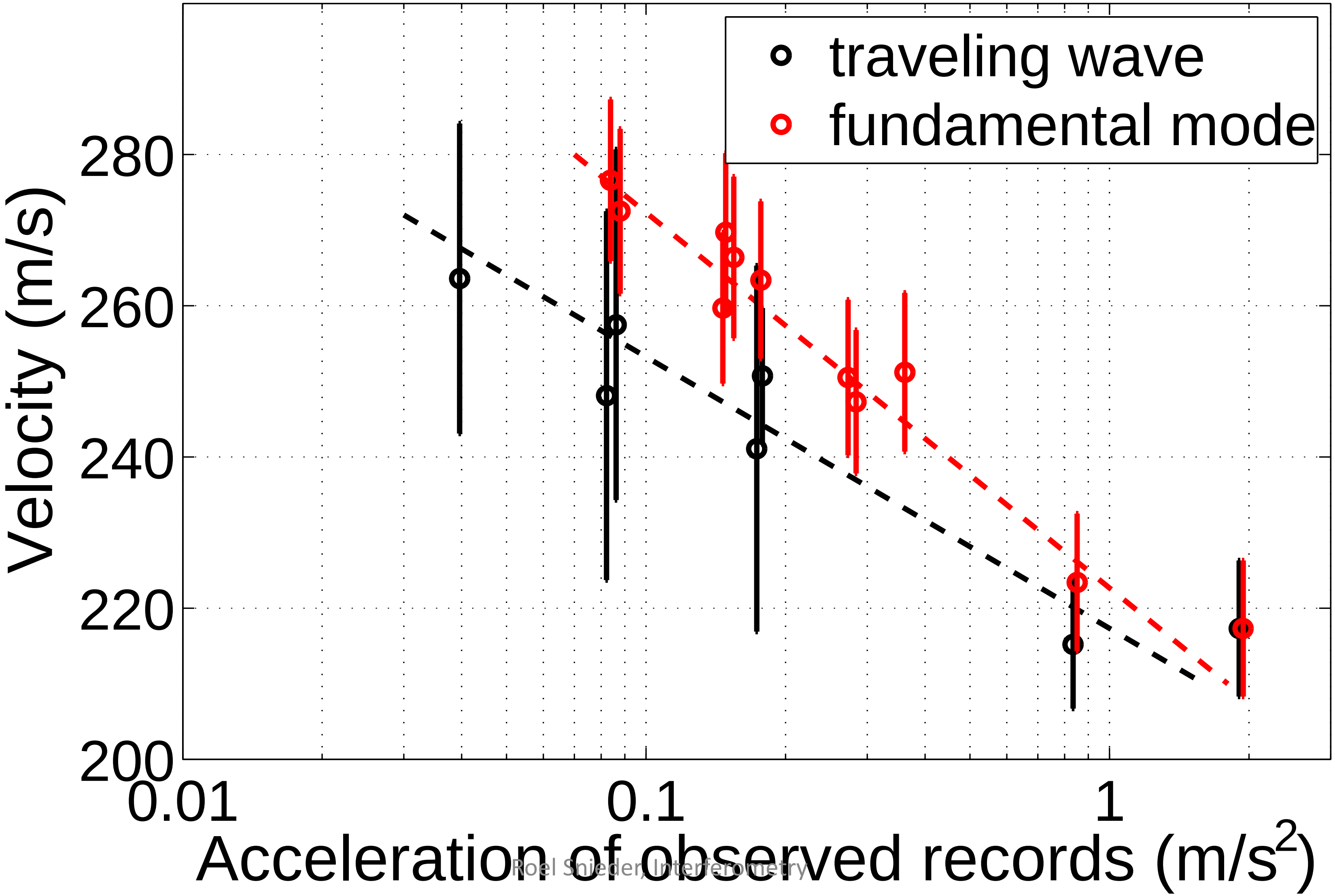

When the source-timing can be used

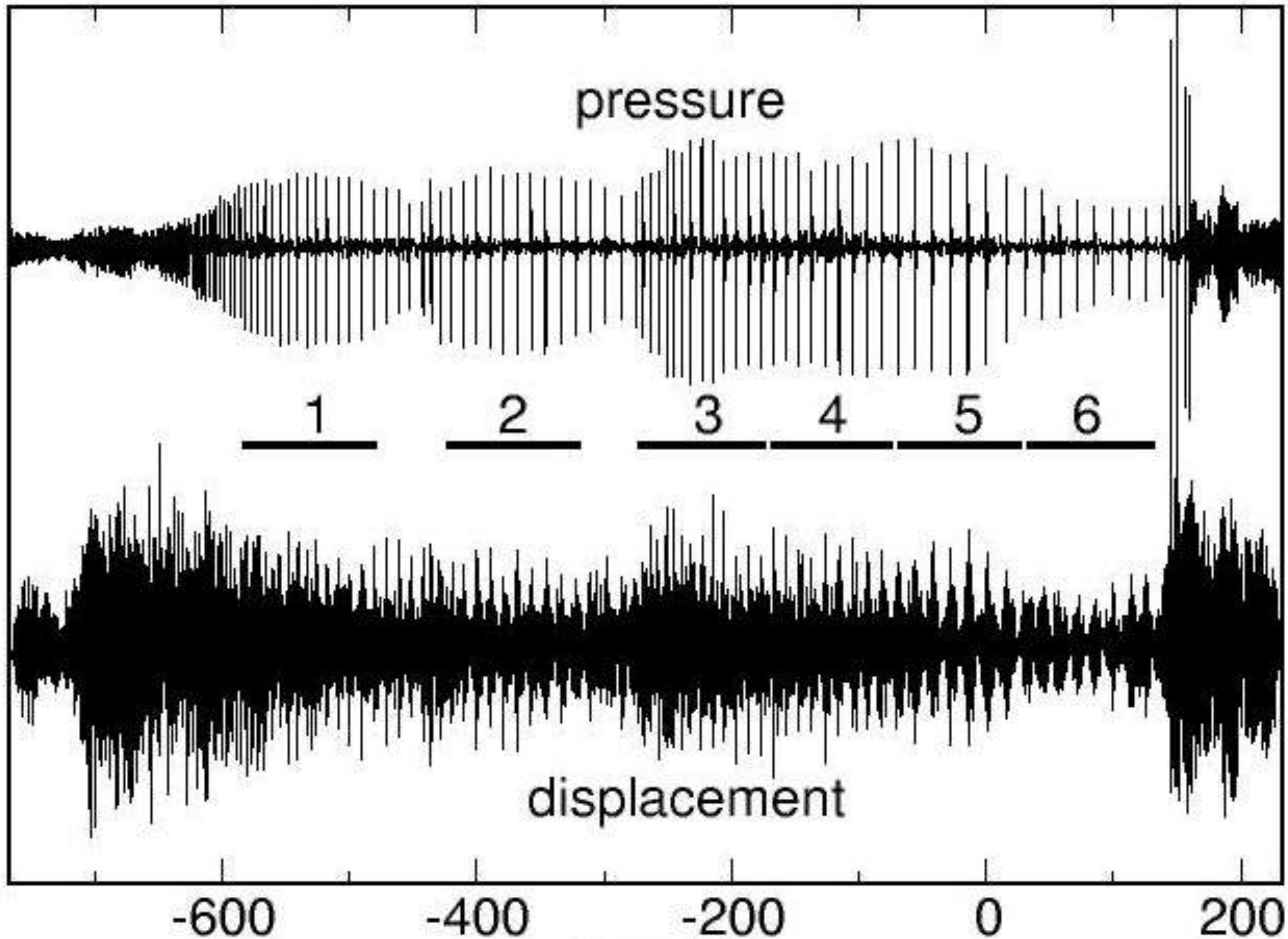
pressure
1
2
3
4
5
6
displacement
-600
-400
-200
0
200
time (s)

Displacement deconvolved with pressure

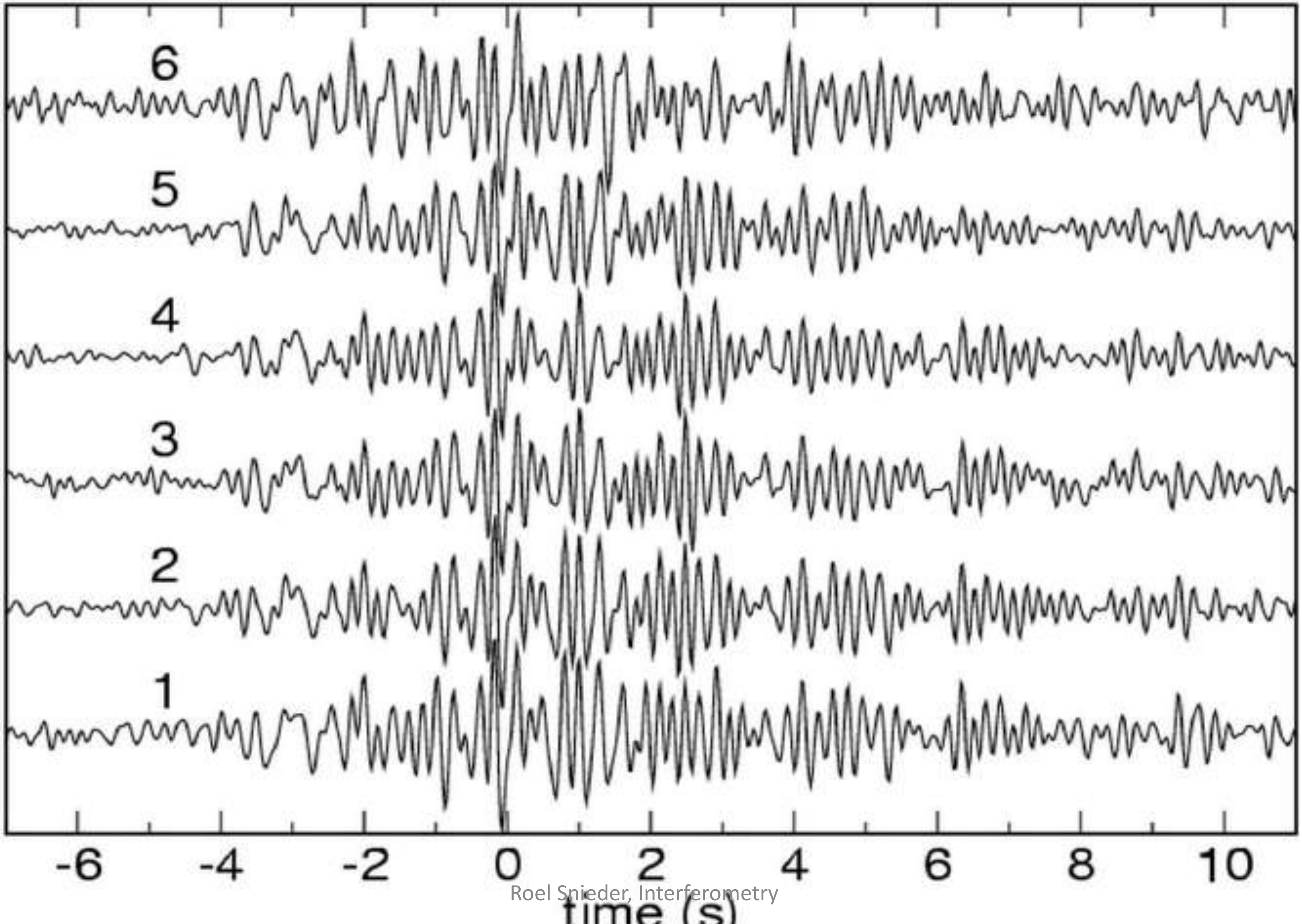

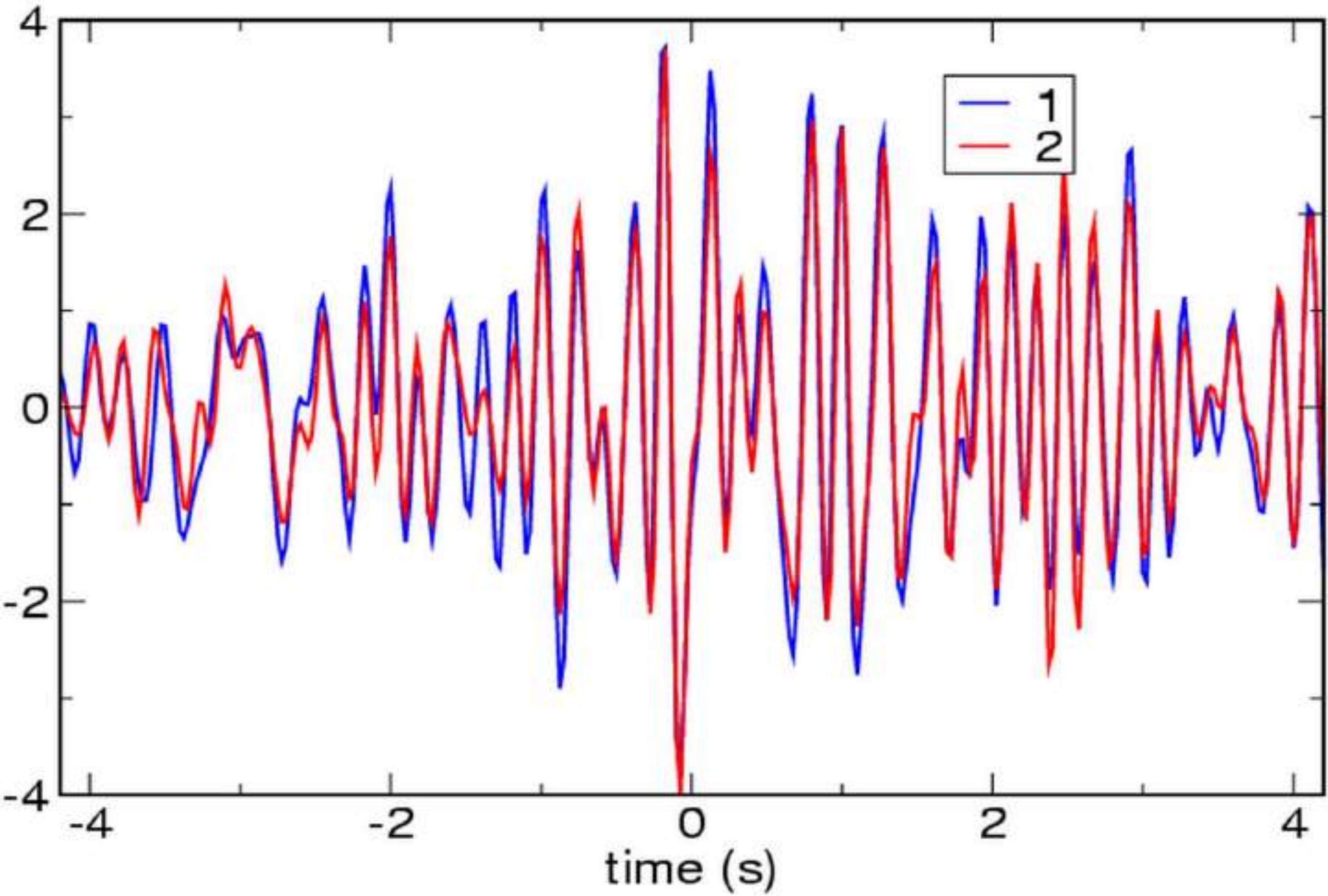

(Snieder, R. and M. Hagerty, Geophys. Res. Lett., 31, L09608, 2004)

Talsperre Eibenstock

Ultraschallsensorik aus der Bauphase

- Entwicklung des E-Moduls/ Druckfestigkeit
- 8 Geber, 4 Empfänger (UNG40/SW40, 40 kHz)
- VEB Projektierung Wasserwirtschaft

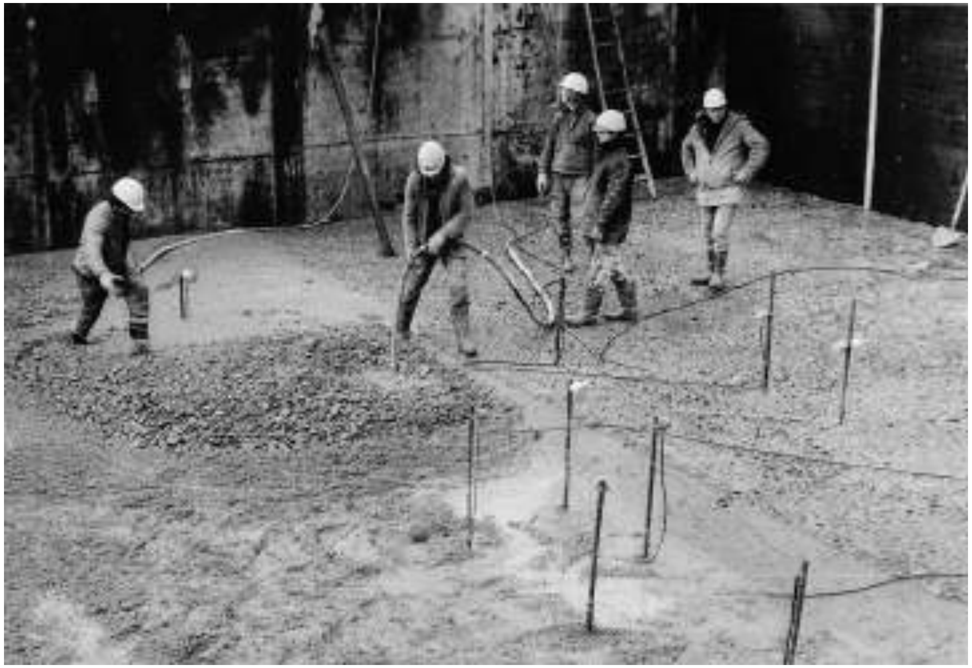

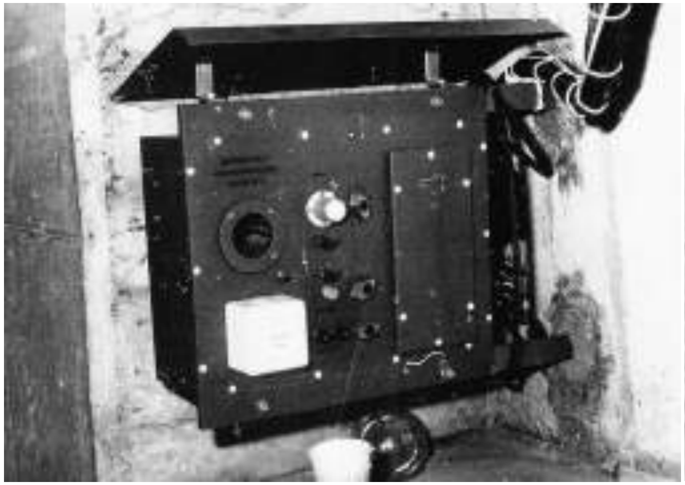

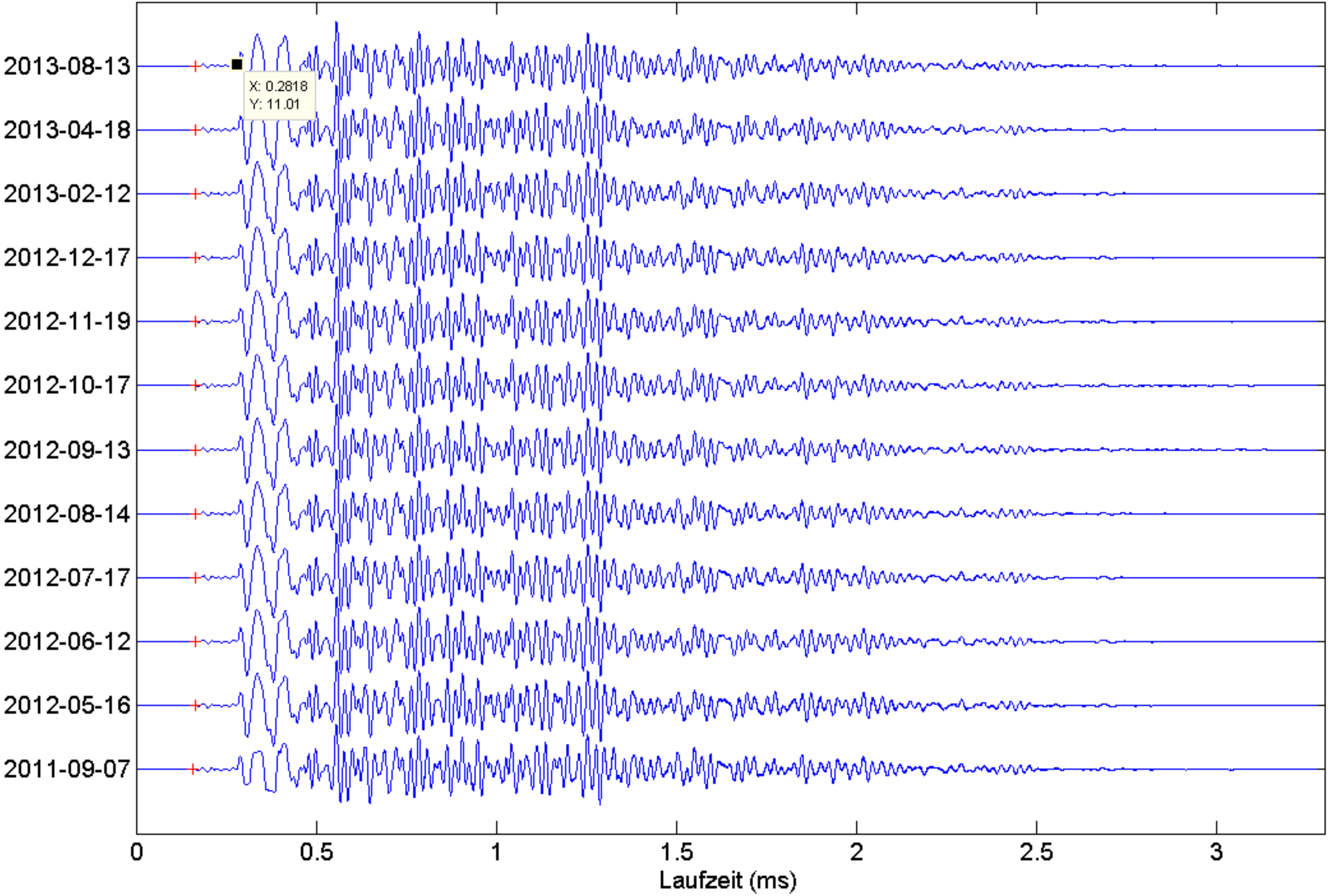

(Niederleithinger, E.; Krompholz, R.; Müller, S.; Lautenschläger, R. & Kittler, J. 36 Jahre Talsperre Einbenstock - 36 Jahre Überwachung des Betonzustands durch Ultraschall Proc. 38. Desdner Wasserbaukolloquium 2015 "Messen und Überwachen im Wasserbau und Gewässer, 2015, 1-10)